Optimizing energy storage and reproduction for Aquifer Thermal Energy Storage.

A scientific approach in enhancing ATES system performance at Achmea Apeldoorn through application of smart extraction and infiltration strategies.

Master Thesis

Joris Groot

3269396
University Utrecht & Tauw. B.v.
1st supervisor: Prof. R. J. Schotting
2nd supervisor: Ir. M. Bloemendal

Preface

This Msc Thesis report is a result of a study about Aquifer Thermal Energy Storage (ATES). This study is performed for the Master Study ‘Earth, Surface and Water’.In this Master I follow the “Hydrology-Track’. I conducted this study at consultancy firm Tauw b.v.

The subject of this thesis concerns improving the energy efficiency of the specific ATES system at Achmea Apeldoorn through application of smart infiltration and extraction strategies. In order to come up with improvements considering the infiltration and extraction rates, an analytical model is built in a worksheet of Excel. The understanding of the physical processes, local subsurface characteristics and system characteristics was essential to create this model. Building the model with the assembled knowledge made this project very educational. The greatest challenge was determining which aspects of the problem needed to be assessed and which not. I considered this to be rather difficult because the amount of paths that may be taken to come up with proper solutions seemed infinite.

I really enjoyed applying all the aspects of geo-hydrology to come up with an analytical solution to this actual problem and I hope you enjoy reading this report as much as I enjoyed working on this problem and finishing this resulting Msc thesis.

Joris Groot
Utrecht, 2013

Aknowledgements

I would not been able to complete this thesis without the help of other people. For this reason and many others I would like those who contributed to making the writing of my thesis such an interesting and pleasant experience.

First of all I would like convey my thanks to my 2 supervisors at Tauw. Martin Bloemendal for introducing me to the problem. His critical analytical view on the problem kept my on the right track in finding proper solutions more than once, and his positive attitude kept me motivated throughout the entire process. Erik Donkers for his help concerning Excel and his enduring patience, critical questions and his always present sense of humor. I learned more at Tauw than I imagined I ever would on beforehand and because of their persistent enthusiastic contribution I am proud of the result, so Thanks!

I would like to thank prof.dr. R. J. Schotting for his enthusiasm concerning the subject and the analytical model, and his critical, very useful comments on my resulting work. Furthermore I would like to thank my girlfriend Nienke, whose inexhaustible positivity I deeply respect and whose patience with me always kept me with both feet on the ground.

Finally I would like to thank all the people at Tauw who contributed to a very comfortable working atmosphere, my family who have always shown their love and (financial) support, and my friends and roommates, on who I can always rely me even during times when I did not seem to have time for them!

Summary

At Achmea Apeldoorn the groundwater velocity is high due to impelled geological features within the subsurface. For the ATES system of Achmea this is a problem, because potential stored thermal energy in the subsurface can be lost from the systems range. Current system management is based on a ’50-50 control strategy’ where the same volume is infiltrated in both the upstream and downstream stream well. In order to reduce energy loss it is investigated if through smartly changing the infiltration and extraction rates, energy loss can be reduced and the system performance of the system can be increased.

A detailed study about the physical processes concerning ATES established that time dependent energy demand and groundwater flow velocity are the parameters which are of most influence on infiltration or extraction rates and on the thermal influence radius of the wells. Understanding of these processes led to the realization of an analytical model that quantifies temperatures of groundwater within the subsurface. In this model the water volume that is infiltrated or extracted is considered to have the shape of a cuboid instead of a cylinder. The model is made one-dimension dependent because the length and the depth are fixed. Groundwater flow is considered to be only lateral. The infiltration and extraction rates that are needed to meet the monthly energy demand can be divided over the 2 wells in every possible ratio, making optimization for infiltration and extraction rates possible.

The analytical model is numerically validated with a numerical groundwater modeling program. The infiltration and extraction rates were then optimized with an iterative solver which focuses on equaling a target cell to a value or minimizing a target cell. Three optimization strategies were applied, which focused on minimizing the energy loss from the system, minimizing the total net pumped volume and compensating for the volume of water that is lost from the system due to groundwater flow.

The results of these optimizations which lead to three different control strategies are assessed with use of assessment criteria. Optimization for the compensation of volume loss for the system, lead to an ‘improved control strategy’ that reduced thermal energy loss from the system and reduced total net volume pumped and thus pumping costs, which increased the Seasonal Performance Factor for the hot and the cold wells. The control strategy was qualitatively accounted for in that the ratios that determine infiltration and extraction volumes per well, confirmed the expectancy that season dependent increased infiltration in upstream wells and increased extraction in the downstream wells would result in greater energy efficiency.

The ‘improved control strategy’ was then tested on its robustness. It was applied on 18 differing energy scenarios which mimicked years of extreme temperatures (i.e. hot summers or cold winters). The ‘improved control strategy’ resulted in financial savings, and total net volume decreasing for everyone of the 18 energy demand scenarios, compared to when the accustomed

’50-50 control strategy’. In an additional robustness test the energy demand scenarios were optimized individually. The ‘improved control strategy’ was compared to optimizations of the individual energy demand scenarios. The result was that not a single percentage for all the optimizations differed for more than 1% with the percentages of the ‘improved control strategy’. This increases the robustness of the ‘improved control strategy’.

The analytical Excel model and the resulting ‘improved control strategy’ provide insight in how ATES system energy efficiency, of systems installed in the subsurface where groundwater flow velocity is high, can be improved compared to accustomed system management. It is expected that the ‘improved control strategy’ is well applicable on other ATES systems. It must however be stressed that individual ratios which determine dividing of volumes of wells, may vary for other systems compared to the ATES system of Achmea, due to local differences in system characteristics and subsurface characteristics.

Contents

Appendices

List of symbols

	Annotation	Unit
Temperature	T	°C
Difference between infiltration and extraction temperature	ΔT	°C
Effective porosity	n_e	-
Volume of interconnected pore space in a porous medium	V_v	m^3
Total volume of porous medium	V_t	m^3
Volumetric water content of porous medium	θ	-
Volumetric flow rate in s-direction	Q_s	m^3/h
Hydraulic conductivity of porous medium in s-direction	K_s	m/day
Hydraulic gradient	$\frac{\Delta h}{\Delta s}$	-
Cross-sectional area	A	m^2
Specific discharge in s-direction	q_s	m/h
Linear velocity in s-direction	v_s	m/h
Transmissivity	T_b	m^2/d
Thickness of a specific layer	b	m
Longitudinal hydrodynamic dispersion in direction of the groundwater flow in the x-direction	D_L	m^2s^{-1}
Transversal dispersivity in the y,z-direction	$D_{T_{y,z}}$	m^2s^{-1}
Longitudinal dispersivity in the x-direction	α_L	m
Transversal dispersivity in the y,z-direction	$\alpha_{T_{y,z}}$	m
Molecular diffusion coefficient	D_{diff}	m^2s^{-1}
Radius of the cylindrical volume of water	$r_{volumewater}$	m
Influence radius of water distributed over the aquifer	$r_{volumewater}$	m
Infiltrated or extracted volume of water	V	m^3
Length of filter screen	H	M
Volumetric heat capacity of a medium	C_m	J*m^{-3}°C^{-1}
Volumetric heat capacity of aquifer, water, soil grains	$C_{a,w,r}$	J*kg^{-3}°C^{-1}
Specific heat capacity of a medium	c_m	J*kg^{-3}°C^{-1}
Density of a medium	ρ_m	kg/m^3
Distance between hot well1 & 2, distance between cold well 1 & 2	L	m
Length of time step in analytical model	Δt	months
Dimensions of infiltrated/extracted cuboid (x,y,z)	$\Delta x, y, z_{cub}$	m

Dimensions of analytical model grid (x,y,z)	$\Delta x, y, z_{grid}$	m
Width of grid cells left of well 1, between the 2 wells, and right of well 2	$\Delta x_{grid\_left,middle,right}$	m
Infiltration/extraction rate	$Q_{\inf, ext}$	m^3/h
Thermal energy demand	P	W
Thermal energy demand	E	J
Cylindrical/cuboid volume of infiltrated or extracted water	$V_{cyl,cub}$	m^3
Total volume lost from the system due to groundwater flow	V_{lost}	m^3
Volume of infiltrated/extracted water in/from cold well1/cold well 2	$V_{\inf, extC1,C2}$	m^3
Membrane filter index	MFI_{mem}	$sec/liter^2$
Design injection Darcy velocity on the walls of the bore hole	v_{inject}	m/h
Specific clogging speed	v_{cl}	m/year
The number of equivalent full load hours the well pumps per year	u_{eq}	-
Radius of the bore-hole	r_0	m
Distance from the well	r	m
Head difference between the initial head h_0 and head h_r after injection or extraction at position r	$h_r - h_0$	m
Width of infiltrated/extracted within each grid cell in the analytical model	$W_{\inf, ext}$	m
Temperature of infiltrated/extracted volume of water	$T_{\inf, ext}$	°C
Volumetric flux per unit volume representing sources and/or sinks of water where *negative* values are extractions, and *positive* values are injections	W	day^{-1}
Time	t	days or months
Specific storage of the porous medium	S_s	m^{-1}
Distribution coefficient for advective heat transport	Kd	m^3/kg
Energy supplied by wells or used by pumps	$E_{wells,pump}$ E	kWh
Power of pumping system	P_{pump}	J/s
Maximum hourly discharge rate	$Q_{\max}$	m^3/h
Gravitational acceleration	g	m/s^2
Efficiency of underwater pump	η	-
Elevation head	H_{pump}	m

1 Introduction

1.1 Aquifer thermal energy storage to save energy

With the decreasing availability of fossil fuels, the increase of global warming and rising energy prices there is a strong need for sustainable energy. One upcoming form of effective sustainable energy is aquifer thermal energy storage (ATES) (Vail and Jenne 1994; IF Technology 1995., Morofsky 1994). In an aquifer thermal energy storage system, heat and cold is stored in and recovered from the ground where the subsurface acts as a storage medium.

ATES systems are installed globally for the past 25 years and the number of ATES systems in the Netherlands currently exceeds 2000 (www.deltares.nl). With the governmental aim to create a green and sustainable energy supply in 2020, the number of ATES systems is increasing in application as well as its popularity. To achieve the governmental requirements of 2% annual energy saving and the increase in share of sustainable energy of 20%, there would have to be 20.000 working ATES systems in 2020 (IF Technology, 2009, www.agentschap.nl). The current expected increase in application of ATES systems however, is much lower (Figure 1.1).

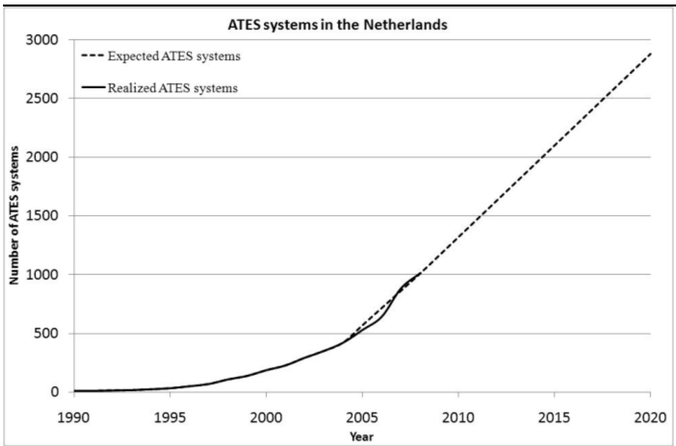

Figure 1.1 ATES systems in the Netherlands until 2020 (IF Technology, 2009).

1.2 ATES technique

During (hot) summer periods, groundwater that is used to cool buildings increases in temperature after which it is stored in the subsurface into the hot well. During (cold) winter periods this hot water is pumped out of the subsurface and is used to supply the building with heat. This releases cold water, under influence of outside temperature, and that is again re-injected in the aquifer into the cold well. This water will serve for cooling purposes during summer (Figure 1.2). This reversible process leads to a zero net-loss of water from the aquifer and can lead to significant energy savings.

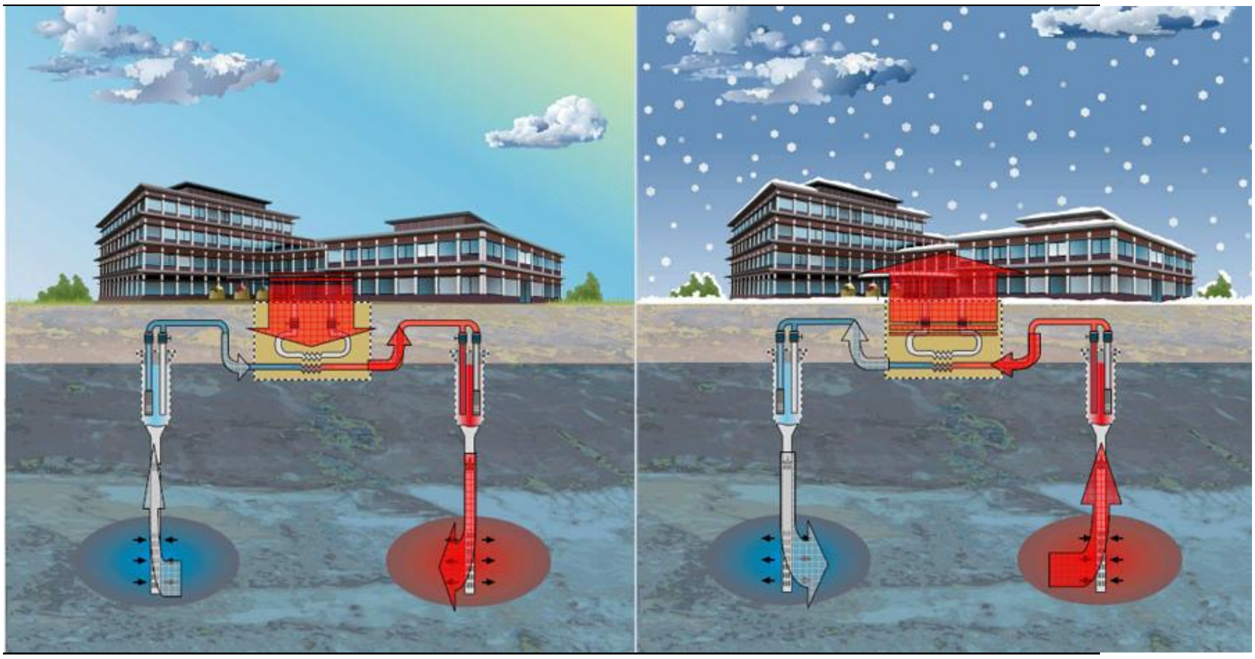

Figure 1.2 ATES system (www.geo-elements.nl).

Water temperatures in the cold well typically lie in the range of 6-10 °C and this is sufficient to effectively cool a building. The water temperatures in the hot well typically lie in the range of 14-18 °C. Preferentially this temperature is increased to temperatures of 35 – 40 °C to meet heating purposes. To increase the water temperature a heat pump is used. The extraction and injection of ATES can place at depths ranging from 10 – 150 meters (Courtois et al., 2007), depending on the depth of the suitable aquifer.

Groundwater flow influences the locality of the stored hot and cold energy in the subsurface. The groundwater flow velocity and direction must be taken into account when an ATES system is installed (Figure 1.3).

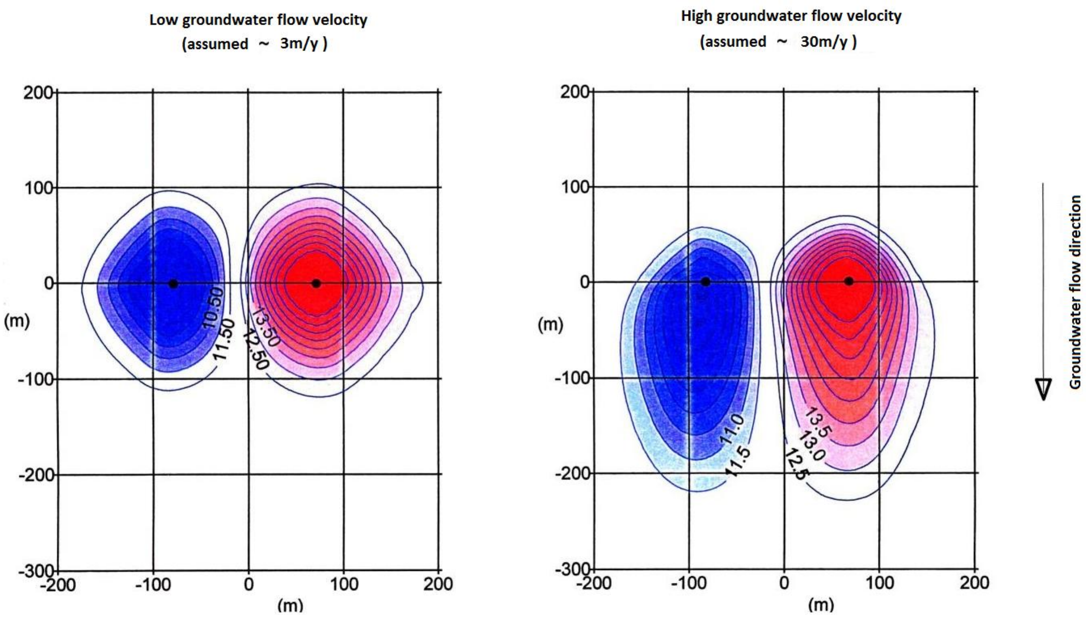

Figure 1.3 Influence of groundwater flow velocity and direction on stored energy in ATES.

1.2.1 Energy efficiency in ATES

The hotter the water that flows into the heat pump the electricity has to be used by the heat pump to increase the waters temperature to the preferred 35 - 40 °C for heating purposes. This results in a lower energy use for the system when peak temperatures (i.e. lowest for the cold well and highest for the hot well, or a high temperature difference (ΔT [°C]) is retrieved from the wells.

A measure for the operating performance of the ATES over the season is called the seasonal performance factor (SPF). The SPF is the ratio of the hot and cold thermal energy delivered through the wells over the electrical energy needed for pumping. The energy efficiency of the ATES system will increases with a higher SPF. This is established if the wells are managed in such a way that the peak temperatures are available when extraction is required, because this results in lower pumping rates (www.sepemo.eu) and less energy used by the heat pump.

1.3 ATES for Achmea

“Consultancy firm Tauw” was given the assignment to design an ATES system for insurance company Achmea in Apeldoorn. Since the campus of Achmea is expanding, their increased need in sustainable energy to provide for new facilities lead to the realization of an ATES system in the subsurface.

The most commonly applied ATES systems are doublets, as is the case at Achmea. For a doublet a pair of tube wells is drilled in the same aquifer with significant lateral distance. One is the hot well and the other the cold well. In the system each well can be used to inject or extract water and the flow direction is therefore reversible. The ATES system of Achmea uses 2 doublets. The hot wells and cold wells are positioned in line with the groundwater flow direction (Figure 1.4).

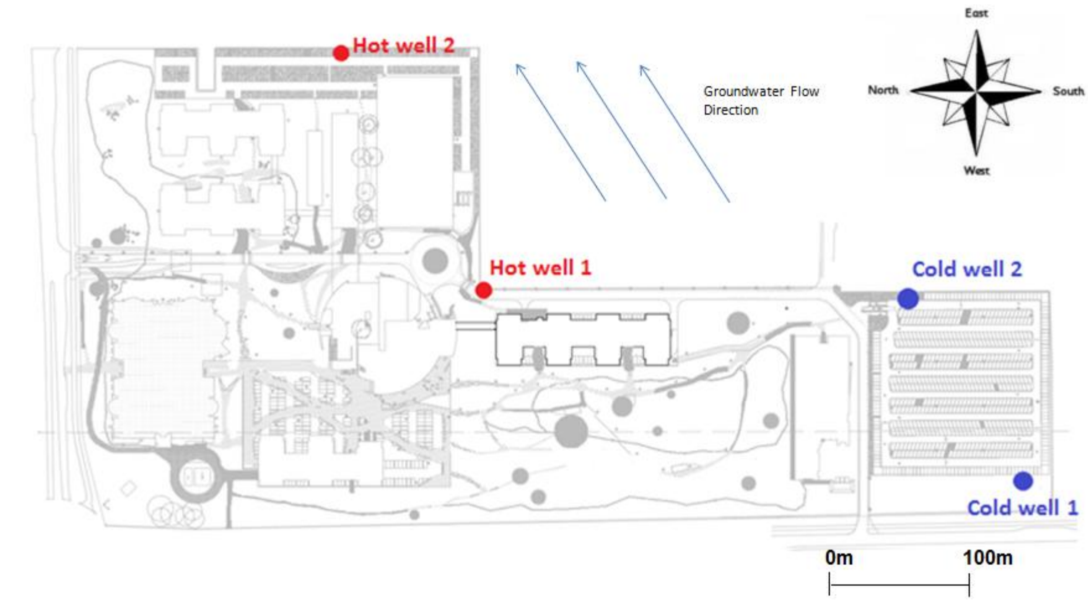

Figure 1.4 Well locations and groundwater flow direction of ATES system Achmea.

Realizing optimal efficiency in energy usage in the ATES system of Achmea is a challenge because Apeldoorn lies in the Veluwe area where natural groundwater flow velocities are high. Due to this high groundwater flow velocity, energy that is stored in the subsurface can be lost from the systems range when this is not taken into consideration during operation. With a thermal influence area with a radius of 60 meters, and groundwater velocity of approximately 37 meters per year (Tauw, 2008) potentially 20% of the infiltrated thermal energy can be lost from the system with an accustomed or straightforward control strategy.

There is limited information present in literature concerning improvement of ATES system management of systems that are installed in the subsurface where groundwater flow velocity is high. System management here relates to infiltration and extraction rates of groundwater during a certain period of time. Additional research may contribute to understanding of this phenomenon and improvement of ATES system efficiency by changing infiltration and extraction rates.

2 Research proposal ATES system Achmea

2.1 Goals

The goal of this research is to conduct a study that will give control options on how thermal energy can best be covered for an ATES system with multiple wells in a high groundwater velocity aquifer. The research must contribute to the control strategy of the wells, optimizing the energy storage and recovery of the ATES system. The research is carried out focusing on the case of Achmea.

2.2 Research Questions

Because of the high groundwater velocities in the subsurface at the site of Campus Achmea Apeldoorn, the loss of thermal energy is apparent. In order to achieve improvement of ATES system management, the following Research Questions with sub-questions/actions are posed:

1: What are the dominating physical processes that occur in the subsurface and in the ATES system, which influence the performance of the ATES system and how can these processes be described?

2: What are the characteristics of the ATES system of Achmea Apeldoorn, i.e. geohydrological subsurface, groundwater flow and system characteristics and energy demands?

3: How can insight in interaction between the 2 hot and the 2 cold wells, with seasonal storage and recovering of thermal energy be obtained?

4: Are there control strategies that can improve the performance of the ATES system of Achmea? And is this control strategy applicable on other systems?

2.3 Methods and approach

1: What are the dominating physical processes that occur in the subsurface and in the building which influence the performance of the ATES system and how can these processes be described?

Understanding of and the ability to mathematically describe the physical processes concerning ATES are of great importance to acquire a thorough understanding in how ATES can best be applied and what parameters need to be considered in search for an improved control strategy.

This question will be answered with a literature and desk study. The mathematical description of the dominating processes will be presented. The most important parameters will be discussed. Where responsible and possible, simplifications will be made by neglecting terms or approaching typical parameters as a constant. The results of this study are presented in Chapter 3; Physical processes.

2: What are the characteristics of the ATES system of Achmea Apeldoorn, i.e. geohydrological subsurface, groundwater flow and system characteristics and energy demands?

In order to answer this question the following sub questions are defined.

<u>What is the composition and what are the properties of the subsurface?</u>

Understanding the geological subsurface features at Achmea Apeldoorn is important because they influence groundwater transport as well as energy transport and storage potential.

This question will be answered with a literature study and using data from a geohydrological survey carried out by Consultancy firm Tauw b.v. (This survey was a requirement for the granting of the permit for applying the ATES system at Achmea). The results of this study are presented in Section 4.1; Subsurface characteristics.

<u>What are the groundwater flow characteristics?</u>

Understanding the behavior of groundwater flow directions and velocities is highly important in relation to the efficiency of the ATES system. Due to high groundwater velocities potential recoverable energy can be lost permanently from the ATES system.

This question will be answered with using the data from a geohydrological survey carried out by Consultancy firm Tauw, and studying data provided by geo-scientific institutes. The results of this study are presented in the Section Groundwater flow characteristics.

<u>What are the system characteristics of ATES Achmea?</u>

Due to direction of groundwater flow the wells are positioned in such a way that infiltrated hot and cold water cannot interfere with each other. The specific depth of the filter screens is adapted to the location of the applicable aquifers is dependent on geological subsurface features. In understanding how to improve system performance, general knowledge about the specific system used at Achmea Apeldoorn is essential.

This question will be answered with (static) data about the ATES system, provided by Achmea Apeldoorn and the system developing contractor. The results of this study are presented in 4.3; System characteristics.

What is the energy demand of ATES of Achmea and how is this demand met through system management?

The buildings at the site of Achmea Apeldoorn are demanding a certain amount of hot and cold energy throughout the year. Understanding what this demand is and how the energy demand is currently met by the ATES system is essential in establishing an optimization strategy.

This question is answered with using data about the energy demand provided by Achmea Apeldoorn. The results of this study are presented in Section 4.3.2

3: How can insight in interaction between the 2 hot and the 2 cold wells, with seasonal storage and recovering of thermal energy be obtained?

In order to understand interaction between the wells, current system management must be understood. The accustomed control strategy must be compared to a future optimized control strategy for the ATES system which can lead to increased energy recovery.

To be able to compare different control strategies, assessment criteria must be set. For that it is needed that the energy loss downstream of the wells, pumping rates and the temperature in the wells is quantified.

The quantification of the temperatures in the wells and energy loss in the subsurface can be established with analytical operations/calculations that describe occurring processes in the ATES system. The different time spans that concern the subsurface, groundwater flow, and system characteristics as well as the energy demand must be accounted for in a governing time scale. Using an analytical model that incorporates this quantification will establish insight in the result of an optimized control strategy compared to the accustomed control strategy the ATES system at Achmea.

Approach

To answer research question 3 an analytical model is built in an Excel spreadsheet. This Excel model quantifies the temperatures in the subsurface in the vicinity of the wells. By calculating the flows and energy transport, thermal energy loss in the subsurface is quantified and can be expressed in financial loss. The description of the Excel model is presented in Chapter 5.

To establish an accurate representation of the reality, the analytical Excel model will be validated qualitatively and by using the results from a simulation in a numerical groundwater modeling program.

The approach in creating the analytical Excel model is visualized in Figure 2.1 and described in Chapter 5.

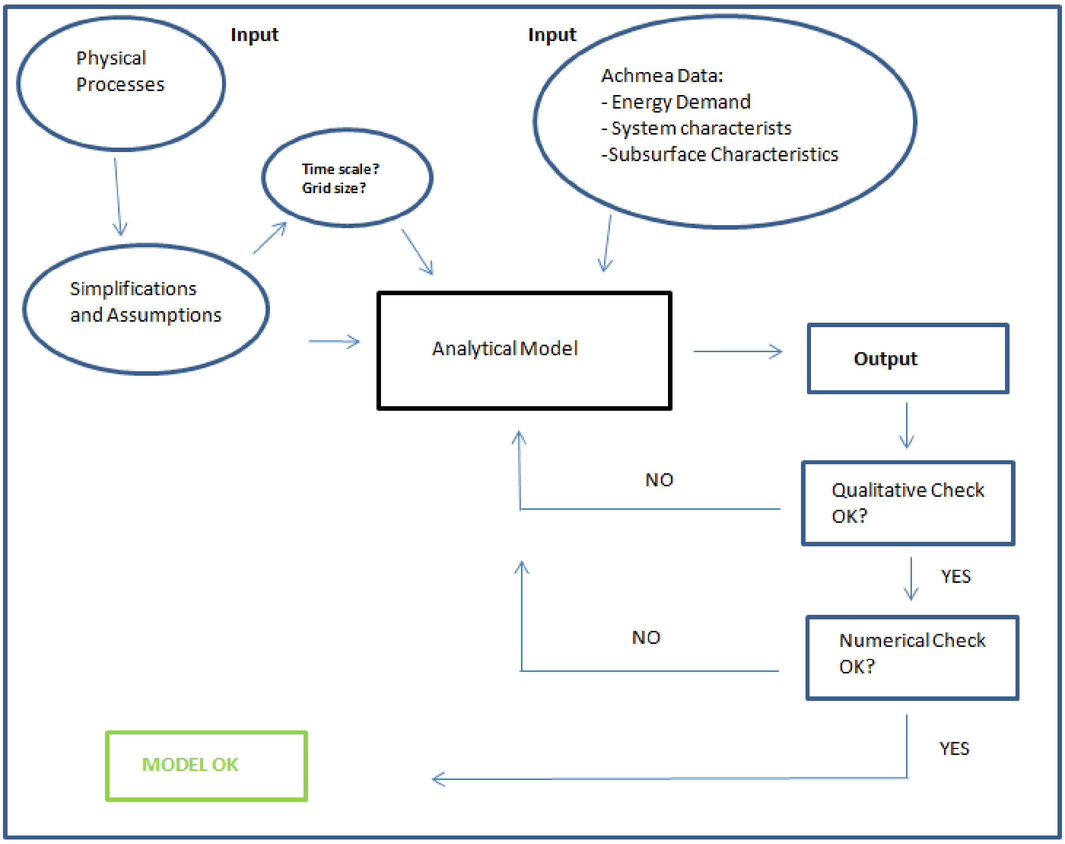

Figure 2.1 Analytical approach in creating analytical Excel model.

4: Are there control strategies that can improve the performance of the ATES system of Achmea? And is this control strategy applicable of other systems?

The accustomed control strategy applied at ATES Achmea can now be visualized. To find a control strategy that can improve the performance of the ATES system, the accustomed control strategy must be optimized.

Optimization

The question is answered by using an iterative solving function on the current control strategy in Excel. For the same energy demand this solver changes the infiltration and extraction rates. The solving method that Excel uses is described and discussed to validate its outcome.
The optimization is performed for several optimization strategies. In these strategies for different 'targets' is optimized (i.e. lowest energy loss, lowest total pumped volume) which will yield different control strategies.

Assessment criteria

In order to judge if the resulting control strategies are in fact improved control strategies, they are assessed based on several criteria. The control strategy that matches the assessment criteria the best will be chosen as the 'improved control strategy'.

Robustness check

A key aspect is to investigate if the 'improved control strategy' optimizes the performance of the ATES system for varying *energy demands. This means: If outside temperatures change in such a way that the energy demand within the building is going to change, will the useful 'optimized control strategy' yield improved results compared to the current control strategy. In order to test the robustness of the 'optimized control strategy' a series of energy demand scenarios is established. These energy demand scenarios mimic variations in annual outside temperature distribution. It is tested if the ATES systems requirements are met and energy loss is reduced is the 'improved control strategy' is applied on these varying energy demand scenarios.*

In an additional check is the 'improved control strategy' compared to the optimization control strategy for the different energy scenarios. This means that an energy demand is predicted and optimization is performed for this prediction. The intensity with which the 'improved control strategy' differs from the optimized control strategy for a varying energy demand is a measure for the robustness of the 'improved control strategy'.

The results, of the comparison between the improved control strategy and the accustomed control strategy and the difference between optimization for energy scenarios, is then qualified.
The approach in finding the improved control strategy and determining its quality is visualized in Figure 2.2 *and described in Chapter 5.*

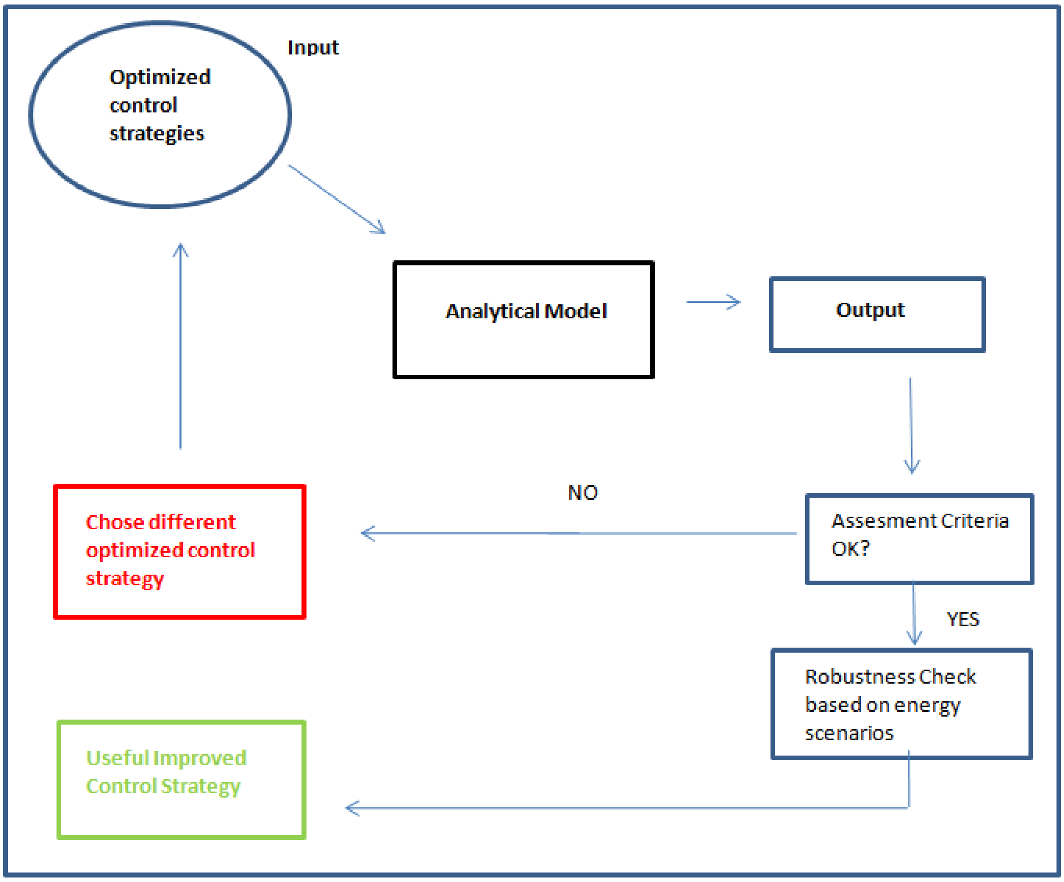

Figure 2.2 Approach for obtaining useful control strategy.

3 Physical processes

In the following Sections the physical processes concerning ATES are described. The Sections focus on mathematically describing water flow and energy transport in porous media.

3.1 Water flow in porous media

An ATES system can only be realized if the there is an appropriate aquifer in the subsurface. Preferentially this permeable region or layer in the saturated zone is not to deeper than 200 meters, has a high hydraulic conductivity (i.e. coarse sand) and is sealed with an impermeable layer.

Grain size

The distribution of grain sizes in an aquifer determines whether or not water is easily transmitted through the porous medium. Sand with larger a larger grain size has greater pore spaces and therefore transmits water better than sand with smaller grains. ATES is applied in aquifers with grain sizes of 200 – 250 μm or larger. The designation of sand according to differing grain size is listed in Table 3.1 (N.V.O.E., 2006).

Table 3.1 Grain sizes of sand

Grain size diameter (μm)	**Designation**
50 – 150	Very fine – Fine sand
150- 300	Middle fine – Middle coarse
300 – 2000	Middle coarse – Very coarse

Effective porosity

The effective porosity in a porous medium is defined by Equation [1].

$$n_e = \frac{V_v}{V_t} \qquad [1]$$

Where n_e is the effective porosity of the porous medium [-]; V_v is the volume of *interconnected* voids that is interconnected and is transmitting flow, within the porous medium [m^3]; V_t is the total volume of the porous medium [m^3]. The effective porosity can differ significantly from the total porosity, if the amount of pores that are not interconnected (i.e. single pore) is high.

The volumetric water content (θ) is a measure for the amount of pore space in a porous medium that is occupied by water in a given total volume V_t , and is defined by Equation [2].

$$\theta = \frac{V_w}{V_t} \qquad [2]$$

Where θ is the volumetric water content [-]; V_w is the volume of water [m^3].

When a porous medium is fully saturated: $n_e = \theta$

When a porous medium is not fully saturated and there is also air inside the pore spaces: $\theta < n_e$ (Fitts, 2002).

A visualization of the difference between a fully and not fully saturated porous medium is presented in Figure 3.1.

1

2

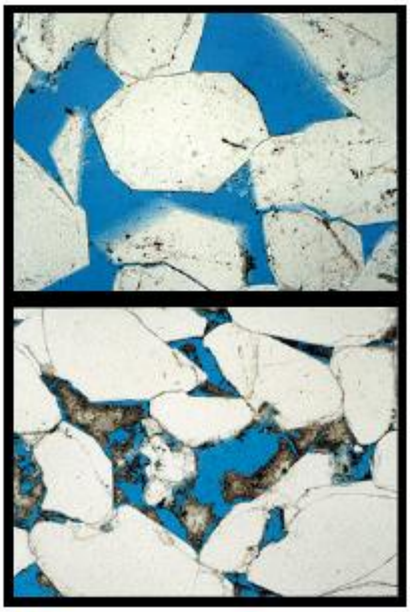

Figure 3.1 Fully saturated porous medium (1) and a not fully saturated porous medium (2) (http://biosystems.okstate.edu/darcy/index.htm).

3.1.1 Darcy's law

One dimensional groundwater flow can be quantified using Darcy's law. Henry Darcy conducted an experiment in which water is forced through a tilted sand filled column. Two small piezometers measured the hydraulic head difference (Δh) within the saturated column Figure 3.2.

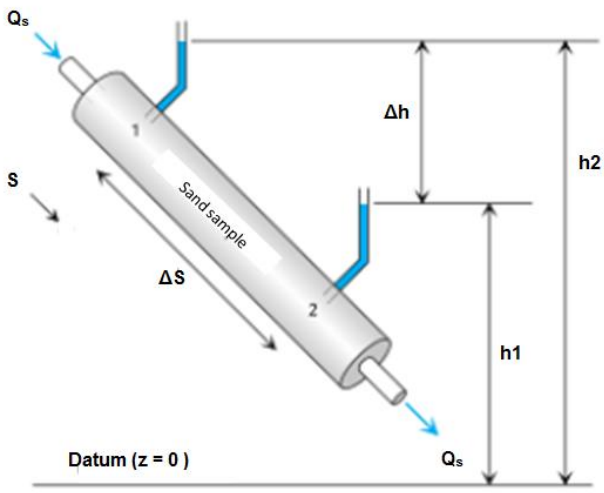

Figure 3.2 Schematic illustration of Darcy's experiment.

The distance between the piezometers is Δs. A steady flow of water is forced through the column at a volumetric flow rate (Q_s). The observations of the conducted experiment showed that the volumetric flow rate is dependent on hydraulic conductivity (K_s), a property which is a measure for the ease that a fluid passes through the porous medium and the cross-sectional area of the column (A). This lead to formation of Darcy's law (Equation [3]) (Fitts, 2002).

$$Q_s = -K_s \frac{\Delta h}{\Delta s} A \quad [3]$$

Where Q_s is the volumetric flow rate in the s direction [m^3/h]; K_s is hydraulic conductivity of the porous medium [m/d]; $\frac{\Delta h}{\Delta s}$ is the hydraulic gradient [-]; A is cross-sectional area [m^2].

The minus sign is in Equation [4] because head decreases in the flow direction. The hydraulic gradient states the rate that the head changes in the s-direction.

Darcy's Law can be rewritten in terms of flux (Equation [4]) when the volumetric flow rate is divided by the cross-sectional area:

$$q_s = \frac{Q_s}{A} = -K_s \frac{\Delta h}{\Delta s} \qquad [4]$$

Where q_s is the specific discharge in the s-direction [m/h]. The specific discharge is sometimes referred to as the Darcy velocity of the groundwater.

Because only a fraction of the cross section is available for water through in a porous medium, due to the presence of grains, the specific discharge is lower than the average linear velocity (v_s). By dividing the specific discharge by the effective porosity, the average linear velocity is shown by Equation [5];

$$v_s = \frac{q_s}{n_e} \qquad [5]$$

Where v_s is the average linear of the water flowing through the porous medium [m/d].

A visualization of specific discharge and average linear velocity is presented in Figure 3.3.

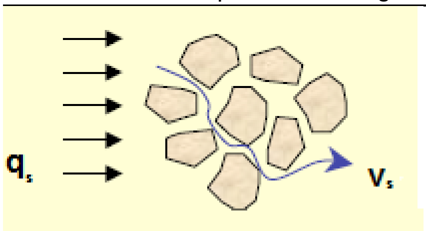

Figure 3.3 Average linear velocity compared with specific discharge.

Heterogeneity and anisotropy

Commonly the hydraulic conductivity is irregularly distributed over the subsurface. Within a heterogeneous material the value of K varies spatially, whereas in a homogeneous material K is consistent over different localities.

Anisotropy implies that the value of K is depending on direction. If a Cartesian coordinate system is used with z being the vertical axis, then from a fixed point of view, the medium is anisotropic if hydraulic conductivity for either of the directions is not equal (i.e. $K_x \neq K_y$). Due to strong horizontal layering in the subsurface, K_z is often smaller than K_x and K_y.

Transmissivity

Hydraulic conductivity can also be measured as an integrated parameter over the thickness of a distinct geological facies or layer. The hydraulic conductivity over an entire layer is called the transmissivity. If the hydraulic conductivity tangential to the layer can be assumed constant over a thickness of a layer, the transmissivity T is given in Equation [6]:

$$T_b = K_s b \qquad [6]$$

Where T_b is the transmissivity of the layer [m^2/d]; b is the thickness of the specific layer [m]; K_s is the hydraulic conductivity of the specific layer [m/d].

Advection

Advection is the movement of mass due groundwater flow velocity. In solute advection, dissolved substances in the water are transported by moving water particles.

Hydrodynamic dispersion in porous media

The principle of hydrodynamic dispersion is visualized in Figure 3.4.

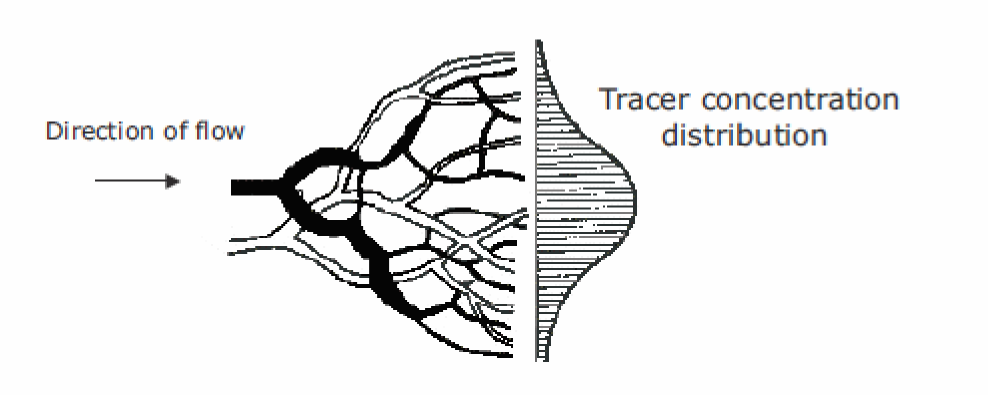

Figure 3.4 Principle of hydrodynamic dispersion (Neri, 2009).

Water with a tracer added if forced through a homogeneous porous medium. The tracer particles spread faster in the direction of the groundwater flow, than perpendicular to it. This is caused by molecular diffusion and mechanical mixing due to mechanical dispersion.

Mechanical dispersion is caused by local velocity differences of the groundwater (Figure 3.5). Velocity of water particles within a porous medium is influenced at pore scale by the soil particles. Due to heterogeneities in soil particle size and pores, the flow velocity of water particles is influenced: Water particles that flows through fine grained soil have limited room to flow through, compared to soil with large grains. Water particles near the soil particles tend to slow down due to friction compared to water particles in the middle of a pore.

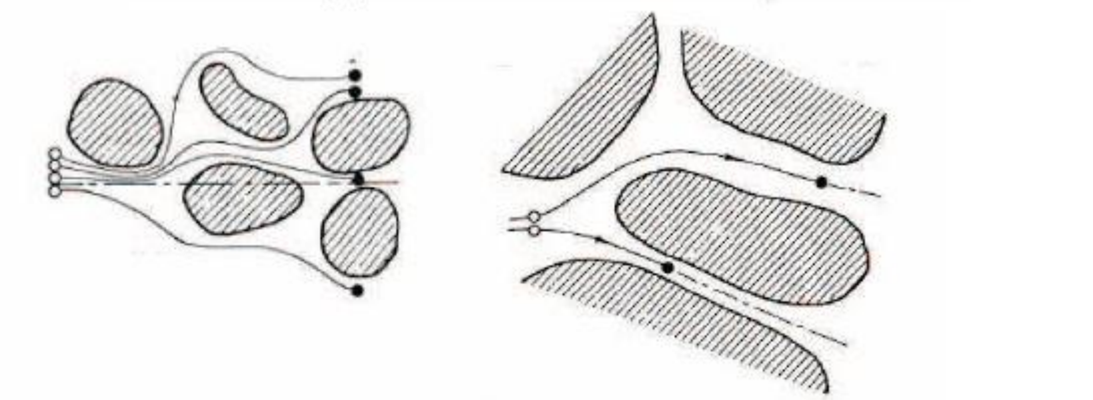

Figure 3.5 Groundwater velocity differences due to pore irregularites (Neri, 2009).

Usually mechanical dispersion is divided in a longitudinal and a transversal component. Quantifying hydrodynamic dispersion is done in combining the mechanical dispersion coefficient and molecular diffusion coefficient through the following Equations [7].

$$D_L = \alpha_L * v_s + D_{diff} \qquad [7]$$
$$D_{T_{y,z}} = \alpha_{T_{y,z}} * v_s + D_{diff}$$

If a Cartesian coordinate system is assumed then: D_L is the longitudinal hydrodynamic dispersion in direction of the groundwater flow in the x direction [m^2s^{-1}]; α_L is the longitudinal dispersivity in the x-direction [m]; D_{T_y} is the transversal hydrodynamic dispersion in the y-direction [m^2s^{-1}]; α_{T_y} is the transversal dispersivity in the y-direction [m]; D_{T_z} is the transversal dispersivity in the z-direction [m^2s^{-1}];; α_{T_z} is the transversal dispersivity in the z-direction [m] ; D_{diff} is the molecular diffusion coefficient [m^2s^{-1}].

3.2 Thermal energy transport in porous media

For thermal energy transport through porous media, infiltration of hot water is considered. Initially the water and the soil grains have the temperature of the ambient groundwater. When hot water infiltrates the aquifer, the soil grains are surrounded by this hot water. The thermal energy of the water is transferred to the soil grains through conduction and the soil grains take over the temperature of the infiltrated water. Because the water surrounds the grains quickly and the grains have a negligible volume, this heat transfer process is considered instantaneously. An infiltrated volume of water through a filter screen has a cylindrical shape. The influence radius of an infiltrated volume of water can be determined through Equation [8]:

$$r_{volumewater} = \sqrt{\frac{V}{\pi H}} \quad [8]$$

Where $r_{volumewater}$ is the radius of the cylindrical volume of water [m]; V is the infiltrated volume of water [m^3]; H is the length of the filter screen of the well [m]

This considers however only the volume of water. In order to achieve the influence radius of the water that is distributed over the aquifer, the effective porosity is used in Equation [9]:

$$r_{waterinaquifer} = \frac{\sqrt{\frac{V}{\pi H}}}{n_e} \quad [9]$$

Where $r_{waterinaquifer}$ is the influence radius of water distributed over the aquifer [m]

This radius considers the volume with both water and soil grains.
It is necessary to establish how the thermal energy spreads over the soil grains and the water (i.e. what is the thermal influence radius of the affected soil grains ?). In order to do so, the volumetric heat capacity is used. The volumetric heat capacity is the specific heat capacity multiplied by the density of the medium through Equation [10]:

$$C_m = c_m \rho_m \quad [10]$$

Where C_m is the volumetric heat capacity of a medium [J*$m^{-3}C^{-1}$]; c_m is the specific heat capacity of a medium [J$kg^{-3}C^{-1}$]; ρ_m is the density of a medium [kg*m^{-3}].
The volumetric heat capacity is a measure of how well a volume of a certain medium can store thermal energy.

The volumetric heat capacity for of the affected volume is determined with using effective porosity and the volumetric heat capacity of the soil grains and water through Equation [11]::

$$C_a = n_e C_w + (1 - n_e) C_r \quad [11]$$

Where C_a is the volumetric heat capacity of the aquifer [2,5*10^6 J*m^{-3}*K^{-1}]; C_w is the volumetric heat capacity of the water[4,2*10^6 J*m-3*C^{-1}]; C_r is volumetric heat capacity of the soil grains [1,77*10^6 J*m^{-3}*C^{-1}] (Tauw, 2009).

The ratio between the volumetric heat capacity of water and volumetric heat capacity of the aquifer yields the thermal influence radius of influence through Equation [12]::

$$R_{th} = \sqrt{\frac{C_w V}{C_a \pi H}} \qquad [12]$$

3.3 Conclusions theoretical background

In getting grip on how infiltrated and extracted water volumes alter the temperature distribution within the subsurface, a correct representation of the thermal influence radius is crucial. The time dependent volume that is pumped in a time step is the predominant parameter that affects the thermal influence radius. This volume is determined through the energy demand (Section 5.2). These volumes can be of an order of magnitude 100-1000 times greater those of the filter length and the ratio between the volumetric heat capacities. Due to heterogeneities and isotropy in the subsurface, the effective porosity, linear groundwater flow velocity and the volumetric heat capacities differ locally in the aquifer where the ATES system is installed. Local differences or inaccuracies in these chosen parameters thus have a significant smaller influence on the thermal influence radius than the time/energy dependent volume based on the energy demand.

4 Site description Achmea

In building the analytical Excel model, information about the local conditions, soil properties and energy demand is essential. The next Section focuses on the description of the site at Achmea. The features described in the following Sections are: Subsurface characteristics, groundwater flow characteristics, system characteristics and the energy demand for ATES at Achmea.

4.1 Subsurface characteristics

The following Section incorporates a detailed description of the subsurface characteristics of the subsurface at the location of Achmea Apeldoorn.

4.1.1 Geological features

Veluwe

The Veluwe is a nature reserve, dominated by glacially uplifted hills, called moraines. These moraines emerged during the pre-last ice age, during the Pleistocene, where unstratified glacial sediment was pushed by the glaciers front into piles and ridges. The deformation caused by glacial activity causes the local subsurface to be strongly impelled (De Vries, 2007). The different formations within the subsurface of the Veluwe therefore are highly tilted, causing an increased hydraulic gradient, which results in high groundwater flow velocity.

The different formations in the subsurface below Apeldoorn are visualized in the REGISS II profile (Figure 4.1). This cross section is composed via interpolation of different well logs over a larger area.

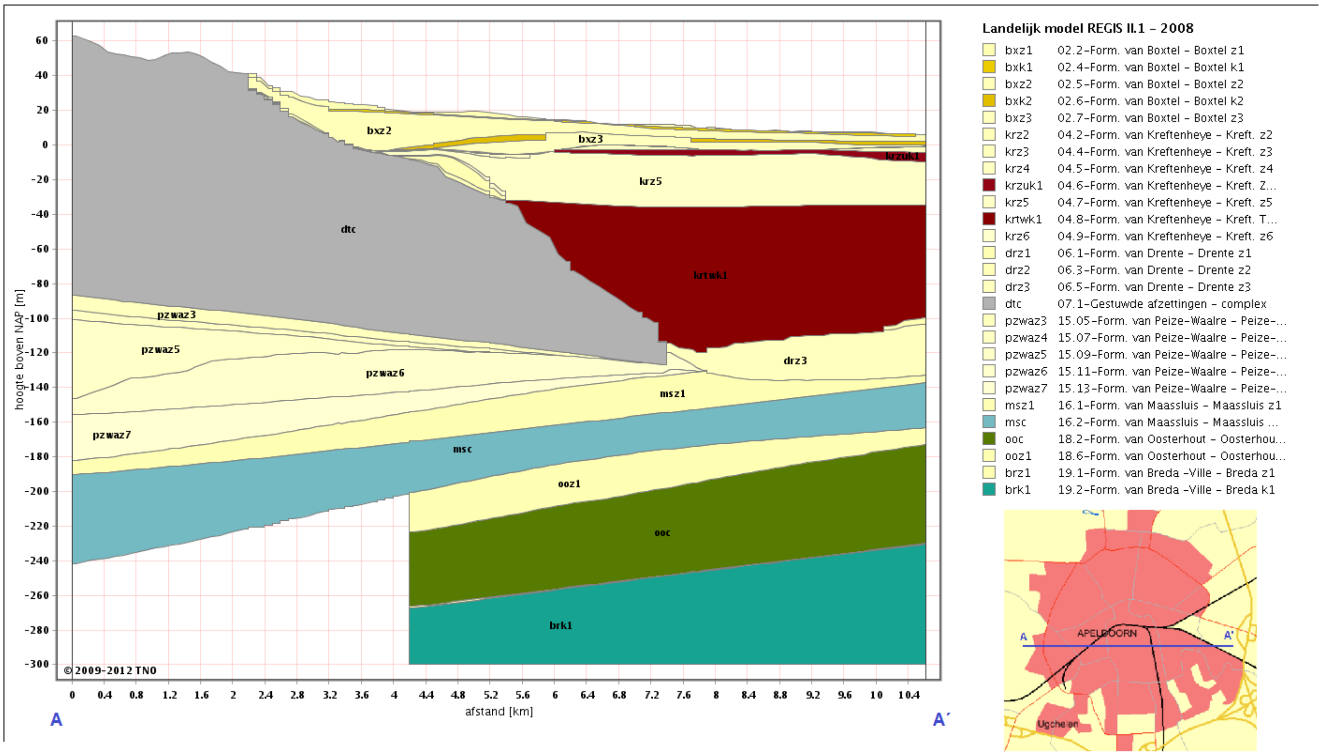

Figure 4.1 Formations below the city of Apeldoorn provided by REGIS (TNO, 2008).

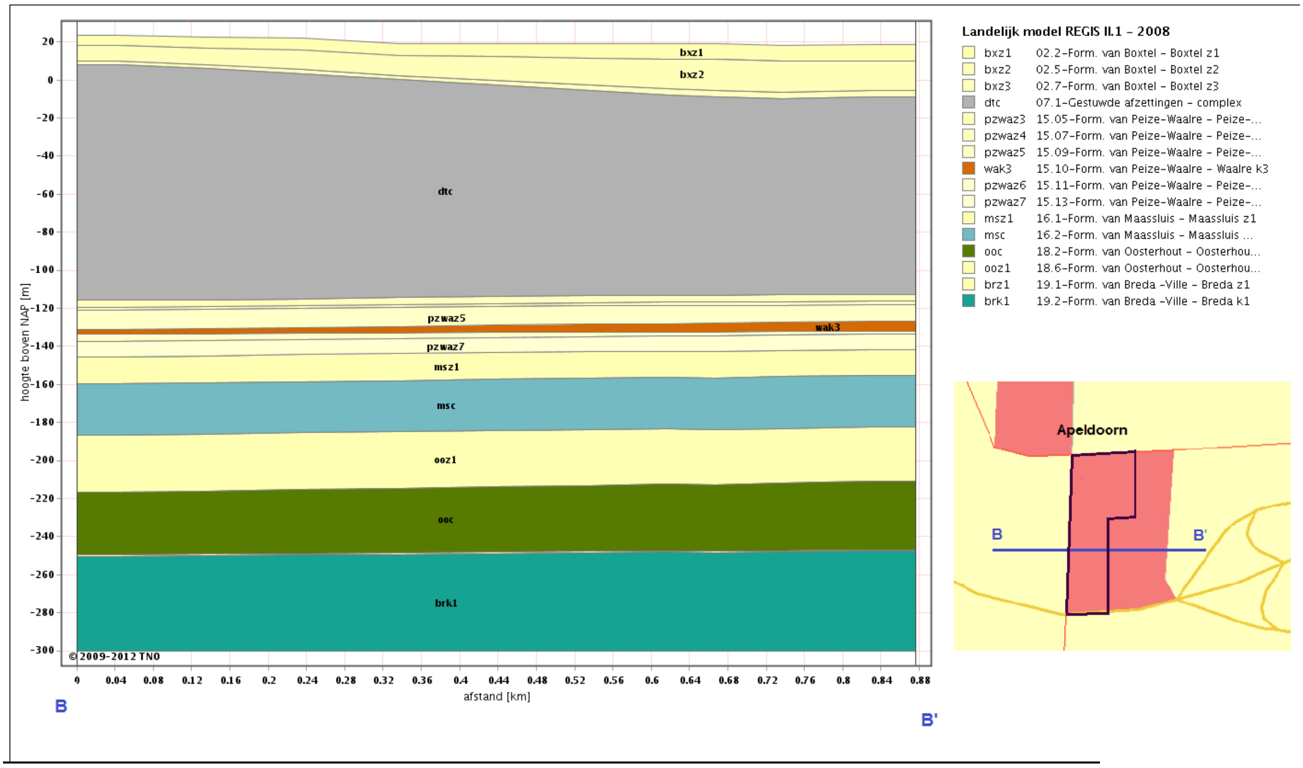

Figure 4.2 Formations in the subsurface of Achmea Apeldoorn provided by REGIS (TNO, 2012).

Combining the REGIS II cross section with several well-logs by (www.dinoloket.nl), and the research regarding the different lithologies, lead to the schematization of the subsurface below the ATES which forms the basis for specific filter locations (Table 4.1).

Table 4.1 Subsurface characteristics

Depth [meters below ground level]	Composition	Geohydrological unit
0-3	Sand	Cover layer
3-25	Sand	Aquifer 1A
25-45	Sand	Aquifer 1B
45-120	**Sand**	**Aquifer 2**
120-140	Clay	Impermeable Layer 2
140-155	Sand	Aquifer 3A
155-160	Clay	Impermeable layer 3A
160-200	Sand	Aquifer 3B
> ca 200	Clay	Hydrological Basis

The ground level at Achmea Apeldoorn is 19 meters above N.A.P. (Dutch reference datum).

The ATES system of Achmea is installed in Aquifer 2 which for the most part consists of the impelled formation of Drenthe (TNO, 2009).

The impelled formation of Drenthe

The geological formation consists of glacial and periglacial deposits from the Saalian period within the Pleistocene. The deposits are mainly related fluvioglacial events where they were deposited by melt water rivers, or from glacio-lacustrine deposits where they were deposited by glacial lakes. Due to glacial movement, the depositions of the Drenthe formation are heavily impelled. The dominant lithologies are:

- Sand, average to very coarse grain size (210 – 2000 μm), weak to strong gravel contents.
- Clay and loam layers, average to strong silt content, of grey-blue to brown-grey color.
- Silty sand layers, fine to average grain size (150-210 μm), of grey-blue to brown-grey color, with locally gravel, rocks and boulders.
- Clay, limited to average silt content, very fine layered (cm-mm), of grey to brown color.

A detailed description of all the geological formations in the subsurface below the ATES system of Achmea is described in Appendix 1

4.2 Groundwater flow characteristics

The next Section gives a detailed description of the groundwater flow characteristics within the subsurface at the location of Achmea Apeldoorn.

Horizontal flow

The natural groundwater temperature at Achmea is approximately 10 °C (Achmea, 2008). Based on the Digital groundwater maps of the Netherlands (hydraulic head and transmissivity, and thickness) (Appendix 2), and drilling core descriptions of the subsurface at Achmea (Bam, 2011) (Appendix 3) the hydraulic conductivities (K_x) and hydraulic gradients $(\frac{\Delta h}{\Delta s})$ for geohydrological units are determined (Tauw, 2009). The total porosity of sand (middle to coarse) is 0,4 (Vereniging voor Landinrichting & Elsevier, 2000). Because no porosity data of the subsurface at Achmea is available, the effective porosity is assumed to be 0,3. The groundwater flow calculations in the following Sections are based on the effective porosity. The horizontal groundwater flow velocity is calculated using Darcy's law. The linear groundwater flow velocity differs for the geohydrological units is shown in
Table 4.2.

Table 4.2 Parameters of hydrogeological units

Hydrogeological Unit	Hydraulic head [meter below ground level]	Direction of flow	Hydraulic conductivity [m/d]	Hydraulic gradient [-]	Groundwater flow velocity [m/y]
Aquifer 1A	2	E-NE	25	$3*10^{-3}$	91,3
Aquifer 1B	5	E-NE	25	$3*10^{-3}$	91,3
Aquifer 2	**5**	**E-NE**	**30**	$\mathbf{1*10^{-3}}$	**36,5**
Aquifer 3A	6	E-NE	60	$8*10^{-4}$	58,4
Aquifer 3B	-	E-NE	10	-	-

The average linear groundwater flow velocity concerning the aquifer in which the ATES system of Achmea is installed, is 36,5 meters per year.

Vertical flow

The head difference
Table 4.2) between Aquifer 2 and Aquifer 3A is 1 meter. The resistance of impermeable layer 2 (Table 4.1), however is circa 3000 days (Appendix 3). This yields a minimal influence of infiltration from Aquifer 2 to Aquifer 3A. This is the only head difference that could result in interference of the groundwater flow in the aquifer in which the ATES system is positioned (Aquifer 2).

4.3 System characteristics and energy demand

The next Section gives a detailed description of the ATES system features at Achmea Apeldoorn and the energy demand.

4.3.1 Location of wells

The wells of the 2 doublets are positioned as shown in (Figure 4.3).

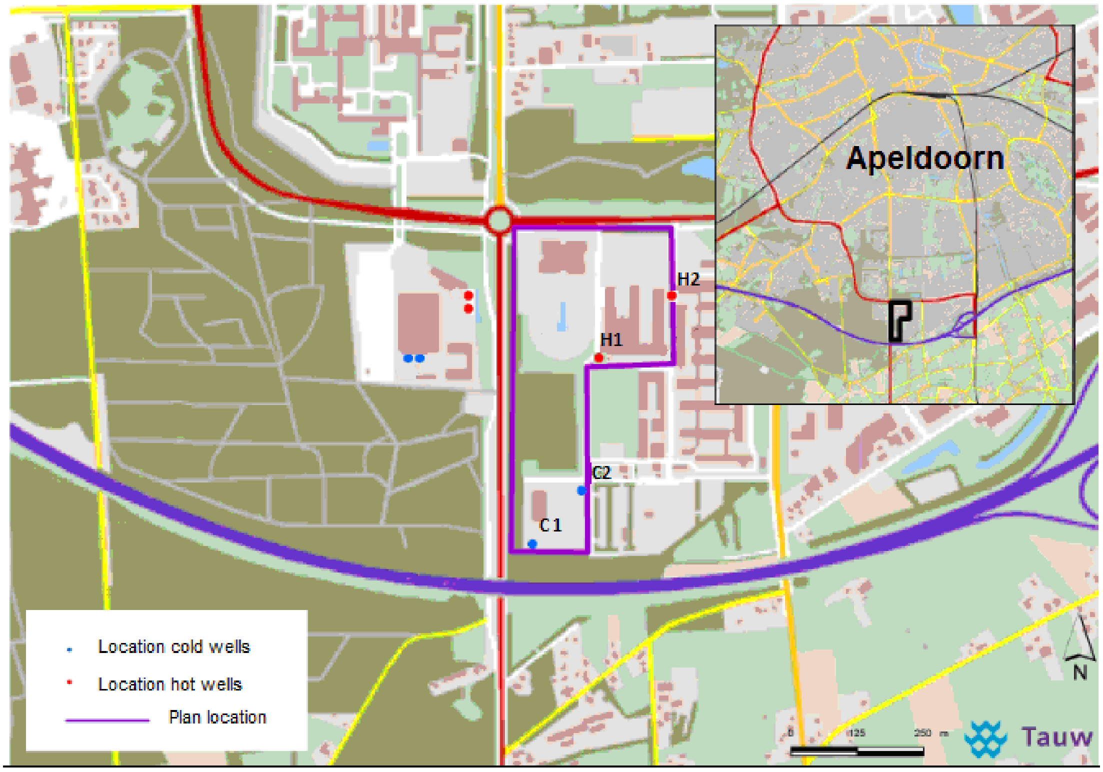

Figure 4.3 The Campus Achmea with the well locations of the ATES system (TAUW, 2009).

The distance between the 2 hot wells is 205 meters and the distance between the cold wells is 165 meters. In a doublet the hot and the cold well are positioned in the same aquifer. Mixing of the injected cold and hot water must be avoided considering potential energy waste. The method to determine the minimum distance between the hot and the cold well is described in Appendix 4.

Locations of wells in the subsurface

The filter screens of the 4 wells are located in the subsurface as presented in Table 4.3 and Appendix 3.

Table 4.3 Well locations in the subsurface.

Well	Depth (meters below ground level)	Lateral distance between wells (m)
Hot well 1	71-91 100-120	205
Hot well 2	94-134	
Cold well 1	77-117	165
Cold well 2	77-92 97-121	

The second cold well and the first hot well both consist of 2 pieces. This is done because of the occurrence of clay layers which disable infiltration or extraction. The top of the second hot well filter is positioned approximately 25 meters deeper that the top of the first hot well. This is done because the drilling core descriptions (Appendix 3) showed that the redox-boundary at location for hot well 2 lies significantly lower than the boundary for hot well 1. The redox-boundary is the boundary that marks the transition from oxygen rich to oxygen poor water. When an ATES system is installed so that it intersects this transition, both oxygen rich and oxygen poor water is extracted through the wells and get mixed. This mixing will cause precipitation of iron in the wells and increases the clogging risk. Therefore the ATES system must be installed either completely above or completely below this boundary.

Buildings

A schematic overview of the expanded campus of Achmea is presented in Figure 4.4.

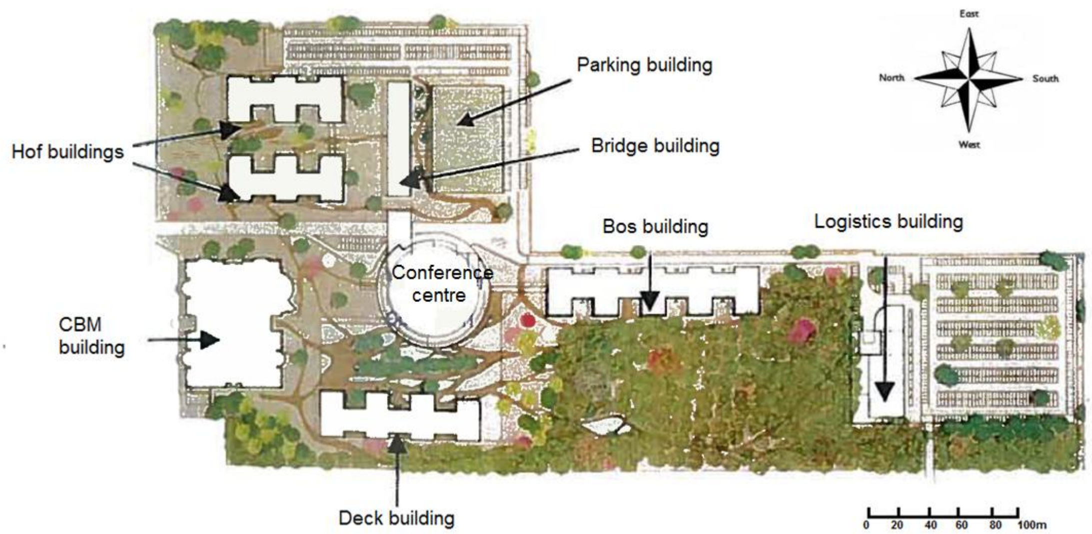

Figure 4.4 Campus of Achmea.

4.3.2 Energetic requirements and discharge

The two doublets of the ATES system must meet the energy demands of the buildings on the Achmea campus. The energetic requirements and corresponding discharge rates are listed in Table 4.4.

The condition that the ATES system has an overall neutral thermal energy balance is met for Achmea Apeldoorn. The permit is requested for an annual total water demand of 1.000.000 m^3.

Table 4.4 Energetic requirements and discharges

Winter period – Hot energy demand	
Power	1664 KW_{th}
Yearly heat demand	2933 MWh_{th}
T Design temperature supply	13 °C
T Design temperature retour	7 °C
Maximum groundwater discharge	236 m^3/h
Total water demand (averaged over a half year)	422.000 m^3
Summer period – Cold energy demand	
Power	2438 KW_{th}
Yearly heat demand	2933 MWh_{th}
T Design temperature supply	11 °C
T Design temperature retour	17 °C
Maximum groundwater discharge	236 m^3/h
Total discharge (averaged over a half year)	422.000 m^3
Difference in thermal balance	
Difference in hot and cold energy demand	0 MWh_{th}
Difference in water demand in summer and winter	0 m^3

(Tauw, 2009)

Initially all the buildings on the Achmea Campus would be connected to the system. In the final stage of the ATES development process it is decided that 2 buildings (Hof buildings and the Bridge buildings) were not going to be built so their energy demand need not to be taken into account. Therefore the total yearly energy demand, which is used in calculations in following

Sections, is multiplied by factor $\frac{2}{3}$, resulting in an energy demand of 1966 MWh both for heating and cooling. The monthly energy demand is more comprehensively explained in Chapter 5.

Hot infiltration temperatures of 17 °C are often not established after cooling within ATES systems. In the calculations in following Sections the infiltration temperature in the hot well is therefore set at 13 °C and the temperatures that will supply the cold energy demand are taken to be the retour temperature from the hot energy demand (7 °C).

4.3.3 Well properties

The well properties for each of the 4 wells in the ATES system are described in Table 4.5. These properties are important because the depth from where the filter screen of a well is installed defines the specific location where the hot or cold water enters in the subsurface. The shape of the infiltrated water body depends on the length of the filter screen and the amount of water that is infiltrated or extracted.

Table 4.5 Well properties

Property	
Maximum designed Darcy speed on borehole	0,96 m/h
Maximum extraction or infiltration rate per well	175 m^3/h
Doublet	2
Wells	4 (2 hot, 2 cold)
Designed filter length per well	50 m
Diameter borehole	1,16 m
Borehole radius	0,58 m
Diameter filter	0,6 m

(Achmea, 2008).

The formulas that are used to determine the maximum designed Darcy speed on the borehole, the filter length and diameter of the borehole are explained in Appendix 4

The drilling state (Appendix 3) showed that the majority of the sand in the aquifer at well locations has favorable conditions (i.e. grain size diameter > 250 µm). Therefore it is decided in the realization phase of the system, that instead of 50 meters filter screen per well, 40 meters filter screen per well is installed, which still enables the maximum infiltration and extraction rates, but which reduced the drilling costs.

4.3.4 Additional devices in the ATES system

To increase the temperature of the water that is extracted from the hot well a heat pump is used. The groundwater is chemically different than the water that runs through the heating and cooling circuits of the buildings. This water therefore should not enter these circuits. To establish this, a countercurrent heat exchange device is used. A detailed description of the heat pump and the countercurrent heat exchange device is given in Appendix 5.

4.3.5 System Management of ATES

The temperature outside the building influences the temperature inside. The temperature inside the building is measured and determines if the ATES system needs to heat or cool. Accordingly hot or cold energy is extracted from the wells to the buildings. The system works most efficient if from the hot well the highest possible temperature, and from the cold well the lowest possible temperature can be extracted (i.e. when ΔT is high). This results in reducing the electrical energy that has to be used by the heat pump. It is important however that the energy stock within the wells is managed. If all the high valuable thermal energy (i.e. highest and lowest temperatures) is extracted in a short period, this can cause problems for efficiently meeting the energy demand in the future. Therefore the energy stock (i.e. the temperatures in the wells) is monitored (Figure 4.5).

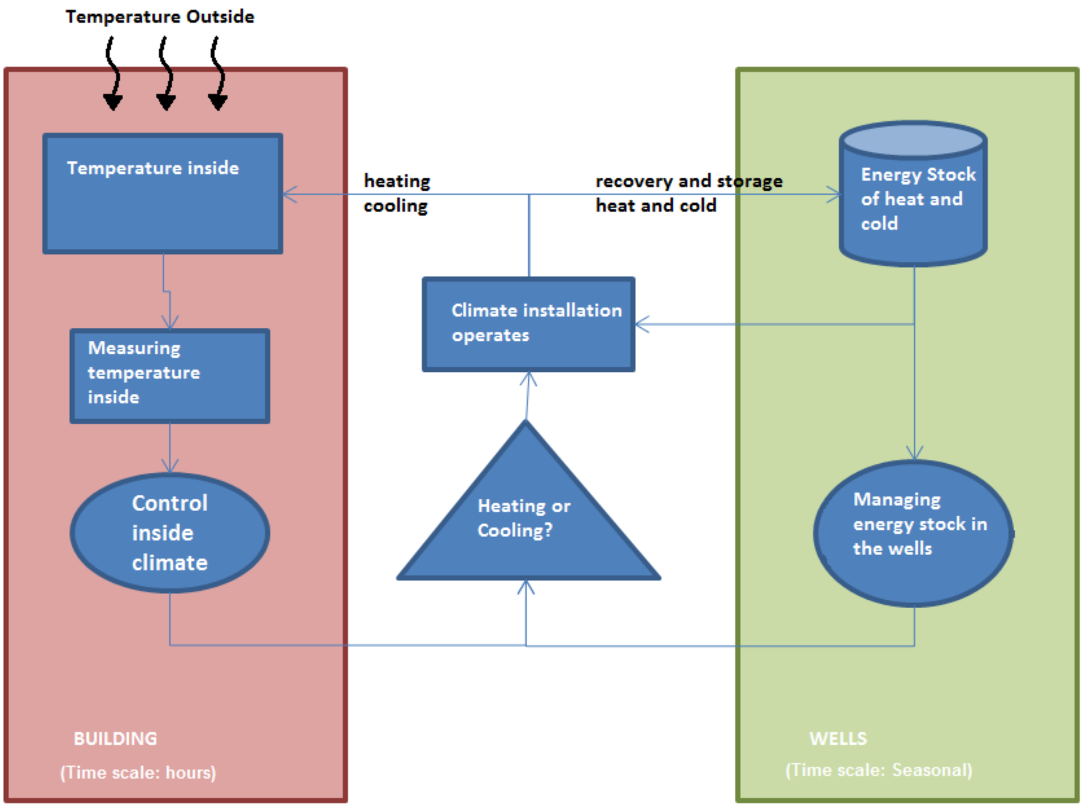

Figure 4.5 System management for an ATES system.

The respectable hot and cold wells are positioned in line with each other, as well as in line with the groundwater flow direction (Figure 4.1). Accordingly, water that is infiltrated in well 1 can be extracted by well 1 but can also be extracted by well 2, when it is transported due to groundwater flow. The wells are positioned in this manner to reduce potential energy loss from the ATES system. The system is able to vary the percentages of infiltration and extraction. This means that it is for example possible to infiltrate 30% of the cold water in cold well 1 and 70% of the cold water in cold well 2.

Current control strategy of ATES Achmea

The current control strategy, with multiple doublets which are positioned in line with each other is to infiltrate and extract, however, with a 50-50 control strategy. This means that the infiltration or extraction rate, desired to fulfill the energy demand, is divided equally over the hot or cold wells. The possibility to change the percentages of infiltration in the different wells is not exploited.

If during peak temperatures (for example: a very cold winter), the energy demand may not be met by the temperatures retrieved from the wells alone (i.e. the heat pumps maximal capacity is exceeded) the system then depends on the conventional boiler for heat supply. This has a negative effect on the efficiency of the ATES system: the SPF decreases.

It is expected that the (50-50) control strategy does not result in the most energy efficient way to operate an ATES system with multiple doublets where groundwater flow velocity is high. In order to limit the use of conventional heating but also preserve energy supply within the wells throughout the year under the influence of peak temperatures outside, smart system management is necessary. The control strategy can be varied by changing the infiltration and extraction rates for the wells for a fixed time step.

5 Temperature transport in the subsurface due to infiltraton and extraction

The groundwater flow differential Equation is simplified to analytical solutions in order to describe the physical processes occurring in the subsurface and concerning ATES. These analytical solutions can be solved in an Excel worksheet. In Excel a boxed-model is created which quantifies the temperatures of groundwater in the subsurface after infiltration or extraction of groundwater. Quantifying the temperature in the subsurface gives insight in if and how much energy is permanently lost from the system. The analytical model is validated with the numerical groundwater modeling program PMWIN.

5.1 Conceptual model

Water infiltrates into the subsurface through the filters screens. The filter screens are of length H [m]. The distance between the wells is length L [m]. The water is distributed in the subsurface in the shape of a cylinder, surrounding the filter (Figure 5.1). The radius r [m] of the cylinder depends on the infiltrated or extracted volume (V_1, V_2 [m^3]) that the system requires to meet the time-dependent energy demand. The groundwater flow causes the infiltrated water from well 1 to flow into the direction of well 2, or when infiltrated in well 2, away from well 2. When the system requires extraction, water within the radius corresponding to extraction volume, is extracted from the aquifer into the filters. In order to create an Excel model which gives a mathematically quantified as well as a visual representation of the ATES system of Achmea, the following simplifications and assumptions are imposed:

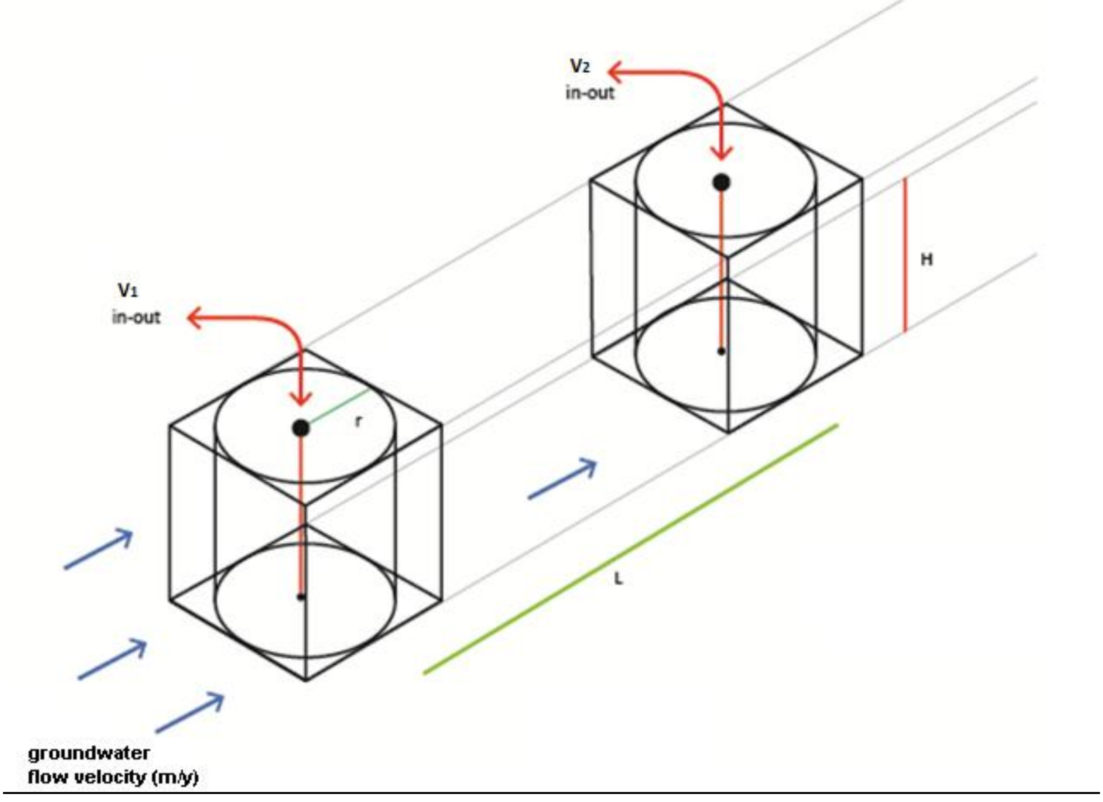

Figure 5.1 Conceptual model.

- Shape of the body of water in the subsurface after infiltration or extraction is not a cylinder, but a cuboid.

  Water with a certain temperature that differs from the groundwater temperature enters the subsurface (at x=0). If water is not extracted within a certain time, the water body with temperature differing from the groundwater temperature is transported in the direction of the groundwater flow after passing of Δt *(Figure 5.2, situation 1). Observed from top-view, if water is extracted within a radius that covers a part of the transported body of water after* Δt *, the overlapping part of the 2 circles is of infiltration temperature, and the rest of the circle is of groundwater temperature (situation 2). The approach to determine the overall temperatures of cylindrical bodies of infiltrated and extracted water is too comprehensive to model accurately in Excel. For this reason the shape of the water body is assured to be a cuboid (Figure 5.1).*

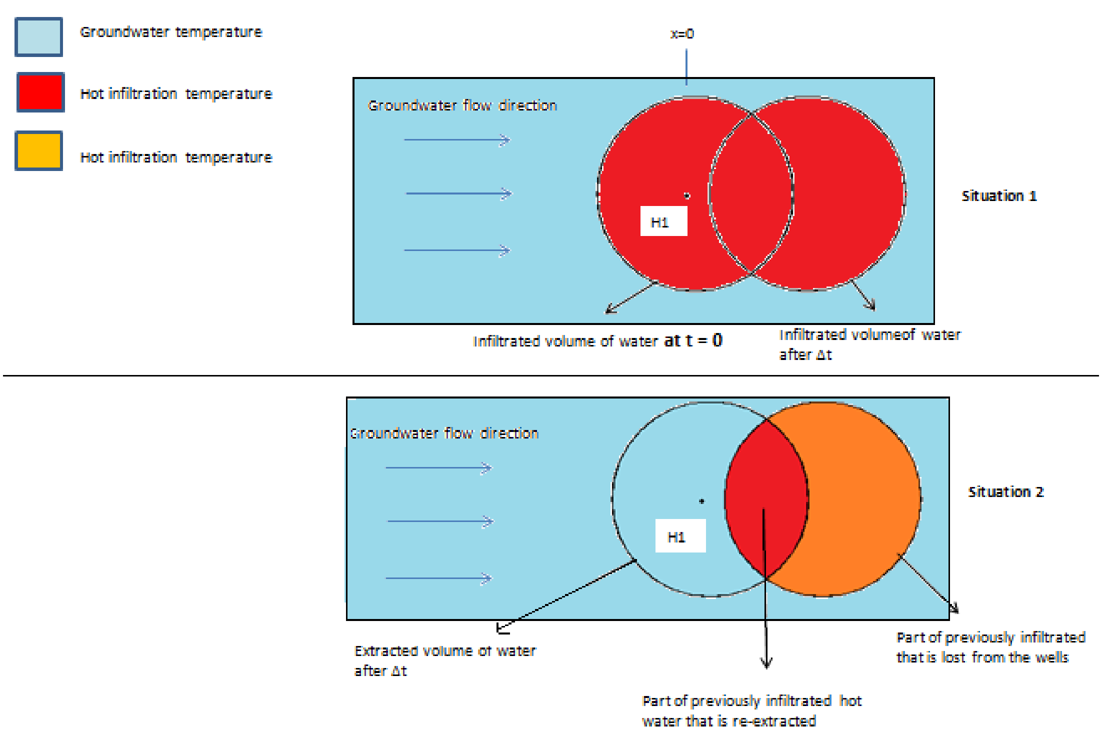

Figure 5.2 Visualisation of proplem for overlapping cylindrical volumes of water.

- The water body in the model is considered 1-dimensional because 2 dimensions (depth and length) of the cuboid are fixed.

  The cuboid has dimensions x, y and z, where Δx_{cub} *is considered the width,* Δy_{cub} *is considered the length and* Δz_{cub} *is considered the height of the cuboid. The volume of the cuboid is equal to the volume of the cylinder. The 4 filters in the 4 different wells are considered to be all of one piece and are positioned at the same depths. This enables water to flow entirely from well 1 into well 2, and thus fixes the* Δz_{cub} *dimension of the cuboid. The length of the cube (*Δy_{cub}*) is also fixed, this means that the shape of the water body is now only dependent on the width of the cuboid, and therefore 1-dimensional (this is more comprehensively explained in the Section 'boxed model'). This results in the neglecting of dispersion effects.*

- Anisotropy

  Because in the previous assumption the spatial dimensions of the problem are reduced to 1 dimension, the horizontal plane, the water volumes are assumed to flow only laterally. This simplification is known as the Dupuit-Forchheimer approximation (Fitts, 2002). This is considered reasonable because even though the large scale geological features within the subsurface at Achmea are impelled, the horizontal layering on the small scale is still strongly evident, limiting flow in the z dimension. Since the water is equally distributed over the cuboid, k_x *is considered equal to* k_y*.*

- Water volumes are infiltrated in, or extracted from subsurface instantaneously per time step. Transport of water due to groundwater flow is also instantaneous.

  Within a certain time period, a certain volume of water is infiltrated or extracted. This is not modeled as a gradual process, but as an instantaneous process, to contribute to simplification of the problem. Because in 1 time step cooling and heating is possible, both effects are modeled in the same time step. Within the same time step the displacement of a volume of water, due to groundwater flow velocity is transported in the boxed model. The size of the time step influences the amount of volume water that is extracted or infiltrated. Therefore this influences the size of Δx_{cub}*. A scaling study is done and in Figure 5.3 is visualized which time dependent processes concern ATES. The appropriate time step size for the Excel model is determined 'months'.*

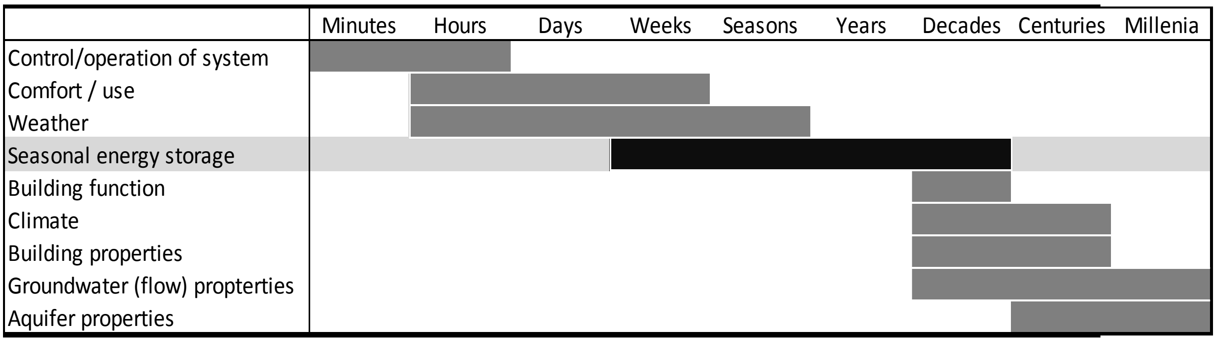

Figure 5.3 Overview of time-dependent processes in ATES.

Any other assumptions that are required for the model to work properly are elaborated in the models Section.

5.2 Analytical boxed-model

The analytical boxed model quantifies the temperatures in the subsurface after injection or extraction and transportation due to groundwater flow through grid cells that contain a certain volume of water with a corresponding temperature. The first action in the model to relate the energy demand of the system in a certain time step with the corresponding extraction and/or infiltration. Once volume of infiltrated or extracted water for a time step is determined its influence on groundwater temperature is quantified in the following three Sections of the model:

- Infiltration
- Extraction
- Transport

The cells that quantify the groundwater temperature are mathematically changed upstream and downstream of the wells after infiltration or extraction, regarding the volume of water that is infiltrated in, or extracted from the subsurface.

Each cell in the box model forms the basis for another cell in the next time step.

5.2.1 Extraction and infiltration rates

The ATES system is designed to provide for a certain yearly energy demand. This energy demand consists of an amount high (for heating purposes) and low (for cooling purposes) thermal energy. This amount of energy is distributed over the amount of time steps that is chosen for the model. The energy amount relates to the extraction or infiltration rate, the specific heat of the groundwater and the temperature difference of the groundwater. This is presented in Equations [13, 14].

$$Q_{\inf,ext} = \frac{P * 3600}{\rho_w c_w \Delta T} \qquad [13]$$

$$V = \frac{E}{\rho_w c_w \Delta T} \quad ` \qquad [14]$$

Where $Q_{\inf,ext}$ is the infiltration or extraction rate [m^3/h]; P is the thermal energy demand [W]; c_w is the specific heat of water [J*kg^{-1} * K^{-1}]; V is the injected or infiltrated volume of water per a given time step [m^3]; E is the thermal energy demand [J]; ΔT is the temperature difference between the water that is extracted and the temperature with which it enters the aquifer again when it returns from the building circuits and is infiltrated [°C].

Because the system consists of 2 doublets, hot or cold energy can be stored in or be extracted from 2 wells, respectively.

Considering for example only infiltration in the cold well for a given month, the total volume of cold water that is infiltrated can be divided over the 2 cold wells with any ratio possible. Within the Excel model, the infiltration rates can be adjusted by varying this ratio, enabling system management. The implementation of dividing total infiltration volumes over the 2 cold wells with any possible ratio is necessary to see the effect of smart system management, opposed to simply splitting the total infiltrating volume so that half of it infiltrates cold well 1, and half of it infiltrates cold well 2 during the same time step, which is the accustomed approach.

Varying this ratio is possible for infiltration and extraction rates, for all 4 wells.

Heating and cooling

If heating and cooling occur within the same time step, this can results in infiltration and extraction for the same well within the same time step. Therefore the net volume that is pumped to meet both high and low thermal energy demands during the same time step is the resulting infiltration or extraction rate which is used in the model; the quantification of temperatures within the subsurface in the Excel model is based on this net infiltration or extraction rate.
When during spring or autumn high and low thermal energy is required within the same month, water is thus being pumped back and forth between the hot and cold wells. Because infiltrated water is extracted within a time span of days/weeks, due to the fluctuating outside temperature, the influence of groundwater flow velocity on the water bodies in the subsurface is assumed negligible.
Whether heating and cooling occurs within the same time step or not, the net infiltration rate must always equal the net extraction rate.

5.2.2 Thermal influence radius

The thermal influence radius of the infiltrated or extracted volume is defined through Equation [12]

This thermal influence radius relates however to the cylindrical volume. The volume of infiltration or extraction of the cylinder is set equal to the volume of a cuboid as shown in the set of Equations [15].

$$\begin{aligned} V_{cyl} &= \pi R_{th}{}^{2} H \\ V_{cub} &= \Delta x_{cub} \Delta y_{cub} \Delta z_{cub} \\ V_{cyl} &= V_{cub} \end{aligned} \qquad [15]$$

Where V_{cyl} is the cylindrical volume of water [m3]; V_{cub} is the cuboid volume of water [m3]; $\Delta x, y, z_{cub}$ are the dimensions of the cuboid volume of water [m]

In Section 5.1 is determined that the dimensions $\Delta y_{cub}, \Delta z_{cub}$ are fixed, to assure a 1-dimension dependent model. This means that with a changing energy demand, infiltrating of extracted volume will change, and this is only visible through a change in Δx_{cub}. This 'Δx_{cub}' is called the width of cuboid volume of infiltrating or extracted water

5.2.3 Boundary conditions and discretization

The cells in the boxed model are cuboid cells which have a fixed volume with a certain temperature. The grid dimensions of the cells ($\Delta x_{grid,} \Delta y_{grid}, \Delta z_{grid}$ [m]) can be increased or decreased which changes the accuracy of the model and corresponding quantification of the thermal distribution in the subsurface.
To ensure that the infiltrated or extracted volumes of water 'fit' nicely in the grid of the Excel model the following rule applies in the model through Equation [16]:

$$\begin{aligned} \Delta y_{grid} &= \Delta y_{cub} \\ \Delta z_{grid} &= \Delta z_{cub} \end{aligned} \qquad [16]$$

Which means that any influence of infiltration or extraction is still only dependent on Δx_{cub}.

Well locations, boundaries and width of grid cells with respect to the x-dimension

From a spatial point of view there can be considered three regions within the excel model:

- The grid cells upstream of hot/cold well 1
- The grid cells between hot/cold wells 1 and 2
- The grid cells downstream of hot/cold well 2

The width of the grid cells upstream of the wells is called Δx_{grid_left}

The width of the grid cells between wells is called Δx_{grid_middle}

The width of the grid cells downstream of the wells is called Δx_{grid_right}

In the excel model, there are 8 grid cells between the wells. Therefore the width of Δx_{grid_middle} is given by Equation [17]:

$$\Delta x_{grid\_middle} = \frac{L}{8} \qquad [17]$$

Where L is the lateral distance between hot/cold well 1 and hot/cold well 2.

Δx_{grid_left} and Δx_{grid_right} are set in the same order of magnitude [25 m]

Boundaries

For the system of ATES Achmea it is not reasonable to expect Δx_{cub} to exceed 100 meters for a given time step. This will cause exceeding of the maximum hourly pumping capacity of the system (Table 4.3). Therefore boundaries are set at 100 meters (4 grid cells) upstream of well 1 and 100 meters downstream of well 2. If infiltration or extraction, however, does cause Δx_{cub} to exceed this length, the calculations within the Excel model considering adjacent cells will become very complex. A simplification of the math concerning exceeding of these boundaries will be more comprehensively explained in the detailed model description.

5.3 Principle of temperature quantification within the grid cells

The temperature quantification within the grid cells that combine establish the temperature distribution in the subsurface, is divided in the Sections ‘Infiltration’, “Extraction’ and “Transport’.

In the infiltration Section, the volume of infiltrated water enters the grid at the location of the wells, and pushes the water that was initially located in the grid to the left and right.

In the extraction Section, the volume of extracted water exits the grid at the locations of the wells, and the water that was initially located in the grid adjacent to this water volume, shifts in the direction of the wells.

In the transport Section, the water distribution after infiltration or extraction is shifted to the right, due to groundwater flow velocity.

Determination of the temperature within a single grid cell is based on the weighted average of water volumes with a different temperature, which may have entered other grid cells due to infiltration, extraction or transport.

The quantification of temperature for the three different Sections is extensively described in Appendix 6.

Qualitative check

Within the model, after implementation of the yearly energy demand, the temperature of the grid cells all are within the range of 7°C – 13 °C, the volumes that are infiltrated and extracted are of the same order of magnitude as monthly rates would be according to Table 4.4, and the temperature distribution is properly visualized, so the model extent is of sufficient size.

5.4 Analytical model validated with numerical solution

In order and validate the analytical Excel model, the subsurface characteristics, groundwater flow characteristics, well locations and time dependent infiltration or extraction rates are simulated in the modeling code Processing Modflow for Windows (PMWIN). This is a simulation system for modeling groundwater flow and transport processes with modular three-dimensional finite-difference groundwater model. Two modules are used in PMWIN: Modflow, and MT3D. Modflow models the groundwater flow, and head distribution after injection and infiltration of water, and MT3D models the temperature distribution after injection or extraction of water with different temperatures. There are 7 layers in the PMWIN model. They represent the top 5 layers from Table 4.1. The layers below the 5th layer from Table 4.1 are not relevant due to impermeable character of layer 5 and are thus neglected. The layer that represents aquifer 2 however is divided in 3 parts, because in the a distinct layer is needed positioning of the wells. The middle part (layer 5) therefore is exactly 40 meters deep. The chosen parameters in for Modflow and MT3D are described and justified in Appendix 7.

The analytical model is considered a valid model if its temperature quantification and distribution corresponds to the results presented by the numerical model when the same input is used.

The excel model is validated through comparing the results of two scenarios in Excel with the results from PMWIN.

In the first scenario it is validated how well the Excel model simulates the temperature transport under influence of groundwater flow, and in the second scenario is validated how well the excel model simulates the temperatures within wells when a variety of infiltration and extraction is simulated.

Scenario 1

The scenario that is used in Excel and PMWIN considers only hot well 1 and simulates 10 years. For the first 12 months, it infiltrates water of 13°C constantly with 1000 m^3/day. After the infiltration period of 1 year, the system is shut down, and the temperature in the subsurface is monitored for the next 9 years. It is chosen to simulate for 10 years, because the influence of groundwater flow is more apparent after 10 years than after, for example after 1 year. The numerical visualization of how the high temperature water body travels through the subsurface is presented in Figure 5.4. The distance traveled by the plume is taken as: The distance from hot well 1, to the left boundary of the traveled high temperature water body.

This boundary is taken where the water has the infiltration temperature minus 0,5 °C (i.e. 12,5 °C). This is considered the transition boundary from high temperature infiltrated (13°C) water to ambient groundwater temperature (10 °C). This transition takes place at x = 277 meters right of hot well 1. The cell left of the target cell has temperature of 12°C so at x = 277 meter the temperature is approximately 12,5°C.

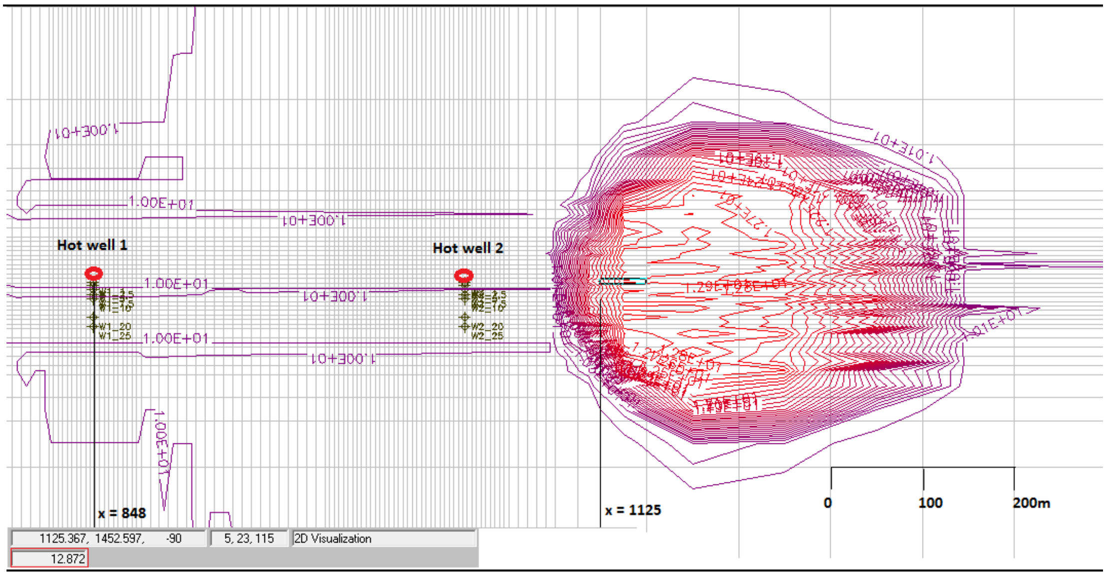

Figure 5.4 High temperature body displacement in PMWIN.

The temperatures in the subsurface at are quantified in the Excel model. The temperatures at x=280 meters from the hot well is presented in Figure 5.5. The shape of the curve represents the movement of the high temperature water body through the subsurface due to groundwater flow. At t=120 (10 years) the temperature is approximately 12,5 °C.

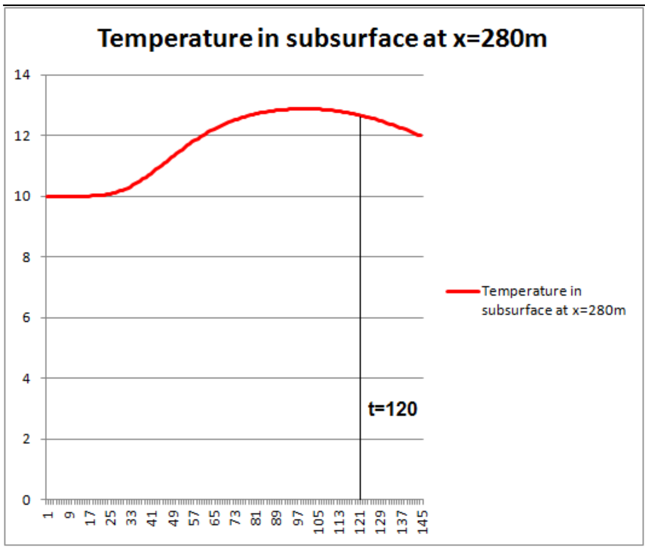

Figure 5.5 Temperature in the subsurface at x=280 meters, for the analytical Excel model.

Scenario 2

The second scenario simulates use of all 4 wells with varying infiltration and extraction rates throughout a period of 10 years. The infiltration and extraction rates result from the annual energy demand which is described in Section 4.1, and visualized in Section 6.1. The difference between the temperatures in the wells for the Excel model and PMWIN is visualized in Figure 5.6.

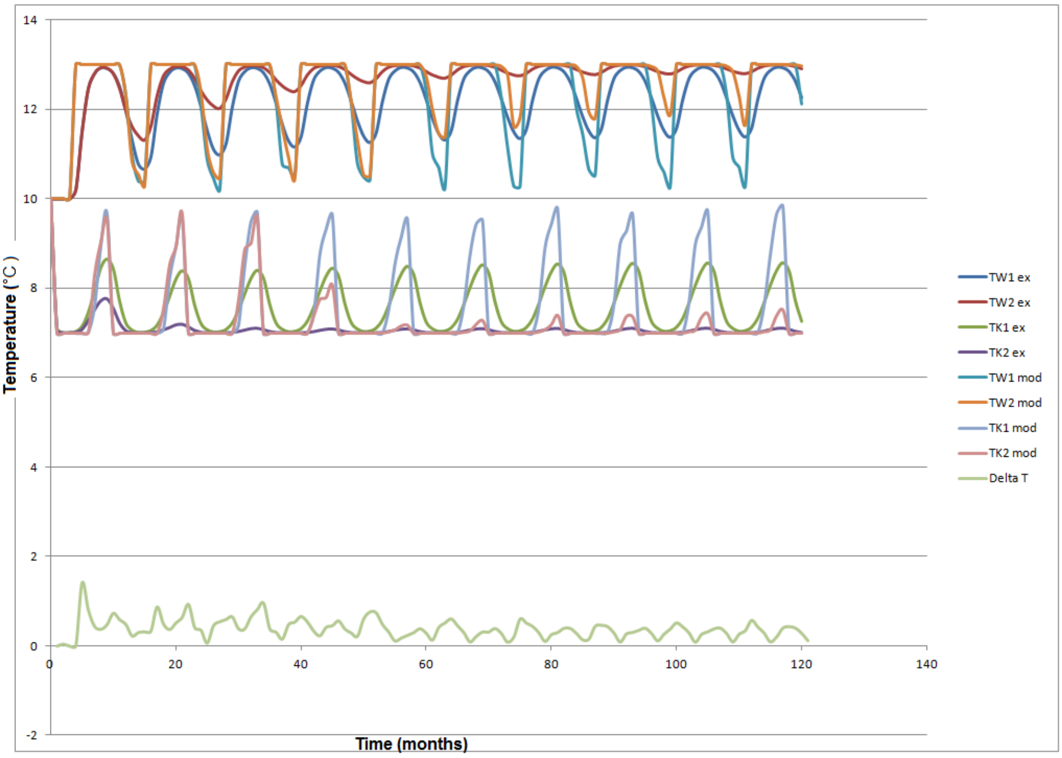

Figure 5.6 Temperatures within wells compared for Excel and PMWIN Modflow.

The temperatures for Excel and PMWIN show the same pattern throughout the 10 years. The average temperature difference between Excel and PMWIN is 0,38 °C per month for their corresponding measuring points. In excel the grid cells are order of magnitude 1000 smaller ($\Delta x, y, z_{grid}$ in Modflow is 2,5 * 2,5 * 2,5 meters). Therefore temperature changes are less gradual in the Modflow model, which increases the difference between measured temperatures. The value of 0,38 °C temperature difference therefore is considered acceptable.

Combining that for groundwater transport with a not complex scenario (1) the temperatures at a certain measuring point (x=280) coincide, and that for implementation of a relative complex scenario (2), the average temperature difference within wells per month is only 0,38 °C, it is concluded that the Excel model thus quantifies the temperature distribution within the subsurface quite accurately.

6 Defining control strategies through optimization

In this Chapter is explained how optimization of the infiltration and extraction rates has led to the an ‘improved control strategy’.

6.1 Control Strategies

Through Equation [20, 21] the infiltration and extraction rates are determined by the analytical Excel model. The energy demand for one year is expected to be equal annually. This implies that the yearly average outside temperature distribution throughout the year is expected to be the same. The way the energy demand of 1955 MWh (Section 4.3.2) for both heating and cooling per year, is distributed over the months, is presented in Figure 6.1.

	Hot KWh	Cold KWh
January	325889	333
February	325889	333
March	195533	130689
April	97767	228456
May	32589	293633
June	333	325889
July	333	325889
August	333	325889
September	130689	195533
October	228456	97767
November	293633	32589
December	325889	333

Figure 6.1 Annual energy demand distribution.

6.1.1 Accustomed approach

The control strategy that is implemented in the ATES system of Achmea is that the infiltration and extraction rates are divided over the 2 hot and the 2 cold wells equally. This is called the ’50-50 control strategy’ (Section 4.3.5).

The ratio (depicted as a percentage below) that defines what amount of the volume is infiltrated or extracted enters which well, is 0,5 for the ’50-50 control strategy’. This occurs for every month of the year and is presented in the following manner:

	H1 ex	C1 Inf	H1 Inf	C1 ex
January	50,0%	50,0%	50,0%	50,0%
February	50,0%	50,0%	50,0%	50,0%

Experience tells that this control strategy is operated in most other multiple doublet ATES systems. It is expected that optimization of these ratios results in a higher energy efficiency for the system. Therefore the '50-50 control strategy' is the reference control strategy against which the results of the optimized control strategies will be compared to.

Energy loss

The temperature of the cells 100 meters laterally right of the second hot and cold well is used to determine the thermal energy loss from the system. Water that has passed that point is stated to be irretrievable by the wells. Therefore the energy that is within these cells is considered to be lost from the system. Through Equation [20, 21] the energy loss per time step is quantified. This energy loss is expressed in Euro's through:

Price of gas:	0,6711 Euro/m^3 gas (www.Eneco.nl 3 year contract)
Price of electricity:	0,2262 Euro/kWh (www.Eneco.nl 3 year contract)
kWh/m^3 gas:	9,4072 (www.warmtepompforum.nl)

When the Excel model simulates the energy demand from Figure 6.1 for 20 years with the '50-50 control strategy' the temperature in the wells and energy loss is represented by Figure 6.2.

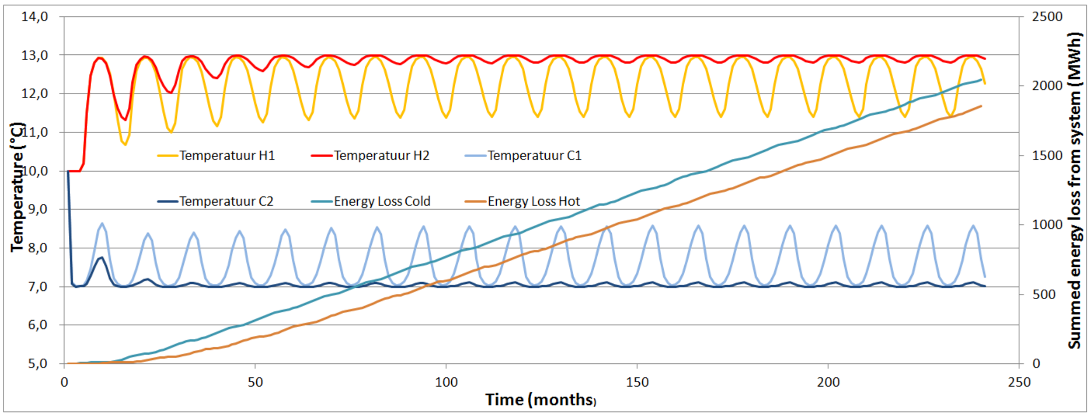

Figure 6.2 Temperatures in wells and energy loss from system.

When the '50-50 control strategy' is applied it takes approximately 3 years for the second hot and cold well to be completely surrounded by water with the infiltration temperature. Because thermal energy that is not extracted from the first hot and cold well flows away and enters the extraction range of the second wells, the temperature fluctuations in the second hot and cold well are relatively small. The temperature fluctuations in the first hot and cold well are higher because the infiltrated energy is extracted after a half year, and the first wells are not replenished with thermal energy due to groundwater flow, like the second wells.

Because the simulation starts in January (during winter) there is a hot thermal energy demand. This results in extraction of groundwater with the ambient temperature (10 °C) and infiltration of cold water. Because infiltration of cold water occurs before infiltration of hot ground water, more cold thermal energy is relatively lost from the system. This effect is enhanced by the fact that the cold wells lie closer to each other. The cold wells range in which thermal energy can be held is thus smaller, which means that at a constant groundwater flow velocity thermal energy loss is higher measured from a fixed point for the cold wells than for the hot wells.

6.2 Optimizing the ’50-50 control strategy’

In order to find a successful control strategy, first the boundary conditions for the model and the solver options for optimization are explained. Then 3 optimization strategies with their corresponding focus are explained. In order to decide if a resulting control strategy is in fact successful the control strategy itself and its results are tested with a set of assessment criteria. After assessment of the resulting control strategies, it is determined if a successful control strategy is achieved.

6.2.1 Boundary conditions in the analytical Excel model and solver options

- The simulation time is 20 years
- The average width of Δx_{cub} of all the infiltrated and extracted volumes can be changed by changing Δy_{cub} (which equals Δy_{grid}) . Preferably the average Δx_{cub} equals Δy_{cub} because this yields the cuboid which resembles the cylindrical volume the most. Through iteration the Δy_{cub} is found to be 28m for the ’50-50 control strategy’. This width is maintained in optimization for a fair comparison.
- The improved control strategy is not applied all 20 years. The first 3 years, the 50-50 control strategy is applied, after that, the following 17 years, the improved control strategy is applied. This is done to prevent very high infiltration and extraction rates in the first three 3 years, due to a low ΔT . In applying the first 3 years as 50-50, the wells have sufficient time to fill with the designed temperatures.
- Δx_{grid_left} for the hot and cold wells is 25 meters
- Δx_{grid_right} for the hot and cold wells is 25 meters
- Δx_{grid_middle} for the cold well is 20,6 meters
- Δx_{grid_middle} for the hot well is 25,6 meters
- (Table 4.3 and Appendix 6).

The ratios that determine what percentage of a volume is infiltrated in or extracted from the subsurface are changed by an iterative solver in Excel. This solver minimizes a target cell or tries to equal the target cell to certain value. The chosen solver options and parameters are described in Appendix 8.

6.2.2 Optimization strategies

The three optimization strategies that are solved are described in the following Section.

- **Optimization strategy 1**

  Minimizing the summed amount of high value thermal energy that is lost from the system.

  The ATES system is considered energy efficient, if high or low thermal energy that is infiltrated is not lost from the system. High value thermal energy is water that is hotter than 12,5 °C and water that is colder than 7,5 °C. The difference with high value thermal energy and the groundwater at 100 meters from the downstream wells is calculated. These differences then are summed. The differences between the groundwater temperature and low value thermal energy are neglected, because it is allowed to flow away. In solving for minimizing the summed differences between high thermal energy and groundwater flow, high value thermal energy loss from the system is reduced.

- **Optimization strategy 2**

  Minimizing the sum of net total pumped volume

  Through Equation [13, 14] established that if parameters are kept constant and $Q_{\inf,ex}$ decreases, ΔT increases. A high ΔT means that high value thermal energy is located in the vicinity of the wells and thermal energy loss. An additional advantage of a high ΔT and of lower infiltration and extraction rates is reducing of electrical pumping costs.

- **Optimization strategy 3**

  Solving for correction of groundwater flow velocity.

  The volume of water that is effectively lost from the system is given through Equation [18] :

  $$V_{lost} = v_s \Delta y \Delta z * 20 \qquad [18]$$

  Where V_{lost} is the total volume lost from the system due to groundwater flow [m^3]; v_s is the linear groundwater flow velocity of 36,5 m/year, Δy is 28m and Δz is 40m. If the sum of the extraction rates for a specific well is added to the summed infiltration rates of a well, the net infiltration or extraction of a specific well is determined. For no volume of water to be lost from the system, the difference between net infiltration/extraction rates of well 1 and well 2, must equal V_{lost} . In solving for correction of the groundwater velocity, the ratios defining the control strategy, will thus be varied in such a way that the volume that would be lost from the system is extracted and infiltrated back into the system again. Varying the ratios should yield for the cold well (Equation [19]):

  $$V_{lost} = V_{\inf C1} - V_{exC2} \qquad [19]$$

Where $V_{\inf C1}$ is the net summed volume infiltrated [m^3] and is a represented as a positive value by the Excel model; V_{exC2} is the net summed volume of extracted water [m^3] and is represented as a negative value by the Excel model

Solving for this optimization strategy means that for 2 target cells (one for the difference between cold well 1 and cold well 2, one for the difference between hot well 1 and hot well 2) is iterated until they both equal V_{lost} .

6.2.3 Assessment criteria

Before optimization is executed it needs to be established when an optimized control strategy establishes a better result compared to the accustomed 50-50 control strategy'.

Whether or not a control strategy is considered successful is determined based on the following assessment criteria:

Criterion 1)

- *Is the energy loss from the system reduced compared to the '50-50 control strategy'?*

Reducing energy loss from the ATES systems range increases the efficiency of the ATES system. Reducing energy loss is established in 2 ways:

 – Total thermal energy loss reduction (in Euros)
 – High value thermal energy loss reduction (in Euros)

This is done, because in reality water that has a thermal value slightly above or below the groundwater temperature (10 °C) may not be of financial value. Therefore the distinction is made between water with all temperatures (this is the total thermal energy loss) and high value thermal cold water (T≤ 9 °C, which is sufficient to cool buildings with) and high value thermal hot water (T ≥ 12,5 °C, which is needed in order to let the heat perform without additional electricity costs). Note that this is a different temperature range then for which is optimized in optimization strategy 1.

Criterion 2)

- *Is the total pumped volume for the desired simulation time lower, compared to when '50-50 control strategy' is applied'?*

Lowering of summed pumped volume yields energy savings, because electrical pumping costs are reduced. Lowering summed pumped volumes is a result from improving extraction temperatures within the wells.

Criterion 3)

- *Can the result of the optimized control strategy qualitatively be explained considering the changed ratios?*

The iterative solver can come up with infinite ways to establish minimizing or equaling a target cell through varying the ratios. It is therefore necessary to be able to account for the altered ratios through a qualitative check.

Criterion 4)

- *Is the chosen grid of the analytical model still able the accurately quantify the temperatures within the subsurface after the optimized control strategy is applied?*

If a control strategy results in such high infiltration rates that the temperature distribution exceeds the boundary of the grid, its potential for applicability decreases.

Criterion 5)

- *Is the seasonal performance factor (SPF) increased?*

If due to application of a certain control strategy the temperatures are managed in such a way that peak temperatures (high ΔT) are available in the wells, this results in less electrical energy needed for pumping (Section 1.2.1), because the infiltration and extraction rates will decrease. Therefore this yields an increase in the seasonal performance factor, which is desired. The way the SPF is calculated is described in Appendix 12.

6.2.4 Results of optimization

The results of optimizing the ’50-50 control strategy’ relative to the ’50-50 control strategy’ by means of the 3 different strategies are presented in Figure 6.3 and Figure 6.4. Detailed results of each optimization for the hot and cold wells separately are presented in Appendix 13.

Optimizing Strategy 1

			H1 ex	H2 ex	C1 Inf	C2 Inf	H1 Inf	H2 Inf	C1 ex	C2 ex
January	325889	333	16,4%	83,6%	100,0%	0,0%	50,0%	50,0%	50,0%	50,0%
February	325889	333	17,6%	82,4%	98,8%	1,2%	50,0%	50,0%	50,0%	50,0%
March	195533	130689	23,1%	76,9%	72,0%	28,0%	66,0%	34,0%	37,5%	62,5%
April	97767	228456	36,8%	63,2%	75,8%	24,2%	73,4%	26,6%	0,0%	100,0%
May	32589	293633	45,6%	54,4%	56,1%	43,9%	84,1%	15,9%	2,4%	97,6%
June	333	325889	50,0%	50,0%	50,0%	50,0%	94,4%	5,6%	4,8%	95,2%
July	333	325889	50,0%	50,0%	50,0%	50,0%	97,5%	2,5%	12,1%	87,9%
August	333	325889	50,0%	50,0%	50,0%	50,0%	95,6%	4,4%	12,7%	87,3%
September	130689	195533	39,0%	61,0%	69,6%	30,4%	68,9%	31,1%	18,1%	81,9%
October	228456	97767	4,8%	95,2%	75,1%	24,9%	72,8%	27,2%	36,4%	63,6%
November	293633	32589	7,3%	92,7%	86,5%	13,5%	55,4%	44,6%	45,5%	54,5%
December	325889	333	9,9%	90,1%	98,7%	1,3%	50,0%	50,0%	49,9%	50,1%
		Average	29,2%	70,8%	73,6%	26,4%	71,5%	28,5%	26,6%	73,4%

Optimizing Strategy 2

			H1 ex	H2 ex	C1 Inf	C2 Inf	H1 Inf	H2 inf	C1 ex	C2 ex
January	325889	333								
February	325889	333	80,7%	19,3%	67,4%	32,6%	49,9%	50,1%	50,0%	50,0%
March	195533	130689	0,0%	100,0%	70,3%	29,7%	49,8%	50,2%	50,0%	50,0%
April	97767	228456	0,0%	100,0%	38,6%	61,4%	0,0%	100,0%	57,5%	42,5%
May	32589	293633	100,0%	0,0%	58,1%	41,9%	57,5%	42,5%	39,4%	60,6%
June	333	325889	91,6%	8,4%	45,6%	54,4%	92,9%	7,1%	85,7%	14,3%
July	333	325889	50,0%	50,0%	49,9%	50,1%	70,8%	29,2%	70,5%	29,5%
August	333	325889	50,0%	50,0%	49,7%	50,3%	66,9%	33,1%	95,9%	4,1%
September	130689	195533	50,0%	50,0%	49,7%	50,3%	70,9%	29,1%	0,0%	100,0%
October	228456	97767	54,3%	45,7%	0,0%	100,0%	36,1%	63,9%	0,0%	100,0%
November	293633	32589	36,3%	63,7%	59,2%	40,8%	61,2%	38,8%	100,0%	0,0%
December	325889	333	87,3%	12,7%	93,6%	6,4%	53,9%	46,1%	93,4%	6,6%
			81,9%	18,1%	70,7%	29,3%	50,1%	49,9%	46,0%	54,0%
		Average	56,8%	43,2%	54,4%	45,6%	55,0%	45,0%	57,4%	42,6%

Optimizing Strategy 3

			H1 ex	H2 ex	C1 Inf	C2 Inf	H1 Inf	H2 inf	C1 ex	C2 ex
January	325889	333	44,0%	56,0%	56,3%	43,7%	50,0%	50,0%	50,0%	50,0%
February	325889	333	44,0%	56,0%	56,6%	43,4%	50,0%	50,0%	50,0%	50,0%
March	195533	130689	46,4%	53,6%	54,1%	45,9%	52,0%	48,0%	47,7%	52,3%
April	97767	228456	47,9%	52,1%	52,1%	47,9%	54,0%	46,0%	45,9%	54,1%
May	32589	293633	49,3%	50,7%	50,7%	49,3%	55,2%	44,8%	44,8%	55,2%
June	333	325889	50,0%	50,0%	50,0%	50,0%	55,9%	44,1%	44,2%	55,8%
July	333	325889	50,0%	50,0%	50,0%	50,0%	56,0%	44,0%	44,2%	55,8%
August	333	325889	50,0%	50,0%	50,0%	50,0%	56,1%	43,9%	44,1%	55,9%
September	130689	195533	47,7%	52,3%	52,0%	48,0%	53,7%	46,3%	46,5%	53,5%
October	228456	97767	45,8%	54,2%	54,0%	46,0%	51,9%	48,1%	48,0%	52,0%
November	293633	32589	44,7%	55,3%	55,1%	44,9%	50,6%	49,4%	49,3%	50,7%
December	325889	333	44,1%	55,9%	55,9%	44,1%	50,0%	50,0%	50,0%	50,0%
		Average	47,0%	53,0%	53,1%	46,9%	53,0%	47,0%	47,1%	52,9%

Figure 6.3 Optimized control strategies.

	Opt1	Opt2	Opt3	
Total thermal energy loss savings (hot and cold compared to '50-50')	535.177	35.036	135.454	Euro
High value thermal energy loss savings (hot and cold compared to '50-50')	473.399	75.222	196.433	Euro
Pumping Costs ('50-50' = -546.916 Euro)	-661.564	-516.501	-534.212	Euro
Total reduced volume of water pumped (compared to '50-50')	-3.717.350	986.196	411.927	m3
SPF Hot Well (compared to 32,4 for '50-50')	27,1	34,3	33,2	[-]
SPF Cold Well (compared to 32,4 for '50-50')	26,4	34,3	33,2	[-]

Figure 6.4 Results of 3 new control strategies.

Strategy 1:

Optimizing for reduction of energy loss yields in fact significant energy loss reduction for total energy loss and high value thermal energy loss and thus in significant financial savings. However the total amount of net volume pumped increases with more than 15 % (Appendix 13).This is explained in that the optimized control strategy focuses on increased infiltration in the first wells and increased extraction in the second wells (>70% on average). This is because for minimum energy loss to occur, all the thermal energy must be extracted before it leaves the systems range. In order to meet the energy demand infiltration rates increase significantly. These rates are increased to such an extent that the temperature distribution is not compatible with the grid (the range of infiltration temperature after 20 years exceeds the left boundary of the excel model). The SPF is not increased, because average the total pumping costs for both wells increase significantly compared to when the '50-50 control strategy' is applied.

Strategy 2:

Optimizing for minimizing the total net pumped volume yields a reduction in total energy loss and high value thermal energy loss, but it is not as significant as for strategy 1. The total pumped volume however does decrease, which will contribute to financial savings. The concern for this strategy is the control strategy itself. Extreme monthly transitions from 100 % infiltration of well 1, to 100 % infiltration in well 2 and vice versa occur. This approach in management of the wells is difficult to account for. It is expected that this specific control strategy is the result of the iterative solvers intention to find the solution for minimizing in the least amount of time. The temperature distribution as a result of this control strategy does fit well in the excel model grid. The SPF is increased, because average the total pumping costs for both wells decrease compared to when the '50-50 control strategy' is applied.

Strategy 3:

Optimizing for the correction of groundwater flow velocity yields a significant total energy loss and high value thermal energy loss reduction, with also a reduction in net total pumped volume. The ratios in the control strategy change gradually according to the time dependent energy demand with relatively small changes (<4% on average). The focus is on increased infiltration of hot well 1 during summer, and increased infiltration of cold well 1 during winter. To compensate for the loss due to groundwater flow, during winter extraction in hot well 2 is increased and during summer extraction in cold well 2 is increased. The temperature distribution as a result of this control strategy fits well in the excel model grid. The SPF is increased, because average the total pumping costs for both wells decreases compared to when the ‘50-50 control strategy’ is applied.

Conclusion
Considering the results, optimizing for correction of the groundwater flow velocity (strategy 3) is considered to establish the best control strategy. This is because it meets all of the assessment criteria. The control strategy yields significant financial savings with very small, gradual variations in the volume distribution ratios which are expected to be well implementable in actual system management. Although the SPF for strategy 2 is higher than for strategy 3, the increased financial savings of strategy 3 outweigh the reduced pumping costs for strategy 2, which is decisive. This chosen control strategy will be referred to as the ‘improved control strategy’ from now on.

6.2.5 Robustness of the ‘optimized control strategy’

In order to test the validity of the ‘optimized control strategy’ a robustness check is performed. In this check, first the ’50-50 control strategy’ is applied on 18 different energy scenarios. In the different energy scenarios, the monthly energy demand for hot or cold energy is increased or decreased, for 1 year or for 2 subsequent years. Since the monthly energy demand relates to the outside temperature, an exceptionally hot or cold summer or winter thus is simulated. An overview of the energy scenarios is presented in Appendix 9
Then the ‘improved control strategy’ is applied on these 18 different energy scenarios. The result of the comparison between applying the ’50-50 control strategy’ and the ‘improved control strategy’ on different energy demand scenarios is presented in Appendix 10

For all the differing energy scenarios, applying the ‘optimized control strategy’ on the differing energy demand scenarios results in financial savings and reduction of pumping rates, compared to applying the ‘50-50 control strategy’. Apparently the ‘improved control strategy’ is a better control strategy compared to the ‘50-50 control strategy’, for a large variety of different scenarios, making it a valid control strategy.

Additional to the fact that ‘optimized control strategy’ resulted in a financial gain for all the energy demand scenarios, another check for the robustness of the ‘improved control strategy’ is performed: For every different energy scenario, the control strategy optimized (i.e. 18 optimizations). This essentially implies that an energy demand scenario (i.e. temperature for a year to come) is predicted, and the optimization is performed in advance. This is done to compare to which extent the ‘improved control strategy’, differs from the control strategies for optimizing for different energy scenarios. Preferentially the ‘optimized control strategy’ for the initial energy demand scenario does not differ to the control strategy resulting from optimizing for the new energy demand scenarios. If this is the case, then annual reprogramming of the control strategy is not necessary. The ‘improved control strategy’ for the initial energy demand is compared with the control strategies that resulted from optimization for the new energy demand scenarios. This comparison is represented in Appendix 11

Scenarios

Optimization of scenarios 1, 2, 3 (a hot summer and a hot winter for 1 year), yields the following changes: During winter, compared to the ‘improved control strategy’ more heat is extracted from H1. This is explained by an abundance of hot thermal energy. During summer, more cold is extracted from C2. This is explained by the shortage of cold thermal energy, and less cold energy is allowed to flow away. The greatest difference for decreasing ratios is -0,59% and the greatest difference for increasing ratios is 0,61%.

Optimization of scenarios 4, 5, 6 (a hot summer an hot winter for 2 consecutive years) yields the same changes as for 1 year, except the effects increase. This is shown in that the greatest difference for decreasing ratios is -0.77 % and the greatest difference for increasing ratios is 0,85%

Optimization of scenarios 7, 8, 9 (a cold summer, and a cold winter for 1 year) yields the following changes: During winter, compared to the ‘improved control strategy’ more heat is extracted from H2. This is explained by the shortage of hot thermal energy and less thermal energy is allowed to flow away. During summer, more cold is extracted from C1. This is explained by the abundance of cold thermal energy. The greatest difference for decreasing ratios is -0,38 % and the greatest difference for increasing ratios is 0,53%.

Optimizing of scenarios 10, 11, 12 (a cold summer, and a cold winter for 2 consecutive years) yields the same changes as for 1 year, except the effects increase. This is shown in that the greats difference for decreasing ratios is -0,60 % and the greatest difference for increasing ratios is 0,76%

Optimizing for scenarios 13, 14,15 (a hot summer, and a cold winter for 1 year) yields the following changes: the ratios shows great similarity with the ‘improved control strategy’ but every ratio decreases or increases more towards the 50% (i.e. the control strategy behaves more like the ’50-50 control strategy’). The differences between the volumes that are divided over well 1 and 2 decrease. This is explained in that if for both seasons the energy demand increases the subsurface buffer capacity needs to increase. To achieve this, equal amounts of hot and thermal energy need be available in the subsurface. The greatest difference for decreasing ratios is -46% and the greatest difference for increasing ratios is 0,24 %.

Optimizing of scenarios 16, 17, 18 (a cold summer, and a cold winter for 2 consecutive years) yields the same changes as for 1 year, except the result in even more similarity with the ’50-50 control strategy’. This is shown in that the greats difference for decreasing ratios is -0,62 % and the greatest difference for increasing ratios is 0,41%. These differences thus contribute to approaching the 50% ratio.

An important aspect of the optimization of the 18 different scenarios is that the not a single percentage in the 18 new control strategies differs more than 1% (i.e. largest difference is -0.77 %) from the percentages in the ‘improved control strategy’. Considering this, and that the differences for optimization of the energy scenarios can all be accounted for and that the overall trend of division of ratios from the ‘improved control strategy’ is maintained, the ‘improved control strategy’ is in fact robust.

Applicability of the ‘improved control strategy’.

It is expected that the improved control strategy is well applicable on other ATES systems that are installed at locations where groundwater flow velocities are high. The pattern in the ‘improved control strategy’ that, dependent on the season, larger volumes are infiltrated in the upstream wells and larger volumes are extracted in the downstream wells, is a shown to be a adequate way to keep thermal energy within the ATES systems range. It is expected that if this pattern is maintained, individual ratios however may vary. This is caused by local differences for different ATES systems, such as volumes involved, distance between corresponding hot and cold wells, and difference in groundwater flow velocity.

7 Discussion

Optimizing infiltration and extraction rates for the ATES system of Achmea through analytical quantification of the groundwater temperature in the subsurface, lead to the establishment of an ‘improved control strategy’. The limitations of the used approach are discussed in the following Sections.

Soil characteristics

In this study several parameters concerning physical processes and subsurface characteristics are taken from related research, articles or provided data. It is not reasonable to accept those values to be completely accurate because due to heterogeneity of the subsurface parameters may differ locally. The values for parameters however have been selected with care in order represent reality as well as possible. If effective porosity and volumetric heat capacity of sand and water are changed within an acceptable margin however, this has a relatively small effect on the ratios in the ‘improved control strategy’: not a single ratio differs with more than 0,4%.

Groundwater flow velocity and direction

The linear groundwater flow velocity is based on hydraulic conductivity maps which do not represent local differences on a detailed level. Small variations in groundwater flow velocity can however significantly affect thermal energy distribution and energy loss reduction, since large volumes of water are involved. This will result in a significant differences in the ratios of the ‘improved control strategy’ when solving is done with a different groundwater flow velocity.

Variations in energy demand

The total energy demand is multiplied by an empirical factor and distributed over the months based on common sense with regard to expected outside temperatures. This energy demand however may differ significantly in reality if simulated, and this will cause significant alterations in the temperature distribution of the groundwater in the subsurface. The effect on the ‘optimized control strategy’ with varying energy demands is more significant: maximum of 0,8% difference. This is however based on varying energy demands for maximum of 2 years, which in reality may be more. Also the factor with which the initial energy demand is multiplied may be increased in reality, which increases the differences in ratios within the ‘improved control strategy’. The increased impact on variations in the ‘improved control strategy’ is explained variations in energy demand, changes the volumes that are pumped and this has a significant larger impact on the thermal influence radius than variations in soil characteristics.

Infiltration temperature

This model considers the hot and cold infiltration temperature to be the same value for every time step. In reality this is not the case because multiple factors which this study does not consider affect the infiltration temperature. If the infiltration temperatures vary with time, this affects the ΔT and thus directly influences the thermal influence radii. In reality the system may need less or more time after installation to fill the wells with sufficient thermal energy than the 3 years simulated in this study. Application of the '50-50 control strategy' for less or more than 3 years will result in a different 'improved optimization strategy' since the temperature distribution in the subsurface will differ.

Simplifications in calculations

Representing the volume as a one-dimension dependent cuboid instead of a cylinder decreases the accuracy of temperature quantification in the subsurface. It is however considered a decent approach in analytically attempting to quantify a problem that is dependent on so many variables, since temperature distribution within the subsurface presented by the analytical model establishes similarities compared to a numerical approach that is considered more accurate.

In assuming that the filter positions are located at the same depth in the subsurface and groundwater flow transports all water from one well to the other, may cause an under estimation of thermal energy loss. Groundwater in reality may pass the top or the bottom of the filter and is thus lost from the system independent of extraction rates.

One of the assessment criteria for judging the quality of the optimized control strategy focuses on if the temperature distribution can be quantified by the model (i.e. is the model extent sufficient). In order to delete this criterion, the amount of grid cells can be increased which increases model extent and accuracy. This however is not done because this is a very time consuming process, since the mathematical formulas that quantify the temperature of a grid cell then become more complex. The temperature of a grid cell is dependent on a fixed number of other grid cells. This number of fixed cells varies for each time step (dependent on thermal influence radius). If the grid is extended, the amount of fixed number of grid cell a single cells temperature is dependent on thus increases. This increases complexity of the model.

In the model the temperatures of extracted groundwater are determined by the weighted averaged of the two grid cells that lie adjacent to the specific well. In reality the temperature of the extracted water is dependent on the total volume that is extracted and this thus reduces the accuracy of representing extraction temperatures.

Quantification of financial assessment criteria

A quantification of electrical costs for the electrical energy that is used by the heat-pump to increase thermal energy for the ATES system is not considered in this study. If a significant increase of thermal energy that is led into the heat pump, decreasing electrical heating costs for the heat-pump, compensates for the possible increased pumping costs, this may lead to a different chosen ‘improved control strategy’. The reduction of energy loss is presented in term of financial savings. This financial saving is a rough approach and may vary greatly in reality. It is however an attractive way to roughly translate the effect of energy reduction to a financial point of view.

8 Conclusion

The physical processes and parameters that predominantly affect an ATES system performance and efficiency are the groundwater flow velocity and the energy demand.

For the campus of Achmea the monthly seasonal dependent energy demand is determined from the total annual energy demand. The energy demand determines the volumes that need to be infiltrated and extracted, which affect the thermal influence radius of thermal energy distribution within the subsurface.

At Achmea Apeldoorn, groundwater flow velocity is high. The 2 doublets of its ATES systems are placed in line with each other, in a dominantly coarse grained sandy aquifer, so upstream infiltrated thermal energy may be extracted by the downstream well, when it is transported due to groundwater flow. With the accustomed '50-50 control strategy' however, energy loss is apparent.

The analytical model that is created quantifies the temperature distribution in the subsurface under influence of infiltration and extraction rates and groundwater flow velocity. Optimization for the correction of total volume of water that leaves the system as a result of the high groundwater flow velocity (Strategy 3), yields the 'improved control strategy'. In this improved control strategy, the ratios which determine the volumes that are infiltrated or extracted as a result of an energy demand are changed compared to the '50-50 control strategy'.

The 'improved control strategy' focuses on, depending on the season, more infiltration in the upstream wells, to keep thermal energy within the systems range and more extraction in the downstream wells, to limit thermal energy loss. This 'improved control strategy' increases the SPF of the ATES system, reduces total pumped volume and thus pumping costs, and reduces thermal energy loss from the system which is represented energetically and financially. Combining this with the established robustness, leads to the consideration that the 'improved control strategy' is in fact an improvement compared to accustomed system management.

This control strategy is applicable on other similar ATES systems. It must however be stressed that individual ratios which determine dividing of volumes of wells, may vary for other systems compared to the ATES system of Achmea, due to local differences in system characteristics and subsurface characteristics.

9 Recommendations

Within this research a variety of problems was encountered which led to a set of recommendations which are described in the following Section.

Increased research of the subsurface of the Netherlands may contribute to more accurate knowledge of local subsurface characteristics. Implementation of more accurate parameters will establish the analytical Excel model to simulate the reality more accurately. Through hydraulic head measurements within the wells of an ATES system, when it is not activated, the local groundwater flow velocity can be more accurately determined than based on the hydraulic head maps provided by Dinoloket. If the determined groundwater velocity of 36,5 m/y differs from the actual groundwater flow velocity, this must be taken into account when establishing a control strategy for future system management.

The ‘improved control strategy’ is established through a very rough estimate of the monthly energy demands for Achmea Apeldoorn. System owners can provide the monthly energy demand from data of the past. Since energy demand is a parameter that greatly influences the infiltration and extraction rates, this data will result in relative great accuracy increase when implemented in the model. Furthermore, infiltration temperatures are not constant as simulated in this study. Temperature measurements within the wells can accurately contribute to more accurately determining the ΔT which then results in more accurate temperature quantification in the model which influences the ‘improved control strategy’. A final contribution that ATES system owners can make to increasing model accuracy is providing data of electrical costs used by the heat pump to increase the extracted groundwater temperature. With this data it can be examined if focusing solely on increasing the extraction temperature is an option, if this effect outweighs additional pumping costs. If the increasing electrical pumping costs for higher infiltration and extraction rates are cancelled out by increased profit due high value thermal energy in the wells, this will cause alterations on the ‘improved control strategy’.

However time consuming; increasing the model extent through adding grid cells will contribute to the accuracy of the temperature quantification. If cell sizes are smaller because extent increases the temperature distribution will become more gradual, yielding a more realistic representation of the real temperatures in the subsurface. It must be taken into account that there is a maximum to the extent of mathematical formula that can be written in Excel and this thus is not exceeded. In increasing model extent, with additional adaptations the model may also function to simulate the groundwater temperature distribution for multiple doublet ATES systems. Since the mathematical foundation for infiltrating and extracting from wells is known for this model, additional wells may be added.

In the model it is assumed that the filters are positioned on equal depths in the subsurface and that all the filters consist of 1 piece. In order to establish a better representation of reality it is possible to divide the subsurface in different layers and model them individually. This accounts for the use of multiple filter pieces per well and the possibility of different layers with different geological features within in the subsurface. This is expected to be relatively easy, because no adaptations are needed to be made, just multiple models are used. An approach to account for the vertical groundwater flow within the Excel model is to extend the model so that not only temperature transport takes place in the lateral direction, but also in the vertical direction. The application of the 2^{nd} dimension in the Excel model is expected to be less easy. The implementation of vertical heat transport and flow will increase accuracy especially in the starting years that the system runs. It is expected that after multiple years however, the temperature within the vicinity of the hot and cold wells will have adapted the infiltration temperature and the influence of vertical heat transport and flow will decrease, making it doubtful if it is worthy of making drastic changes in the current model framework.

With potential predicted climate change, energy demands may change in the future. Differing energy demands may lead to the needing of altering the managing control strategy of ATES system on a large time scale (i.e. decades). A trend of how the control strategy may be varied in the future can be created in assessing KNMI or IPPC climate scenarios. With predicted climate change the change in energy demand can be predicted, which can contribute to understanding the way control strategies should be altered in the future, in order to keep an ATES system performing with maximal efficiency.

Considering the results, the analytical Excel model may function as a helpful ATES system managing tool. Because in the analytical model the parameters; grid cell size, energy demand, infiltration temperatures, time step duration and groundwater flow velocity can easily be adjusted, it is highly flexible to a variety of different input data and the model thus can also be used for other ATES systems than just the system at Achmea. For owners of ATES systems implementation of an' improved control strategy' is relatively easy and cost worthy compared to the estimated financial savings that are currently established by the model for the ATES system of Achmea.

10 References

Buik, N. & Snijders, A.L. (2006). Clogging rate of recharge wells in porous media. Proceedings Megastock, Pomona, NJ, USA.

Courtois, N., Grisey, A., Grasselly, D., Menjoz, A., Noël, Y., Petit, V., & Thiéry, D. (2007). Application of Aquifer Thermal Energy Storage for heating and cooling of greenhouses in France: a pre-feasibility study. Proceedings European Geothermal Congress 2007, Unterhaching, Germany, 30 May-1 June 2007.

Hecht-Méndez, J., Molina-Giraldo, G., Blum, P, & Bayer, P. (2009). Evaluating MT3DMS for Heat Transport Simulation of Closed Geothermal Systems. ***Groundwater***. Vol 48, No.5 (pages 757-770). University of Tübingen.

IF Technology. (1995). ***Underground thermal energy storage: state of the art 1994***. Arnhem, the Netherlands.

IF Technology (2001). ***Ontwerpnormen voor bronnen voor koude-/warmteopslag.*** Research conducted for NOVEM, Projectnr. 149.508-105.0. Arnhem.

IF Technology. (2009). ***20000 ATES systems in the Netherlands in 2020 – Major step towards a sustainable energy supply***. IF Technology, Arnhem, the Netherlands.

Fitts, C. R. (2002). ***Groundwater Science***. Scarborough, Maine: Academic Press.

McDonald, M.G & Harbaugh, A.W. (1984). A modular three-dimensional finite-difference ground-water flow model. USGS Open-File Report: 83-875

Morofsky, E.L. (1994). ATES-Energy Efficiency, Economics and the Environment. ***Proceedings of the International Symposium on Aquifer Thermal Energy Storage***, Tuscaloosa, Ala., 14–15 November 1994. University of Alabama, Tuscaloosa,Ala. pp. 9–14.

Neri, M.G. (2009). Aspects of Transverse Dispersion in Porous Media. Doctoral dissertation, ***Geologica Ultraeictina***. N0.309. Faculteit Geo-Sciences, University Utrecht

N.V.O.E. (2006). ***Nederlandse Vereniging voor Ondergrondse Energieopslagsystemen – Richtlijnen Ondergrondse Energieopslag.*** **Woerden**: NVOE.

Tauw (2008). ***Warmte-/ Koudeopslag Achmea te Apeldoorn***. Definitief ontwerp, 30 July, 2009.

The Engineering Toolbox. (2012). *Water - Thermal Properties*. Retrieved November, 2012, from http://www.engineeringtoolbox.com

TNO. (2009). ***REGIS***. Retrieved October, 2012, from Dinoloket: http://www.dinoloket.nl

Todd, D.K. (1980). ***Groundwater Hydrology***, 2nd ed., John Wiley & Sons, New York, 535p.

De Vries, (2007). ***Geology of the Netherlands.*** Edited by Th.E. Wong, D.A.J. Batjes & J. de Jager. Royal Netherlands Academy of Arts and Sciences, 2007: 295–315

Vail, W.L., & Jenne, E.V. (1994). Optimizing the design and operationof ATES systems. *In* ***Proceedings of the International Symposium on Aquifer Thermal Energy Storage***, Tuscaloosa, Ala., 14–15 November 1994. University of Alabama, Tuscaloosa,Ala. pp. 9–14.

Vereniging voor Landinrichting & Elsevier (2000). ***Cultuur Technisch Vademecum***. Chapter 1, Grond en Bodem. Krips, Meppel.

Websites:

www.deltares.nl
www.tno.nl
www.dinoloket.nl
www.geo-elements.nl
www.enoco.nl
www.warmtepompforum.nl
www.sepemo.eu
http://biosystems.okstate.edu/darcy/index.htm

Appendix

1

Description of geological formations in the subsurface at Achmea Apeldoorn

Description of geological formations

In the following Section a short description of occurring formations (Figure 4.2) in the subsurface below the site of Achmea Apeldoorn is given (www.dinoloket.nl).

Formation of Boxtel

This young geological formation is the upper formation in most parts of the Netherlands. Where it does not outcrop it is usually eroded or overlain by younger river deposits. The varying deposits are from Middle and Late-Pleistocene to Early Holocene. The dominant lithologies are:

-Sand, average to fine grain size (150-300 μm), of light to dark brown color, limestone free to minimum lime stone content

- Silty sand, very fine to average fine grain size (105-210 μm), of light yellow to light grey color, lime stone free to very limestone rich.
- Loam, with occurring peat layers, sometimes clay rich, with grey brown to dark grey color, limestone free to very limestone rich.

Impelled depositions of Drenthe

The formation of Drenthe consist of glacial and periglacial deposits from the Saalian. The deposits are mainly related fluvioglacial events where they were deposited by meltwater rivers, or from glacio-lacustrine deposits where they were deposited by glacial lakes. Due to glacial movement, the depositions of the Drenthe formation are heavily impelled. The dominant lithologies are:

- Sand, average to very coarse grain size (210 – 2000 μm), weak to strong gravel contents.
- Clay and loam layers, average to strong silt content, of grey-blue to brown-grey color.
- Silty sand layers, fine to average grain size (150-210 μm), of grey-blue to brown-grey color, with locally gravel, rocks and boulders.
- Clay, limited to average silt content, very fine layered (cm-mm), of grey to brown color.

Formation of Peize and Waalre

The formation of Peize and the formation of Waalre where deposited simultaneous and therefore transit into each other in the subsurface below Apeldoorn. These two different formations are therefore described as one formation. The formation consists of fluviatile sands from both the Early Pleistocene to Late Pleistocene (Reuverian). The fluviatile facies are deposited by the predecessor of the river Rhine. Sedimentary structures show signs of tidal activity, inferring an estuarine environment. The dominant lithologies are:

- Sand, average to very coarse grain size (210-2000 μm), of light grey to white color, limestone free, gravel with diameter 2-16 mm, quartz fraction within gravel.
- Sand very fine to very coarse grain size (63 – 2000 μm), limestone free to limestone rich content, sporadic shell content, of grey to white-grey color, with occasional red components.

Formation of Maassluis

The formation of Maassluis consist of shallow marine deposited shell and mica containing sands and clays from the Early Pleistocene. Occasionally humus rich layers occur. It covers almost the entire Netherlands. The dominant lithologies are:

-Sand, very small to average grain size (63 - 300 μm), predominantly limestone content, marine shell content, of grey color.
- Clay layers, predominantly limestone content, marine shell content, of grey to dark grey color.

Formation of Oosterhout

The formation of Oosterhout is a Marine formation which was deposited during the Pliocene. The dominant lithologies are:

-Sand, very fine to very coarse grain size (105-420 μm), marine shells with lots of shell-grit, of light grey to grey-green of color, with occasional clay layer.
- Clay and sandy clay, weak to strong silt content, of dark-grey to grey-brown color.
- Shell banks, ranging from decimeters to larger than 10 meters in thickness.

Formation Breda-Ville

The formation of Breda and the formation of Ville where deposited simultaneous and therefore transit into each other at Apeldoorn. De formation is deposited during the Miocene epoch and consists mainly of marine glauconiferous sands and clays. Within fluviatile sands and gravel, locally layers of brown coal (lignite) occur. The dominant lithologies are:

- Sand, very fine to average grain size (105-210 μm), glauconiferous, of grey-green to black-green color, with limestone content, remnants of fish-bones and teeth.
- Clay, glouconiferous, of strong to average silt content, of green to dark-brown color and contains gravel and brown coal.

Appendix

2

Digital groundwater maps of the Netherlands

Geohydrologisch model gl50 (dikten)

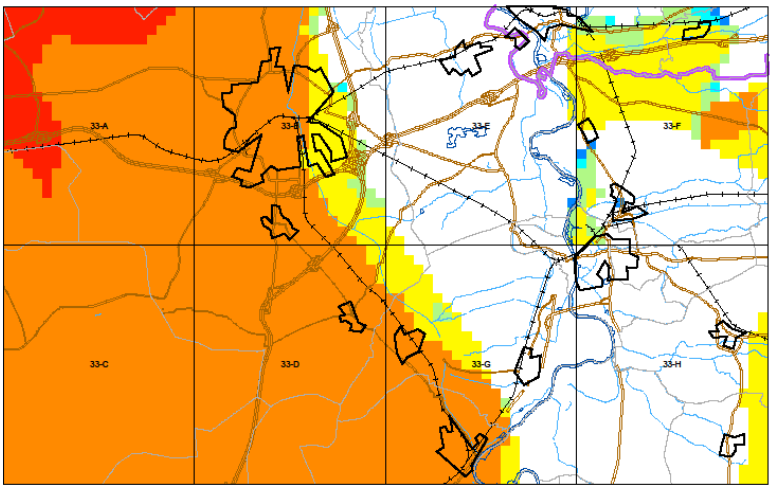

Legenda geohyd. laag

Watervoerend pakket 2 Dikte grid

- 150 - 230.1 (m)
- 30 - 150
- 6 - 30
- 1 - 6
- 0.3 - 1
- 0.05 - 0.3
- 0.01 - 0.05

Legenda topografie

- Kaartbladen 1:25.000
- Gemeentegrenzen
- Nationale grens
- Provinciale grens
- Hoofdwegen
- Spoorwegen
- Waterlopen
- Kustlijnen en oevers
- Steden

Geohydrologisch model gl50 (isohypsen 28-04-1995)

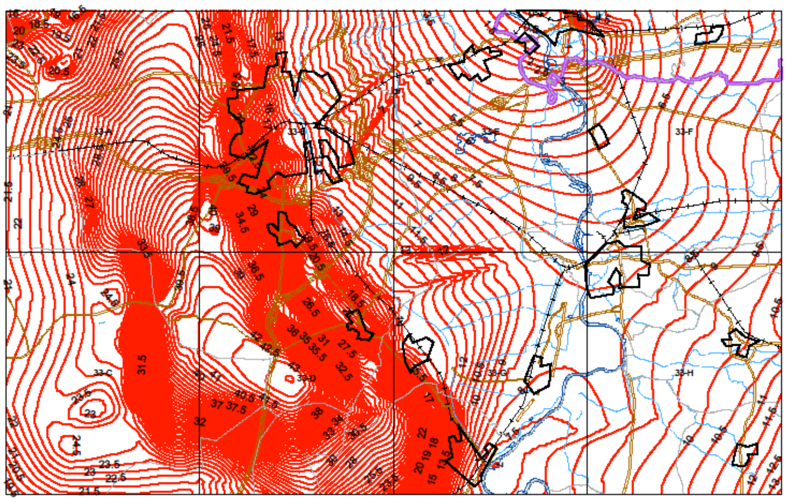

Legenda topografie

- Kaartbladen 1:25.000
- Gemeentegrenzen
- Nationale grens
- Provinciale grens
- Hoofdwegen
- Spoorwegen
- Waterlopen
- Kustlijnen en oevers
- Steden

Legenda geohyd. laag

- Watervoerend pakket 2 Isohypsen (m NAP)

Geohydrologisch model gl50 (kD en c-waarden)

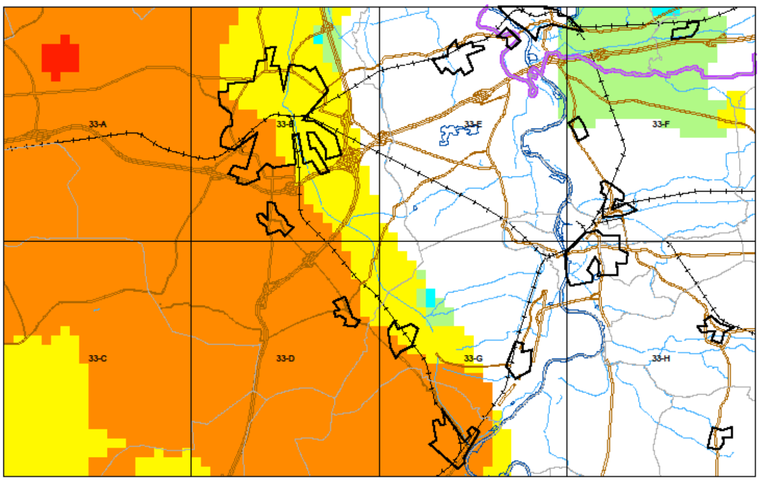

Legenda geohyd. laag

Slecht doorlatende laag 2 c-waarde grid

- 15000 - 28329 (d)
- 3000 - 15000
- 600 - 3000
- 100 - 600
- 30 - 100
- 5 - 30
- 1 - 5

Legenda topografie

- Kaartbladen 1:25.000
- Gemeentegrenzen
- Nationale grens
- Provinciale grens
- Hoofdwegen
- Spoorwegen
- Waterlopen
- Kustlijnen en oevers
- Steden

Grondwaterkaart 9 (IJsseldal) zuid Versie: 1 (2002)

Geohydrologisch model gl50 (kD en c-waarden)

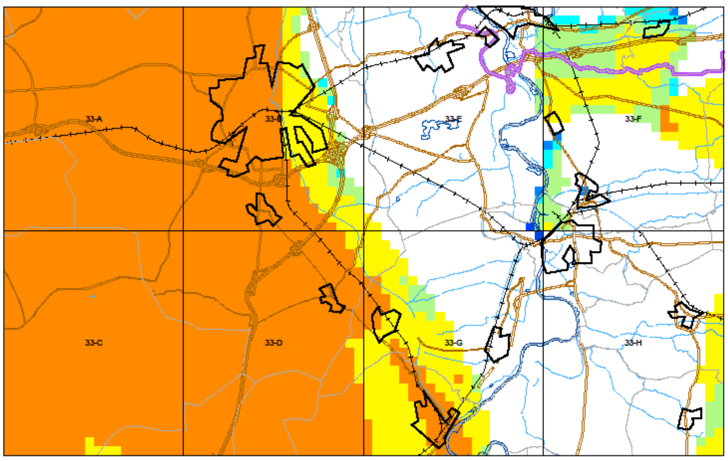

Legenda geohyd. laag

Watervoerend pakket 2 kD-waarde grid

- 10000 - 12184 (m2/d)
- 2000 - 10000
- 500 - 2000
- 100 - 500
- 20 - 100
- 5 - 20
- 1 - 5

Legenda topografie

- Kaartbladen 1:25.000
- Gemeentegrenzen
- Nationale grens
- Provinciale grens
- Hoofdwegen
- Spoorwegen
- Waterlopen
- Kustlijnen en oevers
- Steden

Appendix

3

Drilling core description and well locations

De Ruiter Boringen en Bemalingen bv

Plaats/project	: Apeldoorn/Achmea Campus	Datum uitvoering	:	17-02-2011 t/m 28-02-2011
Boringnummer	: K1	Werknummer	:	3220268
Boormethode	: Zuigboren/luchtliften	Boordiameter	:	Ø1000 mm
Boormeester	: M. v/d Slot H. Meke			
Beschrijver	: M. v/d Slot H. Meke			

Diepte der lagen in meters -/- maaiveld van	tot	Hoofdnaam	µm	Grondsoort	Gesteldheid, kleur, Bijmengsel
0,00	1,00	Zand	420	Uiterst grof	zwak siltig, zwak humeus, bruin
1,00	2,00	Zand	450	Uiterst grof	zwak siltig, bruin
2,00	3,00	Zand	450	Uiterst grof	zwak siltig, bruin
3,00	4,00	Zand	450	Uiterst grof	zwak siltig, bruin
4,00	5,00	Zand	450	Uiterst grof	zwak siltig, bruin
5,00	6,00	Zand	450	Uiterst grof	zwak siltig, bruin
6,00	7,00	Zand	450	Uiterst grof	zwak siltig, bruin
7,00	8,00	Zand	450	Uiterst grof	zwak siltig, bruin
8,00	9,00	Zand	450	Uiterst grof	zwak siltig, bruin
9,00	10,00	Zand	450	Uiterst grof	zwak siltig, bruin
10,00	11,00	Zand	450	Uiterst grof	zwak siltig, bruin
11,00	12,00	Zand	450	Uiterst grof	zwak siltig, bruin
12,00	13,00	Zand	450	Uiterst grof	zwak siltig, bruin
13,00	14,00	Zand	450	Uiterst grof	zwak siltig, bruin
14,00	15,00	Zand	450	Uiterst grof	zwak siltig, bruin
15,00	16,00	Zand	350	Zeer grof	zwak siltig, bruin
16,00	17,00	Zand	350	Zeer grof	zwak siltig, bruin
17,00	18,00	Zand	350	Zeer grof	zwak siltig, bruin
18,00	19,00	Zand	350	Zeer grof	zwak siltig, bruin
19,00	20,00	Zand	350	Zeer grof	zwak siltig, bruin
20,00	21,00	Zand	420	Uiterst grof	zwak siltig, bruin, grind
21,00	22,00	Zand	420	Uiterst grof	zwak siltig, bruin, grind
22,00	23,00	Zand	420	Uiterst grof	zwak siltig, bruin
23,00	24,00	Zand	420	Uiterst grof	zwak siltig, bruin
24,00	25,00	Zand	420	Uiterst grof	zwak siltig, bruin
25,00	26,00	Zand	420	Uiterst grof	zwak siltig, bruin
26,00	27,00	Zand	250	Matig grof	zwak siltig, grijsbruin
27,00	28,00	Zand	250	Matig grof	zwak siltig, grijsbruin
28,00	29,00	Zand	250	Matig grof	zwak siltig, grijsbruin, grind, kleibrokjes
29,00	30,00	Zand	250	Matig grof	zwak siltig, grijsbruin, grind, kleibrokjes
30,00	31,00	Zand	420	Uiterst grof	zwak siltig, grijsbruin, grind
31,00	32,00	Zand	420	Uiterst grof	zwak siltig, grijsbruin
32,00	33,00	Zand	420	Uiterst grof	zwak siltig, grijsbruin
33,00	34,00	Zand	420	Uiterst grof	zwak siltig, grijsbruin
34,00	35,00	Zand	420	Uiterst grof	zwak siltig, grijsbruin

De Ruiter Boringen en Bemalingen bv

Plaats/project	Apeldoorn/Achmea Campus	Datum uitvoering	:	16-03-2011 t/m 29-03-2011
Boringnummer	K2	Werknummer	:	3220268
Boormethode	Zuigboren/luchtliften	Boordiameter	:	Ø1000 mm
Boormeester	M. v/d Slot, H. Meke	Grondwaterstand	:	4,80 m - mv
Beschrijver	M. v/d Slot, H. Meke			

Diepte der lagen in meters -/- maaiveld

van	tot	Hoofdnaam	µm	Grondsoort	Gesteldheid, Kleur, Bijmengsel
0,00	1,00	Zand	250	Matig grof	zwak siltig, roestbruin
1,00	2,00	Zand	250	Matig grof	zwak siltig, roestbruin
2,00	3,00	Zand	250	Matig grof	zwak siltig, roestbruin
3,00	4,00	Zand	310	Zeer grof	zwak siltig, roestbruin
4,00	5,00	Zand	460	Uiterst grof	zwak siltig, roestbruin, sterk grindig
5,00	6,00	Zand	460	Uiterst grof	zwak siltig, roestbruin, sterk grindig
6,00	7,00	Zand	460	Uiterst grof	zwak siltig, roestbruin, sterk grindig
7,00	8,00	Zand	460	Uiterst grof	zwak siltig, roestbruin, sterk grindig
8,00	9,00	Zand	460	Uiterst grof	zwak siltig, roestbruin, sterk grindig
9,00	10,00	Zand	460	Uiterst grof	zwak siltig, roestbruin, sterk grindig
10,00	11,00	Zand	460	Uiterst grof	zwak siltig, roestbruin, sterk grindig
11,00	12,00	Zand	460	Uiterst grof	zwak siltig, roestbruin, sterk grindig
12,00	13,00	Zand	600/1200	Uiterst grof	zwak siltig, roestbruin, sterk grindig
13,00	14,00	Zand	600/1200	Uiterst grof	zwak siltig, roestbruin, sterk grindig
14,00	15,00	Zand	600/1200	Uiterst grof	zwak siltig, roestbruin, sterk grindig
15,00	16,00	Zand	600/1200	Uiterst grof	zwak siltig, roestbruin, sterk grindig
16,00	17,00	Zand	600/1200	Uiterst grof	zwak siltig, roestbruin, sterk grindig
17,00	18,00	Zand	600/1200	Uiterst grof	zwak siltig, roestbruin, sterk grindig
18,00	19,00	Zand	600/1200	Uiterst grof	zwak siltig, roestbruin, sterk grindig
19,00	20,00	Zand	600/1200	Uiterst grof	zwak siltig, roestbruin, sterk grindig
20,00	21,00	Zand	600/1200	Uiterst grof	zwak siltig, roestbruin, sterk grindig
21,00	22,00	Zand	600/1200	Uiterst grof	zwak siltig, roestbruin, sterk grindig
22,00	23,00	Zand	600/1200	Uiterst grof	zwak siltig, roestbruin, sterk grindig
23,00	24,00	Zand	600/1200	Uiterst grof	zwak siltig, roestbruin, sterk grindig
24,00	25,00	Zand	600/1200	Uiterst grof	zwak siltig, roestbruin, sterk grindig
25,00	26,00	Zand	600/1200	Uiterst grof	zwak siltig, roestbruin, sterk grindig
26,00	27,00	Zand	600/1200	Uiterst grof	zwak siltig, roestbruin, sterk grindig
27,00	28,00	Zand	600/1200	Uiterst grof	zwak siltig, roestbruin, sterk grindig
28,00	29,00	Zand	600/1200	Uiterst grof	zwak siltig, roestbruin, sterk grindig
29,00	30,00	Zand	600/1200	Uiterst grof	zwak siltig, roestbruin, sterk grindig
30,00	31,00	Zand	420	Uiterst grof	zwak siltig, grijs
31,00	32,00	Zand	420	Uiterst grof	zwak siltig, grijs
32,00	33,00	Zand	500	Uiterst grof	zwak siltig, grijs
33,00	34,00	Zand	500	Uiterst grof	zwak siltig, grijs
34,00	35,00	Klei		Stevig	zwak siltig, grijs

bam
infra

De Ruiter Boringen en Bemalingen bv

Plaats/project	:	Apeldoorn/Achmea Campus	Datum uitvoering	:	01-03-2011 t/m 14-03-2011
Boringnummer	:	W1	Werknummer	:	3220268
Boormethode	:	Zuigboren/luchtliften	Boordiameter	:	Ø1000 mm
Boormeester	:	H. Meke, P. Bel			
Beschrijver	:	H. Meke, P. Bel			

Diepte der lagen in meters -/- maaiveld

van	tot	Hoofdnaam	µm	Grondsoort	Gesteldheid, kleur, Bijmengsel
0,00	1,00	Zand	310	Zeer grof	zwak siltig, bruin
1,00	2,00	Zand	310	Zeer grof	zwak siltig, bruin
2,00	3,00	Zand	310	Zeer grof	zwak siltig, bruin
3,00	4,00	Zand	310	Zeer grof	zwak siltig, bruin
4,00	5,00	Zand	310	Zeer grof	zwak siltig, bruin
5,00	6,00	Zand	310	Zeer grof	zwak siltig, bruin
6,00	7,00	Zand	350	Uiterst grof	zwak siltig, bruin, kleibrokjes
7,00	8,00	Zand	350	Uiterst grof	zwak siltig, bruin, kleibrokjes
8,00	9,00	Zand	350	Uiterst grof	zwak siltig, bruin, kleibrokjes
9,00	10,00	Zand	350	Uiterst grof	zwak siltig, bruin, kleibrokjes
10,00	11,00	Zand	350	Uiterst grof	zwak siltig, bruin, kleibrokjes
11,00	12,00	Zand	350	Uiterst grof	zwak siltig, bruin, kleibrokjes
12,00	13,00	Zand	420	Uiterst grof	zwak siltig, bruin, sterk grindig
13,00	14,00	Zand	420	Uiterst grof	zwak siltig, bruin, sterk grindig
14,00	15,00	Zand	420	Uiterst grof	zwak siltig, bruin, sterk grindig
15,00	16,00	Zand	420	Uiterst grof	zwak siltig, bruin, sterk grindig
16,00	17,00	Zand	600	Uiterst grof	zwak siltig, bruin, sterk grindig
17,00	18,00	Zand	800/2000	Uiterst grof	zwak siltig, bruin
18,00	19,00	Zand	800/2000	Uiterst grof	zwak siltig, bruin, sterk grindig
19,00	20,00	Zand	800/2000	Uiterst grof	zwak siltig, bruin, stenen
20,00	21,00	Zand	800/2000	Uiterst grof	zwak siltig, bruin, sterk grindig
21,00	22,00	Zand	800/2000	Uiterst grof	zwak siltig, bruin, sterk grindig
22,00	23,00	Zand	600	Uiterst grof	zwak siltig, bruin, sterk grindig
23,00	24,00	Zand	600	Uiterst grof	zwak siltig, bruin
24,00	25,00	Zand	600	Uiterst grof	zwak siltig, bruin
25,00	26,00	Zand	600	Uiterst grof	zwak siltig, bruin
26,00	27,00	Zand	600	Uiterst grof	zwak siltig, bruin
27,00	28,00	Zand	600	Uiterst grof	zwak siltig, bruin
28,00	29,00	Zand	600	Uiterst grof	zwak siltig, bruin
29,00	30,00	Zand	600	Uiterst grof	zwak siltig, bruin
30,00	31,00	Zand	310	Zeer grof	zwak siltig, bruin
31,00	32,00	Zand	310	Zeer grof	zwak siltig, bruin
32,00	33,00	Zand	400	Zeer grof	zwak siltig, bruin
33,00	34,00	Zand	350	Zeer grof	zwak siltig, bruin
34,00	35,00	Zand	350	Zeer grof	zwak siltig, bruin

De Ruiter Boringen en Bemalingen bv

Plaats/project	:	Apeldoorn/Achmea Campus	Datum uitvoering	:	1 maart 2011
Boringnummer	:	W2	Werknummer	:	3220268
Boormethode	:	Zuigbore/Vluchtliften	Boordiameter	:	Ø1000 mm
Boormeester	:	B. Oodam	Grondwaterstand	:	1,70 m - mv
Beschrijver	:	B. Oodam			

Diepte der lagen in meters -/- maalveld

van	tot	Hoofdnaam	µm	Grondsoort	Gesteldheid, Kleur, Bijmengsel
0,00	1,00	Zand	240	Matig grof	matig siltig, geelgrijs
1,00	2,00	Zand	240	Matig grof	matig siltig, geelgrijs
2,00	3,00	Zand	240	Matig grof	matig siltig, geelgrijs
3,00	4,00	Zand	700	Uiterst grof	matig siltig, geelgrijs, grindjes
4,00	5,00	Zand	800	Uiterst grof	matig siltig, geelgrijs, grindjes
5,00	6,00	Zand	600	Uiterst grof	matig siltig, geelgrijs, grindjes
6,00	7,00	Zand	800	Uiterst grof	matig siltig, geelbruin
7,00	8,00	Zand	500	Uiterst grof	matig siltig, geelbruin
8,00	9,00	Zand	500	Uiterst grof	matig siltig, geelbruin
9,00	10,00	Zand	480	Uiterst grof	matig siltig, geelbruin
10,00	11,00	Zand	450	Uiterst grof	matig siltig, geelbruin
11,00	12,00	Zand	380	Zeer grof	matig siltig, geelbruin
12,00	13,00	Zand	350	Zeer grof	matig siltig, geelbruin
13,00	14,00	Zand	350	Zeer grof	matig siltig, geelbruin
14,00	15,00	Zand	420	Uiterst grof	matig siltig, geelbruin
15,00	16,00	Zand	450	Uiterst grof	matig siltig, geelbruin
16,00	17,00	Zand	450	Uiterst grof	matig siltig, geelbruin
17,00	18,00	Zand	350	Zeer grof	matig siltig, geelbruin
18,00	19,00	Zand	350	Zeer grof	matig siltig, geelbruin
19,00	20,00	Zand	350	Zeer grof	matig siltig, geelbruin
20,00	21,00	Zand	350	Zeer grof	matig siltig, geelbruin
21,00	22,00	Zand	350	Zeer grof	matig siltig, geelbruin
22,00	23,00	Zand	480	Uiterst grof	matig siltig, geelbruin
23,00	24,00	Zand	500	Uiterst grof	matig siltig, geelbruin, grindjes
24,00	25,00	Zand	500	Uiterst grof	matig siltig, geelbruin, grindjes
25,00	26,00	Zand	700	Uiterst grof	matig siltig, geelbruin, grindjes
26,00	27,00	Zand	480	Uiterst grof	matig siltig, geelbruin, grindjes
27,00	28,00	Zand	490	Uiterst grof	matig siltig, geelbruin, grindjes
28,00	29,00	Zand	500	Uiterst grof	matig siltig, geelbruin, grindjes
29,00	30,00	Zand	450	Uiterst grof	matig siltig, geelbruin, grindjes
30,00	31,00	Zand	800	Uiterst grof	matig siltig, geelbruin, grindjes
31,00	32,00	Zand	900	Uiterst grof	matig siltig, geelbruin, grindjes
32,00	33,00	Zand	470	Uiterst grof	matig siltig, geelbruin, grindjes
33,00	34,00	Zand	460	Uiterst grof	matig siltig, geelbruin, grindjes
34,00	35,00	Zand	500	Uiterst grof	matig siltig, geelbruin, grindjes

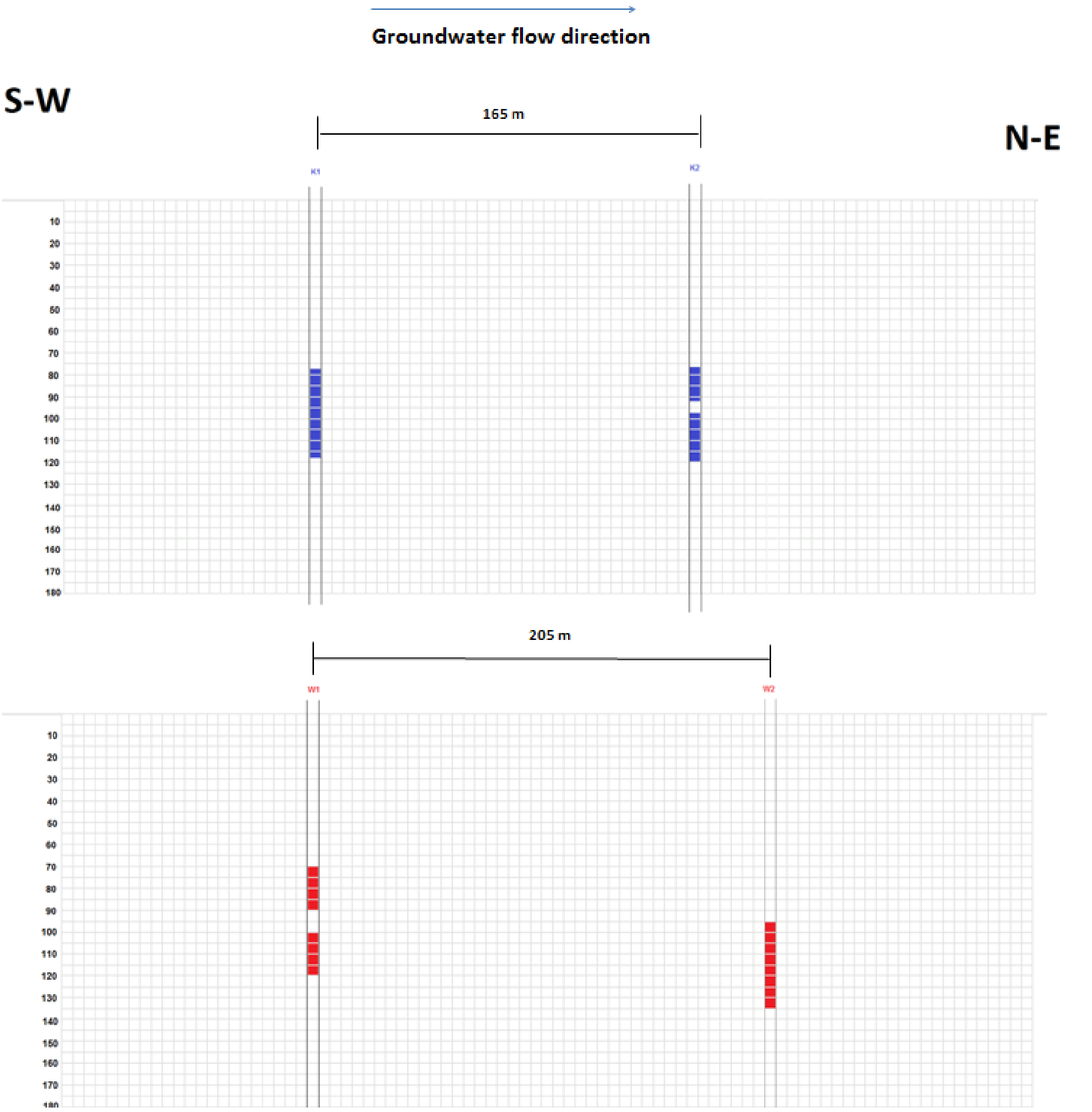

Well locations in the subsurface.

Appendix 4

Well design formulations

Well design formulations

There is a maximum allowed Darcy flow velocity on the walls of bore hole. This standard for injection wells is given by Equation [1A] (NVOE, 2006) and if not exceeded, limits well-clogging.

$$v_{inject} = 1000\left(\frac{K_s}{150}\right)^{0.6} \sqrt{\frac{v_{cl}}{2MFI_{mem} u_{eq}}} \qquad [1A]$$

Where v_{inject} is the design injection Darcy velocity on the walls of the bore hole [m/h]; v_{cl} is the specific clogging speed [m/year]; MFI_{mem} is the measured membrane filter index [s/l^2] (Buik et al., 2006) ; u_{eq} is the number of equivalent full load hours the well pumps per year [-].

In designing the ATES system, Tauw calculated the Darcy velocity for the worst-case scenario. Therefore, in the well-designing stage, hydraulic conductivity of k = 20 m/d is used instead of 30 m/d. The specific clogging speed is set at 0.1 m/year, the MFI is set at 2 s/l^2 and the total amount of equivalent full load hours [h] per year on 2400 (NVOE, 2006.,Tauw, 2009).

This results in a design injection velocity of 0.96 m/h on the bore hole wall.

The maximal allowed Darcy flow velocity on the walls of the bore hole in case of extraction is given by Equation [2A]:

$$v_{extract} = \frac{K_s}{12} \qquad [2A]$$

(IF, 2001, N.V.O.E., 2006).

Where $v_{extract}$ is the design extraction Darcy velocity on the walls of the bore hole [m/h].

With a maximum required discharge for the ATES system, the radius of the bore hole and the filter length are determined through Equation [3A]

$$v_{design} = \frac{Q_{\inf, ex}}{2\pi r_0 H} \qquad [3A]$$

Where $Q_{\inf, ex}$ is the infiltration or extraction rate of the well [m/h]; r_0 is the radius of the bore-hole [m].

The radius of the bore hole is cost-technically preferred to be 50 centimeters. This can vary however because it is interdependent on the filter length. The length of filter and width of borehole consequently influence the shape of the hot or cold water body in the subsurface. In the case of limited room for an ATES system, wells might be placed close to each other. In order to prevent thermal energy mixing, deeper wells with small bore-hole radius are needed.

Within the determined borehole radius, gravel is deposited around the filter screen. This is done to prevent well-clogging. The filter screen radius therefore is the radius of the borehole, minus 25 cm.

Influence on the hydraulic head in the subsurface

When water is injected in or extracted from the subsurface, this has influence on the hydraulic head level in the aquifer. For the maximum amount of head difference that is allowed for any ATES system in the Netherlands the following principle is applied:

Maximum allowed head difference $< 0{,}2 *$ *depth of the top of the filter* (N.V.O.E., 2006).

The steady state drawdown of a single well is calculated through Equation [4A]

$$h_r - h_0 = \frac{Q}{2\pi T}\ln\left(\frac{r}{r_0}\right) \qquad [4A]$$

Where r = distance from the well [m]; $h_r - h_0$ is the head difference between the initial head h_0 and head h_r after injection or extraction at position r [m]

Thermal influence radius

The minimum distance between the hot and cold well is depending on the amount of water that is pumped per season, the specific heat of the water, the specific heat of the aquifer, the volumetric flow rate of the groundwater and filter length. Minimum distance between the hot and cold well is determined via Equation [5A].

$$L = 3R_{th} \qquad [5A]$$

Where L is the minimum distance between the hot and the cold well [m]; R_{th} is the thermal influence radius of infiltrated and extracted volumes of water [m] [m]. If thermal radii for the hot and the cold well are considered the same, and for distance between the hot and cold well 2 times the thermal influence radius of either well is applied this results in touching of touching of the areas of influence of the two wells. To prevent this, the minimum distance of 3 thermal radii is assumed to be sufficient to prevent mixing of hot and cold water (N.V.O.E., 2006).

Appendix

5

Description of additional devices used in the ATES system of Achmea

Heat pump

The water in the cold well is cold enough to be used for cooling purposes within the building. The hot water, stored in the hot well however is not hot enough to fulfill the hot energy demands. Therefore a heat pump is used.

A heat pump is used to increase the temperature of the water of the hot well. Preferentially this temperature is raised t 35 – 40 °C which is sufficient for effective heating of the building.

The heat pump extracts thermal energy from the hot water via compression of the medium. After the water is lead through the heating circuits of the building and cools again it is brought into an expansion valve where it is depressed, energy is used and this results in further cooling of the water.

Countercurrent heat exchange device

The water that is pumped through the wells is of different chemical composition compared to the water that runs through the heating and cooling circuits within the buildings. For this reason these water types must not be mixed. Via a countercurrent heat exchange device the thermal energy from the water from the wells is brought into the heating and cooling circuits. The two chemically different bodies of water with a thermal gradient flow in opposite directions and exchange thermal energy. The hot water becomes cold and the cold water becomes hot. This transfers the energy from the wells through the countercurrent heat exchange device from and to the heating and cooling circuits.

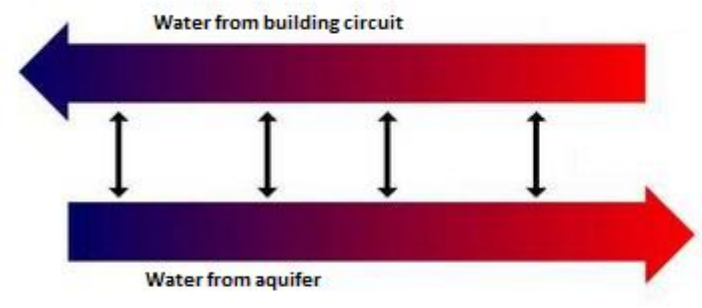

Countercurrent heat exchange device.

Appendix

6

Temperature quantification in the analytical Excel model

Infiltration Section

For the following Sections, the cold wells are used as an example.

Every grid cell is considered to be full of water of a certain temperature. In time step t0, when the system is not working, this temperature is the groundwater temperature. During winter there is a net demand of hot energy in the first time step (t1), water is extracted from the hot wells and infiltrated in the cold wells. The volume of water that is infiltrated is divided over the 2 grid cells adjacent to the wells:

$$W_{\inf} = \frac{\Delta x_{cub}}{2}$$

Where $W_{\inf}$ is the width of the infiltrated volume considered within each cell [m].

Water that is infiltrated pushes water that was initially adjacent to the wells to the left and the right. This means, that if the if $W_{\inf} > \Delta x_{grid}$, the water that was initially in the grid cells adjacent to the well, will shift into grid cells next to it.
Since $W_{\inf}$ can vary, the content of each grid cell can have different values which is further explained in the following Section:

Scenario 1a

The target cell is the grid cell below A1 and its weighted temperature.

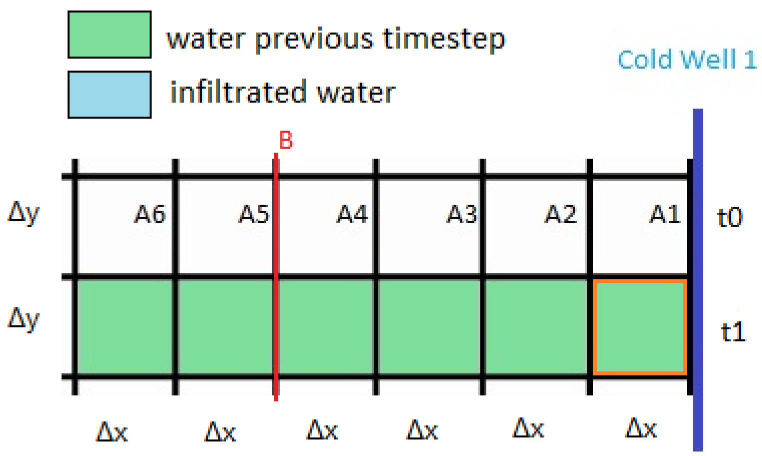

- If $W_{\inf} = 0$, then the temperature of that cell is the same as the temperature of A1, since no water enters.

Scenario 1b

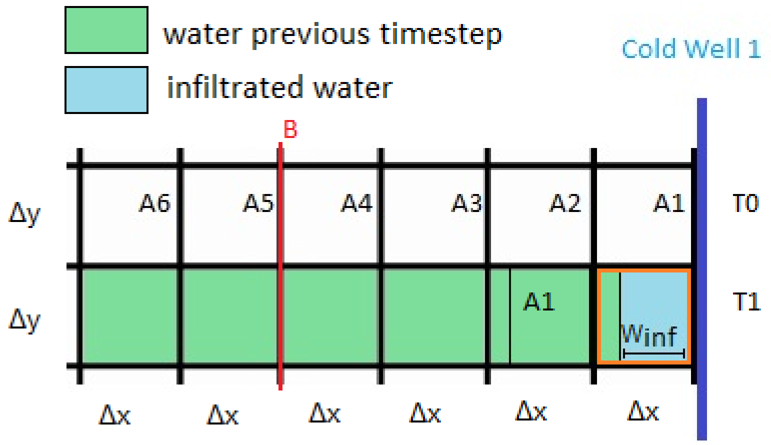

If $W_{inf} < \Delta x$, then the temperature of the cell is the weighted average of the temperature of the infiltrated water and the remaining water. Thus:

- If $W_{inf} < \Delta x$, then the temperature of the cell is: $((W_{inf} * T_{inf}) + ((\Delta x - W_{inf})*A1)) / \Delta x$
- If $W_{inf} \geq \Delta x$, then the temperature of the cell is: T_{inf}

Scenario 2a

The target cell is the gridcell below A2 and its weighted temperature.

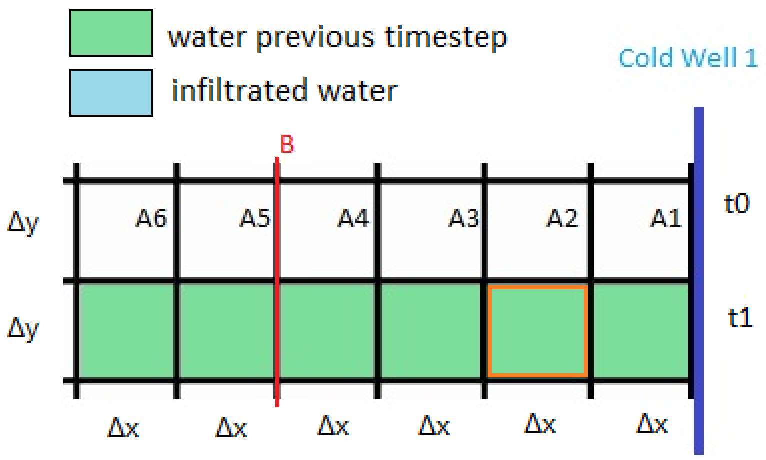

- If $W_{inf} = 0$, then the temperature of that cell is the same as the temperature of A2, since no water enters.

Scenario 2b

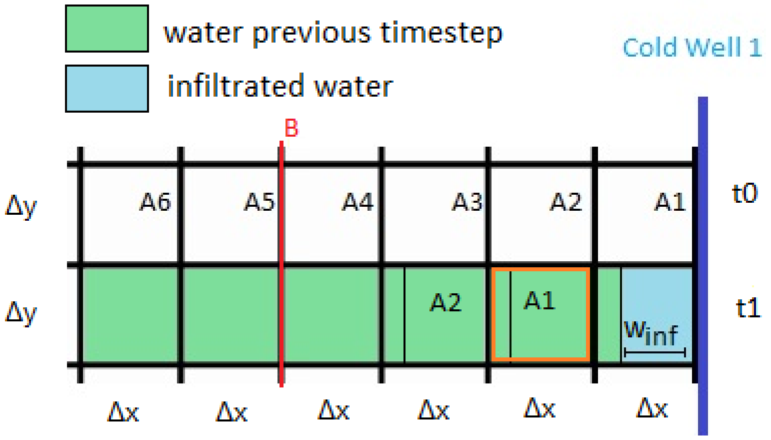

If $W_{inf} < \Delta x$, then the temperature of the cell is the weighted average of the temperature of the infiltrated water and the remaining water. Thus:

- If $W_{inf} < \Delta x$, then the value of the cell is: $((W_{inf} * A1) + ((\Delta x - W_{inf}) * A2)) / \Delta x$

Scenario 2c

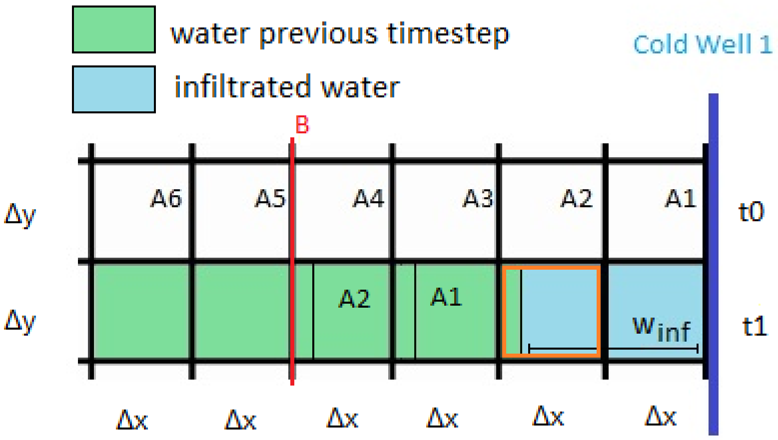

- If $W_{inf} < 2 * \Delta x$ then the temperature of the cell is: $(((W_{inf} - \Delta x) * T_{inf}) + ((\Delta x - (W_{inf} - \Delta x)) * A1)) / \Delta x$

- If $W_{inf} \geq 2 * \Delta x$, then the temperature of the cell is: T_{inf}

As shown in the examples above, every instant that L_{inf} exceeds the next Δx, the number of cells from the previous time step that the temperature of the target cell depends on, increases.

Scenario 3

For the target cell below A3 therefore applies the following:

- If $W_{inf} = 0$ the temperature of the cell is: A3
- If $W_{inf} < \Delta x$ the temperature of the cell is:
  $((W_{inf} * A2) + (\Delta x – (W_{inf} * A3))) / \Delta x$
- If $W_{inf} < 2 * \Delta x$ the temperature of the cell is:
  $(((W_{inf} - \Delta x) * A1) + ((\Delta x- (W_{inf} - \Delta x)) * A2)) / \Delta x$
- If $W_{inf} < 3 * \Delta x$ the temperature of the cell is:
  $(((W_{inf} – (2 * \Delta x) * T_{inf}) + ((\Delta x – (W_{inf} – (2 * \Delta x)) * A1)) / \Delta x$
- If $W_{inf} \geq 3 * \Delta x$, then the temperature of the cell is: T_{inf}

Scenario 4

For the target cell below 4 therefore applies the following:

- If $W_{inf} = 0$ the temperature of the cell is: A4
- If $W_{inf} < \Delta x$ the temperature of the cell is:
  $((W_{inf} * A3) + (\Delta x – (W_{inf} * A4))) / \Delta x$
- If $W_{inf} < 2 * \Delta x$ the temperature of the cell is:
  $(((W_{inf} - \Delta x) * A2) + ((\Delta x- (W_{inf} - \Delta x)) * A3)) / \Delta x$
- If $W_{inf} < 3 * \Delta x$ the temperature of the cell is:
  $(((W_{inf} – (2 * \Delta x) * A1) + ((\Delta x – (W_{inf} – (2 * \Delta x)) * A2)) / \Delta x$
- If $W_{inf} < 4 * \Delta x$ the temperature of the cell is:
  $(((W_{inf} – (3 * \Delta x) * T_{inf}) + ((\Delta x – (W_{inf} – (3 * \Delta x)) * A1)) / \Delta x$
- If $L_{inf} \geq 4 * \Delta x$, then the temperature of the cell is: T_{inf}

Boundaries

Boundary 1 lays 4 cells on the left of cold Well 1 and boundary 2 lays 4 cells on the right of cold well 2. These boundaries visualize the maximal possible infiltration and extraction range for the

model.
If these boundaries are exceeded within a single time step (i.e. width of area of influence/2 > 4x Δx left) this has consequences for the accuracy of the model. This however is unlikely since this would exceed the maximal allowed pumping rate which this ATES system is physically not capable of pumping.
Therefore for the temperatures of these grid cells, the same approach as for scenario 4 is used. The exception however is that if the width exceeds Δx*8, the temperature of this cell does not become the T_{inf} but the temperature of the cell that was adjacent to the well in the previous time step.

The content of all the cells in the infiltration Section from time step 1 (t1), are based on the groundwater temperatures from time step 0 (t0) from the infiltration Section.

The content of all the cells in the infiltration Section from time step 2 (t1), are based on the groundwater temperatures from time step 1 (t1) from the transportation Section (paragraph 8,6).

Extraction Section

When extraction occurs, water disappears from the model. This means that water adjacent to the cells from which water disappears, should shift and fill up their place. With extraction, the length of extraction (W_{ext}) is converted to a percentage. This percentage determines the number of cells next to the well that is pumped out of the subsurface. Because Δx left of cold well 1, between the wells, and to the right of cold well 2 can differ, and extraction rates for cold well 1 and cold well 2 can differ, there are 4 percentages of extraction that must be accounted for.

Consider the following scenario:

Scenario 1a

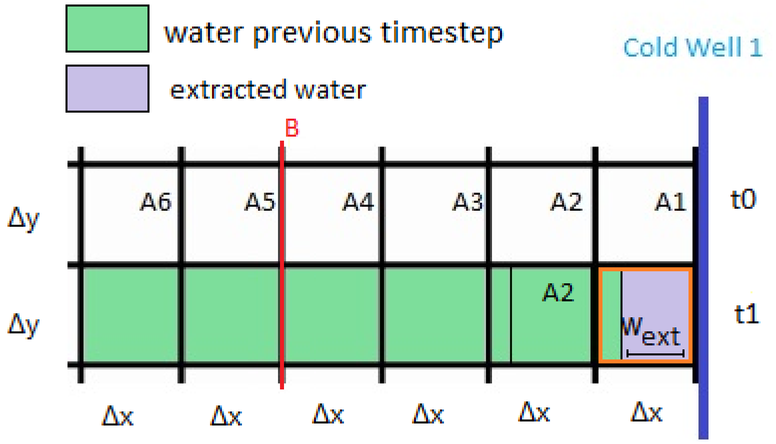

The width of extraction, divided by Δx is smaller than 1.
With W_{ext} = $Width_{area\ of\ influence}$ / 2

Then:
$W_{ext} / \Delta x < 1$

This results in the calculation of the weighted averaged of the remnant in the target cell and the part of the adjacent cell (A2) that will be pulled in the target cell. This is shown below.

- If 'percentage' < 1; then the temperature of the target cell is:

(1- 'percentage') * A1 + ('percentage' * A2)

Scenario 1b

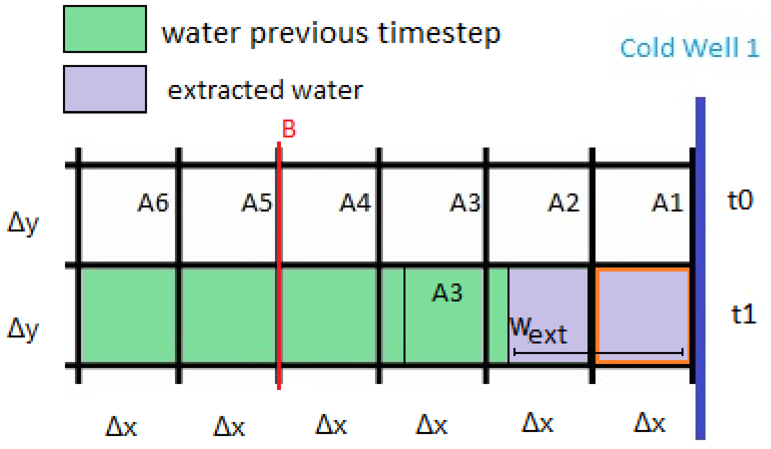

The length of extraction, divided by Δx , is larger than 1, but smaller than 2.

$2 > W_{ext} / \Delta x < 1$

This results in the calculation of the weighted averaged of the remnant in the cell below cell A2 cell and the part of the adjacent cell (A3) that will be pulled in the target cell. This is shown below.

- If 'percentage' < 2; then the temperature of the target cell is:

(2- 'percentage') * A2 + (1 –(2 -'percentage'))* A3

Scenario 1c

The length of extraction, divided by Δx, is larger than 2 but smaller than 3.
$3 > W_{ext} / \Delta x < 2$

This results in the calculation of the weighted averaged of the remnant in the cell below cell A3 cell and the part of the adjacent cell (A4) that will be pulled in the target cell. This is shown below.

If 'percentage' < 3; then the temperature of the target cell is:
(3- 'percentage') * A3 + (1 –(3 -'percentage'))* A4
If 'percentage > 3; then the temperature of the target cell is:
A4

If W_{ext} is 3 times larger than Δx, the temperature is simply taken as cell A4. This is done accordingly, because it is not expected for this system to have such high extraction rates.

Because each cell within a given side of the well, and therefore with their own extraction length and accompanying Δx, experiences the same shift, when extracted, the same formula is applied to every cell in the grid. The difference is lies in the different accompanying Δx and extraction percentages.

If extraction rates increase, it is possible that temperatures of cells are to shift, which initially lie within the extraction area of the other well. Therefore, of the third and fourth cell to the right of well C1 and the third and fourth cells to the left of well C2, the formula is not extended to the same length as left of C1 and right of C2. This is done because it is not preferred to use the content of cells which might be extracted, if the 2 wells extract simultaneously. Their content now only depends on 1 cell within the area of extraction of the other well. On the far left of well C1 and on the far right of well C2, the content of the cells will depend on cells to the models extend: they can use content of the cells as long as they exist.

The content of all the cells in the extraction Section from time step 1 (t1), are based on the groundwater temperatures from the infiltration Section from time step 1 (t1).

Transport Section

In the transport Section the groundwater velocity is divided by the Δx. This is the percentage of the cell that shifts into the other cell due to groundwater flow.

'percentage' = groundwater flow velocity (per time step) / Δx

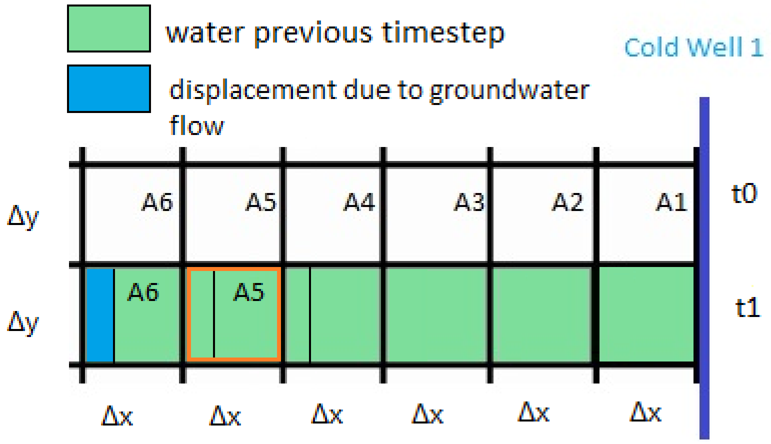

The temperature of the target cell now is:

- 'percentage' * A6 + (1 – 'percentage') * A5

The same formula is used for all the cells, with the exception that the percentage is based on the length of Δx, accordingly with the location of the cell.

The content of all the cells in the transportation Section from time step 1 (t1), are based on the groundwater temperatures from the extraction Section from time step 1 (t1).

Appendix

7

Parameters Modflow and MT3D

The governing partial differential Equation [6A] for a confined aquifer used in MODFLOW is:

$$\frac{\partial}{\partial x}[k_{xx}\frac{\partial h}{\partial x}]+\frac{\partial}{\partial y}[k_{yy}\frac{\partial h}{\partial y}]+\frac{\partial}{\partial z}[k_{zz}\frac{\partial h}{\partial z}]+W=S_s\frac{\partial h}{\partial t} \qquad [6A]$$

(McDonald et al., 1984).

Where $k_{xx,yy,zz}$ are the values of hydraulic conductivity along the *x*, *y*, and *z* coordinate axes [m/day]; h is the hydraulic head [m]; W is a volumetric flux per unit volume representing sources and/or sinks of water where *negative* values are extractions, and *positive* values are injections [day^{-1}]; S_s is the specific storage of the porous material [m^{-1}]; t is time [day].

Grid and mesh size

The model extent is 2000 meters by 2000 meters, with major grid cells of 100 by 100 meters. At the locations of the 4 wells, the cell sizes gradually decrease to the extent of 2,5 by 2,5 meters, which is also the case for the left and right boundaries of the model, where groundwater flow initiates, and the head distribution is defined. The wells are positioned entirely in layer 5 of the model.

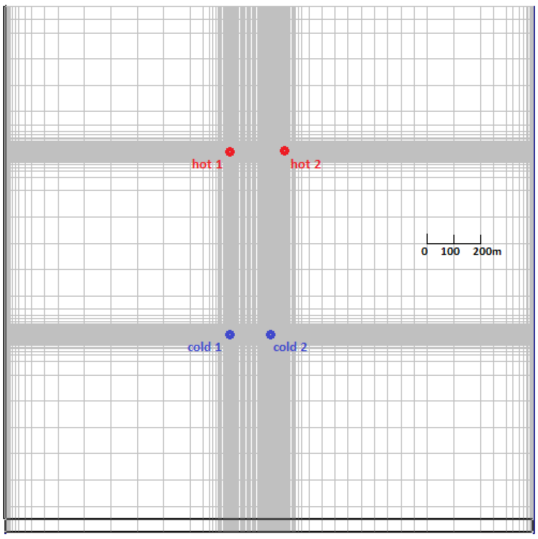

Mesh size PMWIN model of ATES Achmea.

Modflow Parameters

Time

The model runs for 10 years, in 120 periods. Every period has length 30 days . The simulation type is 'transient flow simulation'.

Initial and prescribed hydraulic heads

Using Darcy's law, the calculated that the head difference over the model extent (2000 meters) yields 2 meters. Therefore the hydraulic head level in every layer on the most left part of the grid is set t one and the hydraulic head level in each layer of the most right part of the grid is set to minus one. The rest of all the grid cells is set to zero. The only exception is for the top (covering) layer, which is completely set to zero, because no horizontal groundwater flow is allowed through this layer.

Horizontal and vertical hydraulic conductivity

The horizontal hydraulic conductivities are all equal to those listed in Table 4.1, with the exception of layer 3 (the layer above the aquifer in which the wells are positioned). This layer has a lower horizontal hydraulic conductivity compared to Table 4.1, because in accordance to the Excel model, no flow is allowed above and below the target aquifer. The vertical hydraulic conductivity is taken as the horizontal hydraulic conductivity divided by 2 for all the layers (Todd, 1980).

Effective porosity

The effective porosity for the entire model is set at 0,3 (Chapter 3).

MT3D parameters

Initial concentration

The initial concentration for the entire model is set at 10. This corresponds to the natural groundwater temperature.

Advection

The advection parameters are not altered from the pre-listed parameters suggested by PMWIN.

Solution Scheme: Hybrid MOC/MMOC (HMOC)

Particle Tracking Algorithm: Hybird 1st order Euler and 4th order Runge-Kutta

Simulation Parameters	
Max. number of total moving particles (MXPART)	1000000
Courant number (PERCEL)	0,75
Concentration weighting factor (WD)	0,5
Negligible relative concentration gradient (DCEPS)	0,00001
Pattern for initial placement of particles (NPLANE)	1
No. of particles per cell in case of DCCELL<=DCEPS (NPL)	2
No. of particles per cell in case of DCCELL>DCEPS (NPH)	16
Minimum number of particles allowed per cell (NPMIN)	2
Maximum number of particles allowed per cell (NPMAX)	30
Multiplier for the particle number at source cells (SRMULT)	1
Pattern for placement of particles for sink cells (NLSINK)	0
No. of particles used to approximate sink cells (NPSINK)	10
Critical relative concentration gradient (DCHMOC)	0,01

Advection parameters used in PMWIN.

Dispersivity

Longitudinal dispersivity: 1,0 m

Transversal dispersivity in the y-direction: 1,0 m

Transversal dispersivity in the z-direction: 1,0 m

Because the thermal energy is directly conducted to the soil grains, the energy front is considered a sharp front, which means that transversal dispersivity is neglected, and therefore is considered the same as longitudinal dispersivity.

Chemical reaction

The MT3D program is used to simulate solute transport through porous media. Because the governing Equations for solute transport are mathematically identical the Equations for heat transport, heat transport is modeled as advective solute transport in MT3D. (Hecht-Méndez et al., 2009)

The heat exchange between water and solid in MT3D is expressed with the distribution coefficient. The distribution coefficient is expressed as the ratio between specific heat of the solid in the aquifer and the volumetric heat capacity of the water through Equation [7A]

$$Kd = \frac{c_r}{\rho_w c_w} \qquad [7A]$$

Where Kd the distribution coefficient for advective heat is transport [m^3/kg]; c_r is the specific heat of the soil grains [J/kg^3/K^1]; and $\rho_w c_w$ is the volumetric heat capacity of water (J/m^3/K^1)

The specifc heat capacity of sand soil grains: 0,835 $J*g^{-3}*K^{-1}$
The specific heat capacity of water = 4,19 $J*g^{-3}*K^{-1}$
Density of water = 1000 kg/m^3
This yields Kd=1,99 $*10^{-4}$ m^3/kg

(Engineering Toolbox, 2012)

Appendix 8

Excel solver options and parameters

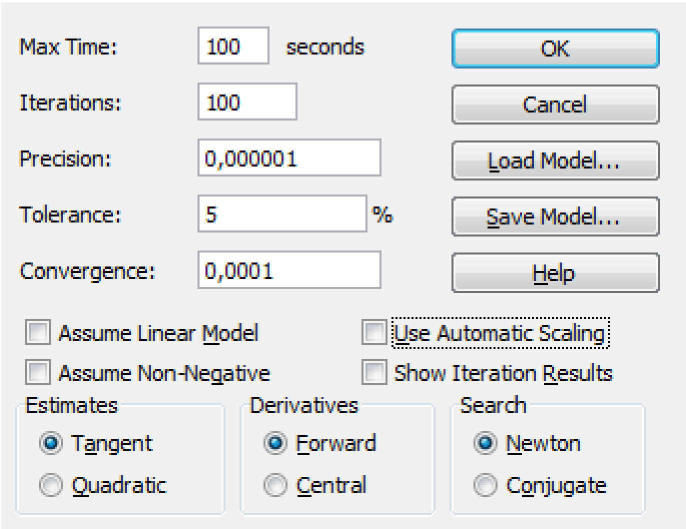

Solver parameters.

Solver Options

You can control advanced features of the solution process, load or save problem definitions, and define parameters for both linear and nonlinear problems. Each option has a default setting

Max time Limits the time taken by the solution process. While you can enter a value as high as 32,767, the default value of 100 (seconds) is adequate for most small problems.

Iterations Limits the time taken by the solution process by limiting the number of interim calculations. While you can enter a value as high as 32,767, the default value of 100 is adequate f

Precision Controls the precision of solutions by using the number that you enter to determine whether the value of a constraint cell meets a target or satisfies a lower or upper bound. Prec (zero) and 1. Higher precision is indicated when the number that you enter has more decimal places — for example, 0.0001 is higher precision than 0.01.

Tolerance The percentage by which the target cell of a solution satisfying the integer constraints can differ from the true optimal value and still be considered acceptable. This option appli tolerance tends to speed up the solution process.

Convergence When the relative change in the target cell value is less than the number in the **Convergence** box for the last five iterations, Solver stops. Convergence applies only to nonli between 0 (zero) and 1. A smaller convergence is indicated when the number that you enter has more decimal places — for example, 0.0001 is less relative change than 0.01. The smaller t solution.

Assume Linear Model Select to speed the solution process when all relationships in the model are linear and you want to solve a linear optimization problem.

Assume Non-Negative Causes Solver to assume a lower limit of 0 (zero) for all adjustable cells for which you have not set a lower limit in the **Constraint** box in the **Add Constraint** dialo

Use Automatic Scaling Select to use automatic scaling when inputs and outputs have large differences in magnitude — for example, when maximizing the percentage of profit based on r

Show Iteration Results Select to have Solver pause to show the results of each iteration.

ESTIMATES

Specifies the approach that is used to obtain initial estimates of the basic variables in each one-dimensional search.

Tangent Uses linear extrapolation from a tangent vector.

Quadratic Uses quadratic extrapolation, which can improve the results on highly nonlinear problems.

DERIVATIVES

Specifies the differencing that is used to estimate partial derivatives of the objective and constraint functions.

Forward Use for most problems, in which the constraint values change relatively slowly.

Central Use for problems in which the constraints change rapidly, especially near the limits. Although this option requires more calculations, it might help when Solver returns a message t

SEARCH

Specifies the algorithm that is used at each iteration to determine the direction to search.

Newton Uses a quasi-Newton method that typically requires more memory but fewer iterations than the Conjugate gradient method.

Conjugate Requires less memory than the Newton method but typically needs more iterations to reach a particular level of accuracy. Use this option when you have a large problem and iterations reveals slow progress.

Load Model Displays the **Load Model** dialog box, where you can specify the reference for the model that you want to load.

Excel Equation solver paramters description.

Appendix

9

Energy demand scenarios for robustness check

Scenario		1	2	3	4	5	6
Type		Hot Summer, Hot Winter					
Factor with which	Hot	0,5	0,5	0,5	0,5	0,5	0,5
initial energy demand	Cold	1,5	1,5	1,5	1,5	1,5	1,5
is multiplied							
Which year(s) is energy		5	10	15	5	10	15
demand varied?					6	11	16
Scenario		7	8	9	10	11	12
Type		Cold Summer, Cold Winter					
Factor with which	Hot	1,5	1,5	1,5	1,5	1,5	1,5
initial energy demand	Cold	0,5	0,5	0,5	0,5	0,5	0,5
is multiplied							
Which year(s) is energy		5	10	15	5	10	15
demand varied?					6	11	16
Scenario		13	14	15	16	17	18
Type		Hot Summer, Cold Winter					
Factor with which		1,5	1,5	1,5	1,5	1,5	1,5
initial energy demand		1,5	1,5	1,5	1,5	1,5	1,5
is multiplied							
Which year(s) is energy		5	10	15	5	10	15
demand varied?					6	11	16

Appendix

10

Results of comparison between application of ’50-50 control strategy’ and ‘improved control strategy’ on the 18 differing energy demand scenarios

	OPT		1	2	3	4	5	6	7	8	9	10	11	12	13	14	15	16	17	18	
Cold Energy Demand 20 years	39.146.667	kwh	40.125.333	40.125.333	40.125.333	41.104.000	41.104.000	41.104.000	38.168.000	38.168.000	38.168.000	37.189.333	37.189.333	37.189.333	40.125.333	40.125.333	40.125.333	41.104.000	41.104.000	41.104.000	kwh
Cold Energy Demand 20 years	8.854.976	euro	9.076.350	9.076.350	9.076.350	9.297.725	9.297.725	9.297.725	8.633.602	8.633.602	8.633.602	8.412.227	8.412.227	8.412.227	9.076.350	9.076.350	9.076.350	9.297.725	9.297.725	9.297.725	euro
Cold Energy Losses 20 years (50-50)	464.818	euro	416.780	417.013	418.991	375.569	376.150	381.783	477.407	477.348	476.569	485.193	485.127	483.627	459.263	459.417	459.485	454.460	454.710	454.807	euro
Cold Energy Losses 20 years (opt)	363.658	euro	299.103	303.872	311.524	270.389	277.704	290.748	391.047	394.459	391.755	405.245	408.623	404.469	353.909	355.363	355.988	346.647	348.788	350.084	euro
Hot Energy Demand 20 years	39.146.667	kwh	38.168.000	38.168.000	38.168.000	37.189.333	37.189.333	37.189.333	40.125.333	40.125.333	40.125.333	41.104.000	41.104.000	41.104.000	40.125.333	40.125.333	40.125.333	41.104.000	41.104.000	41.104.000	kwh
Hot Energy Demand 20 years	2.792.867	euro	2.723.046	2.723.046	2.723.046	2.653.224	2.653.224	2.653.224	2.862.689	2.862.689	2.862.689	2.932.511	2.932.511	2.932.511	2.862.689	2.862.689	2.862.689	2.932.511	2.932.511	2.932.511	euro
Hot Energy Losses 20 years (50-50)	133.267	euro	140.538	138.949	138.356	143.375	141.648	140.648	117.625	118.348	119.031	106.431	106.173	107.877	132.668	131.897	131.823	131.578	130.583	130.471	euro
Hot Energy Losses 20 years (opt)	98.972	euro	113.024	111.267	109.539	118.149	116.052	113.668	81.143	81.318	83.290	74.015	73.808	77.085	97.544	97.069	97.026	96.011	95.326	95.356	euro
Cold Energy Savings	447.215	kwh	520.234	500.180	475.095	464.989	435.218	402.450	381.784	366.443	374.952	353.439	338.214	349.948	465.756	460.009	457.546	476.627	468.265	462.968	kwh
Cold Energy Savings	101.160	euro/20 years	117.677	113.141	107.467	105.180	98.446	91.034	86.360	82.889	84.814	79.948	76.504	79.158	105.354	104.054	103.497	107.813	105.921	104.723	euro/20 year
Cold Energy Savings	5.058	euro/year	5.884	5.657	5.373	5.259	4.922	4.552	4.318	4.144	4.241	3.997	3.825	3.958	5.268	5.203	5.175	5.391	5.296	5.236	euro/year
Cold Energy Savings (compared to 50-50)	21,8	%	28,2	27,1	25,6	28,0	26,2	23,8	18,1	17,4	17,8	16,5	15,8	16,4	22,9	22,6	22,5	23,7	23,3	23,0	%
Hot Energy Savings	480.699	kwh	385.650	388.022	403.917	353.583	358.766	378.175	511.355	519.028	500.972	454.362	453.643	431.610	492.313	488.170	487.745	498.531	494.187	492.197	kwh
Hot Energy Savings	34.295	euro/20 years	27.514	27.683	28.817	25.226	25.596	26.980	36.482	37.029	35.741	32.416	32.365	30.793	35.123	34.828	34.798	35.567	35.257	35.115	euro/20 year
Hot Energy Savings	1.715	euro/year	1.376	1.384	1.441	1.261	1.280	1.349	1.824	1.851	1.787	1.621	1.618	1.540	1.756	1.741	1.740	1.778	1.763	1.756	euro/year
Hot Energy Savings (compared to 50-50)	25,7	%	19,6	19,9	20,8	17,6	18,1	19,2	31,0	31,3	30,0	30,5	30,5	28,5	26,5	26,4	26,4	27,0	27,0	26,9	%
TOTAL savings	6.773	euro/year	7.260	7.041	6.814	6.520	6.202	5.901	6.142	5.996	6.028	5.618	5.443	5.498	7.024	6.944	6.915	7.169	7.059	6.992	euro/year
TOTAL savings	135.455	euro/20 years	145.191	140.824	136.284	130.406	124.042	118.015	122.841	119.919	120.555	112.364	108.869	109.951	140.477	138.882	138.294	143.380	141.179	139.838	euro/20 year
TOTAL savings	22,6	%	26,1	25,3	24,5	25,1	24,0	22,6	20,6	20,1	20,2	19,0	18,4	18,6	23,7	23,5	23,4	24,5	24,1	23,9	%
Total water pumped initial	17.733.226	m3	17.842.423	17.854.904	17.864.554	18.069.958	18.087.801	18.110.207	17.905.330	17.877.785	17.878.852	18.166.269	18.111.575	18.117.136	18.137.726	18.138.230	18.138.633	18.543.112	18.543.703	18.544.577	m3
Total water pumped after	17.321.299	m3	17.461.802	17.477.982	17.488.326	17.737.802	17.753.795	17.767.831	17.539.214	17.506.850	17.503.692	17.837.711	17.778.653	17.773.543	17.720.962	17.722.792	17.724.151	18.122.373	18.125.198	18.128.206	m3
Savings	411.927	m3/20 years	380.620	376.922	376.227	332.156	334.006	342.376	366.116	370.934	375.160	328.557	332.922	343.593	416.764	415.439	414.482	420.739	418.506	416.371	m3/20 years
Total water pumped after per year	866.065	m3/year	873.090	873.899	874.416	886.890	887.690	888.392	876.961	875.343	875.185	891.886	888.933	888.677	886.048	886.140	886.208	906.119	906.260	906.410	m3/year
High value temperature Loss (50-50)	773	°C	774	767	756	746	734	722	723	723	723	707	702	705	764	773	769	765	766	760	°C
High value temperature Loss (Opt)	364	°C	409	419	401	422	428	406	400	406	402	419	425	418	357	366	366	354	367	371	°C
Difference	409	°C	365	348	355	323	306	316	323	318	321	288	277	287	407	407	403	411	399	390	°C

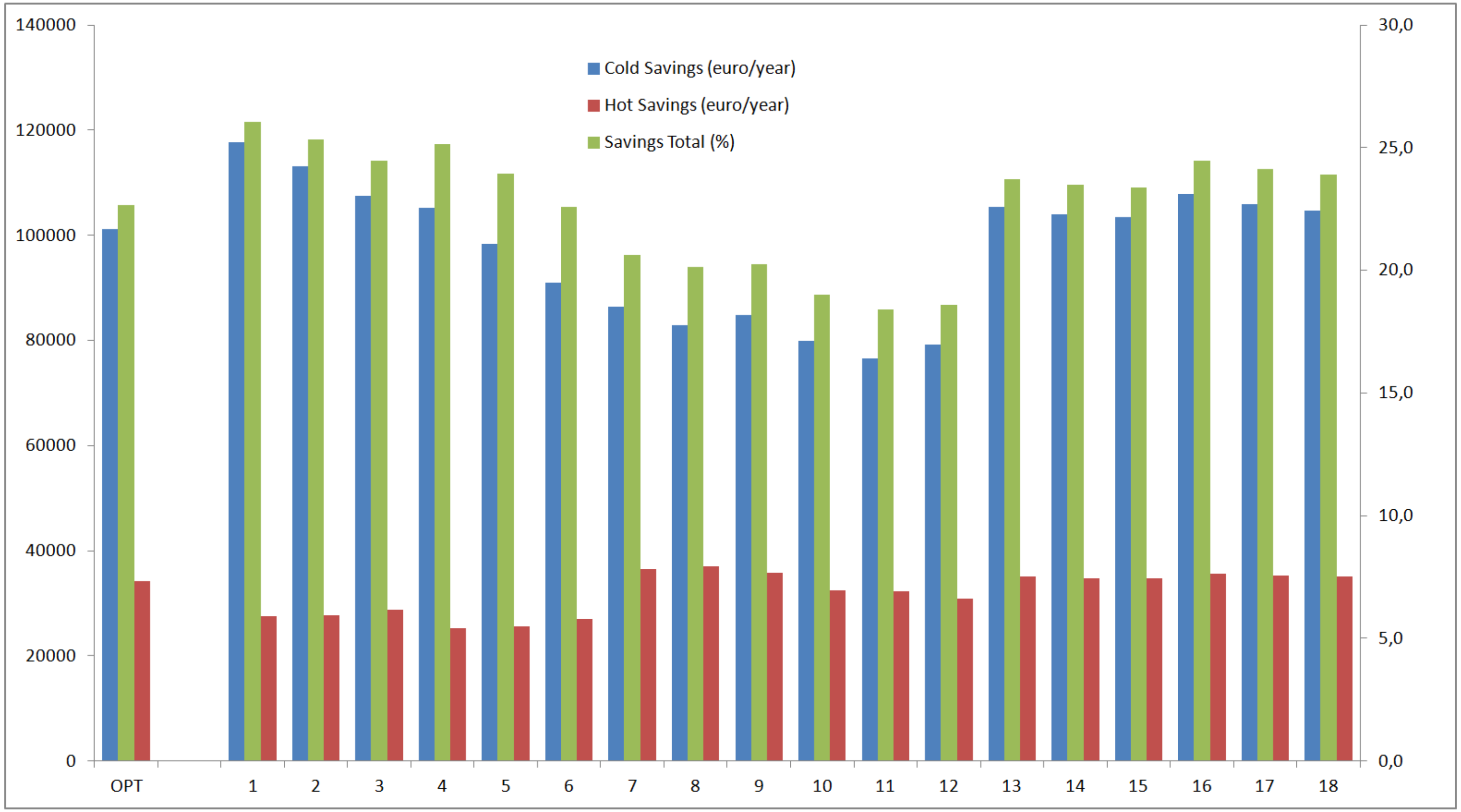
Cold Savings (euro/year)
Hot Savings (euro/year)
Savings Total (%)
140000
120000
100000
80000
60000
40000
20000
0
30,0
25,0
20,0
15,0
10,0
5,0
0,0
OPT
1
2
3
4
5
6
7
8
9
10
11
12
13
14
15
16
17
18

Appendix

11

Comparison between optimized control strategy with initial energy demand, and optimized control strategy with varying energy demands

Improved control strategy

	H1 ex	C1 Inf	H1 Inf	C1 ex
January	44,04%	56,28%	50,01%	49,99%
February	43,99%	56,61%	50,01%	49,99%
March	46,42%	54,10%	52,03%	47,67%
April	47,88%	52,09%	54,05%	45,92%
May	49,32%	50,67%	55,19%	44,77%
June	49,99%	50,01%	55,89%	44,19%
July	49,99%	50,01%	56,00%	44,19%
August	49,99%	50,01%	56,13%	44,12%
September	47,65%	52,03%	53,73%	46,51%
October	45,84%	54,01%	51,92%	47,95%
November	44,69%	55,15%	50,62%	49,34%
December	44,11%	55,93%	50,01%	49,99%

In the next Sections the left set of ratios are the control strategies that result from optimization of the differing energy demand scenarios and the right set of ratios contains the absolute difference of these control strategies with the 'improved control strategy' for the initial energy demand.

S1	44,64%	56,15%	50,01%	49,99%	0,59%	-0,13%	0,00%	0,00%
	44,60%	56,28%	50,01%	49,99%	0,61%	-0,33%	0,00%	0,00%
	46,77%	53,80%	52,04%	47,43%	0,35%	-0,30%	0,01%	-0,24%
	48,17%	51,93%	53,91%	45,49%	0,29%	-0,16%	-0,14%	-0,43%
	49,41%	50,62%	55,07%	44,26%	0,09%	-0,05%	-0,12%	-0,50%
	49,99%	50,01%	55,82%	43,62%	0,00%	0,00%	-0,07%	-0,57%
	49,99%	50,01%	56,09%	43,60%	0,00%	0,00%	0,09%	-0,59%
	49,99%	50,01%	56,38%	43,54%	0,00%	0,00%	0,25%	-0,58%
	47,89%	52,05%	53,94%	46,16%	0,23%	0,03%	0,21%	-0,36%
	46,26%	54,08%	52,03%	47,75%	0,42%	0,07%	0,11%	-0,21%
	45,22%	55,24%	50,65%	49,26%	0,52%	0,09%	0,04%	-0,08%
	44,70%	55,96%	50,01%	49,99%	0,58%	0,03%	0,00%	0,00%
S2	44,51%	56,24%	50,01%	49,99%	0,47%	-0,05%	0,00%	0,00%
	44,47%	56,50%	50,01%	49,99%	0,49%	-0,11%	0,00%	0,00%
	46,69%	53,98%	52,06%	47,49%	0,27%	-0,11%	0,04%	-0,18%
	48,11%	52,04%	53,97%	45,60%	0,23%	-0,06%	-0,08%	-0,32%
	49,39%	50,65%	55,12%	44,39%	0,07%	-0,02%	-0,07%	-0,38%
	49,99%	50,01%	55,82%	43,76%	0,00%	0,00%	-0,07%	-0,43%
	49,99%	50,01%	55,97%	43,74%	0,00%	0,00%	-0,03%	-0,45%
	49,99%	50,01%	56,17%	43,67%	0,00%	0,00%	0,03%	-0,44%
	47,84%	52,02%	53,79%	46,24%	0,18%	-0,01%	0,07%	-0,27%
	46,17%	54,01%	51,95%	47,80%	0,33%	0,00%	0,04%	-0,15%
	45,11%	55,16%	50,63%	49,28%	0,41%	0,01%	0,01%	-0,06%
	44,58%	55,93%	50,01%	49,99%	0,46%	0,00%	0,00%	0,00%
S3	44,56%	56,10%	50,01%	49,99%	0,51%	-0,18%	0,00%	0,00%
	44,52%	56,26%	50,01%	49,99%	0,53%	-0,36%	0,00%	0,00%
	46,72%	53,80%	52,05%	47,47%	0,30%	-0,30%	0,03%	-0,20%
	48,13%	51,94%	53,95%	45,55%	0,25%	-0,15%	-0,09%	-0,37%
	49,39%	50,62%	55,13%	44,34%	0,08%	-0,05%	-0,06%	-0,42%
	49,99%	50,01%	55,89%	43,71%	0,00%	0,00%	0,00%	-0,48%
	49,99%	50,01%	56,16%	43,69%	0,00%	0,00%	0,16%	-0,50%
	49,99%	50,01%	56,45%	43,63%	0,00%	0,00%	0,31%	-0,49%
	47,86%	52,03%	53,97%	46,21%	0,21%	0,00%	0,25%	-0,31%
	46,22%	54,02%	52,04%	47,79%	0,38%	0,01%	0,13%	-0,17%
	45,16%	55,16%	50,66%	49,27%	0,46%	0,02%	0,04%	-0,07%
	44,63%	55,88%	50,01%	49,99%	0,51%	-0,04%	0,00%	0,00%

S4	44,87%	56,09%	50,01%	49,99%	0,82%	-0,19%	0,00%	0,00%
	44,84%	56,31%	50,01%	49,99%	0,85%	-0,30%	0,00%	0,00%
	46,90%	53,85%	52,09%	47,35%	0,48%	-0,25%	0,06%	-0,33%
	48,27%	51,96%	53,93%	45,35%	0,40%	-0,14%	-0,12%	-0,57%
	49,44%	50,63%	55,10%	44,10%	0,12%	-0,05%	-0,09%	-0,67%
	49,99%	50,01%	55,83%	43,44%	0,00%	0,00%	-0,06%	-0,75%
	49,99%	50,01%	56,01%	43,42%	0,00%	0,00%	0,01%	-0,77%
	49,99%	50,01%	56,21%	43,35%	0,00%	0,00%	0,08%	-0,77%
	47,98%	51,96%	53,82%	46,04%	0,33%	-0,07%	0,09%	-0,48%
	46,41%	53,89%	51,97%	47,71%	0,57%	-0,12%	0,05%	-0,24%
	45,41%	55,06%	50,64%	49,23%	0,72%	-0,08%	0,02%	-0,12%
	44,92%	55,81%	50,01%	49,99%	0,80%	-0,11%	0,00%	0,00%
S5	44,82%	56,04%	50,01%	49,99%	0,78%	-0,24%	0,00%	0,00%
	44,79%	56,28%	50,01%	49,99%	0,80%	-0,34%	0,00%	0,00%
	46,87%	53,83%	52,10%	47,37%	0,45%	-0,27%	0,07%	-0,30%
	48,25%	51,95%	53,96%	45,38%	0,38%	-0,14%	-0,09%	-0,53%
	49,43%	50,62%	55,13%	44,15%	0,12%	-0,05%	-0,06%	-0,62%
	49,99%	50,01%	55,86%	43,49%	0,00%	0,00%	-0,03%	-0,70%
	49,99%	50,01%	56,05%	43,47%	0,00%	0,00%	0,05%	-0,72%
	49,99%	50,01%	56,25%	43,41%	0,00%	0,00%	0,12%	-0,71%
	47,97%	51,95%	53,84%	46,07%	0,31%	-0,08%	0,12%	-0,45%
	46,38%	53,85%	51,98%	47,74%	0,55%	-0,16%	0,07%	-0,21%
	45,38%	55,01%	50,64%	49,24%	0,68%	-0,14%	0,03%	-0,11%
	44,88%	55,76%	50,01%	49,99%	0,77%	-0,17%	0,00%	0,00%
S6	44,84%	55,92%	50,01%	49,99%	0,80%	-0,36%	0,00%	0,00%
	44,80%	56,08%	50,01%	49,99%	0,82%	-0,54%	0,00%	0,00%
	46,89%	53,68%	52,08%	47,36%	0,47%	-0,42%	0,05%	-0,31%
	48,24%	51,88%	53,97%	45,35%	0,36%	-0,21%	-0,08%	-0,56%
	49,43%	50,60%	55,17%	44,12%	0,11%	-0,07%	-0,02%	-0,65%
	49,99%	50,01%	55,97%	43,46%	0,00%	0,00%	0,08%	-0,73%
	49,99%	50,01%	56,23%	43,43%	0,00%	0,00%	0,23%	-0,76%
	49,99%	50,01%	56,51%	43,38%	0,00%	0,00%	0,38%	-0,74%
	47,97%	51,95%	54,01%	46,05%	0,32%	-0,07%	0,29%	-0,47%
	46,42%	53,85%	52,06%	47,73%	0,58%	-0,16%	0,15%	-0,22%
	45,41%	55,00%	50,67%	49,23%	0,72%	-0,15%	0,05%	-0,11%
	44,91%	55,71%	50,01%	49,99%	0,79%	-0,22%	0,00%	0,00%

S7	43,68%	56,16%	50,01%	49,99%	-0,37%	-0,12%	0,00%	0,00%
	43,62%	56,49%	50,01%	49,99%	-0,36%	-0,12%	0,00%	0,00%
	46,19%	54,03%	51,99%	47,88%	-0,23%	-0,07%	-0,03%	0,21%
	47,76%	52,07%	53,99%	46,26%	-0,11%	-0,03%	-0,06%	0,34%
	49,26%	50,66%	55,15%	45,21%	-0,05%	-0,01%	-0,04%	0,44%
	49,99%	50,01%	55,84%	44,69%	0,00%	0,00%	-0,05%	0,50%
	49,99%	50,01%	55,93%	44,69%	0,00%	0,00%	-0,07%	0,50%
	49,99%	50,01%	56,03%	44,64%	0,00%	0,00%	-0,11%	0,53%
	47,51%	52,05%	53,62%	46,80%	-0,15%	0,02%	-0,11%	0,29%
	45,58%	53,92%	51,86%	48,19%	-0,26%	-0,10%	-0,06%	0,24%
	44,38%	55,07%	50,60%	49,42%	-0,31%	-0,07%	-0,02%	0,07%
	43,75%	55,85%	50,01%	49,99%	-0,36%	-0,07%	0,00%	0,00%
S8	43,67%	56,20%	50,01%	49,99%	-0,38%	-0,08%	0,00%	0,00%
	43,62%	56,53%	50,01%	49,99%	-0,37%	-0,08%	0,00%	0,00%
	46,18%	54,05%	52,01%	47,86%	-0,24%	-0,05%	-0,02%	0,19%
	47,77%	52,08%	54,00%	46,23%	-0,11%	-0,02%	-0,05%	0,32%
	49,27%	50,67%	55,16%	45,17%	-0,05%	0,00%	-0,03%	0,41%
	49,99%	50,01%	55,86%	44,65%	0,00%	0,00%	-0,03%	0,46%
	49,99%	50,01%	55,95%	44,65%	0,00%	0,00%	-0,04%	0,46%
	49,99%	50,01%	56,06%	44,61%	0,00%	0,00%	-0,07%	0,49%
	47,51%	52,06%	53,64%	46,78%	-0,15%	0,04%	-0,08%	0,26%
	45,56%	53,94%	51,88%	48,19%	-0,28%	-0,08%	-0,04%	0,24%
	44,36%	55,10%	50,60%	49,41%	-0,33%	-0,05%	-0,01%	0,07%
	43,73%	55,88%	50,01%	49,99%	-0,38%	-0,04%	0,00%	0,00%
S9	43,77%	56,13%	50,01%	49,99%	-0,27%	-0,15%	0,00%	0,00%
	43,71%	56,34%	50,01%	49,99%	-0,28%	-0,28%	0,00%	0,00%
	46,25%	53,91%	51,98%	47,80%	-0,17%	-0,19%	-0,05%	0,13%
	47,80%	52,00%	53,96%	46,12%	-0,08%	-0,09%	-0,08%	0,20%
	49,28%	50,64%	55,12%	45,04%	-0,04%	-0,03%	-0,07%	0,27%
	49,99%	50,01%	55,86%	44,50%	0,00%	0,00%	-0,03%	0,31%
	49,99%	50,01%	56,05%	44,50%	0,00%	0,00%	0,05%	0,31%
	49,99%	50,01%	56,28%	44,44%	0,00%	0,00%	0,15%	0,33%
	47,54%	52,10%	53,84%	46,69%	-0,11%	0,07%	0,11%	0,17%
	45,65%	54,02%	51,98%	48,11%	-0,19%	0,01%	0,06%	0,16%
	44,46%	55,17%	50,63%	49,39%	-0,23%	0,02%	0,02%	0,05%
	43,83%	55,90%	50,01%	49,99%	-0,28%	-0,02%	0,00%	0,00%

S10	43,52%	56,09%	50,01%	49,99%	-0,53%	-0,19%	0,00%	0,00%
	43,46%	56,31%	50,01%	49,99%	-0,53%	-0,31%	0,00%	0,00%
	46,09%	53,89%	51,89%	47,98%	-0,33%	-0,21%	-0,14%	0,31%
	47,73%	52,00%	53,79%	46,41%	-0,15%	-0,09%	-0,25%	0,49%
	49,23%	50,65%	54,96%	45,41%	-0,09%	-0,02%	-0,23%	0,64%
	49,99%	50,01%	55,67%	44,91%	0,00%	0,00%	-0,22%	0,72%
	49,99%	50,01%	55,83%	44,91%	0,00%	0,00%	-0,17%	0,72%
	49,99%	50,01%	56,03%	44,87%	0,00%	0,00%	-0,11%	0,76%
	47,43%	52,09%	53,65%	46,93%	-0,22%	0,07%	-0,08%	0,42%
	45,47%	53,94%	51,87%	48,29%	-0,37%	-0,07%	-0,04%	0,34%
	44,27%	55,12%	50,60%	49,45%	-0,43%	-0,03%	-0,02%	0,10%
	43,60%	55,88%	50,01%	49,99%	-0,51%	-0,05%	0,00%	0,00%
S11	43,49%	56,13%	50,01%	49,99%	-0,56%	-0,16%	0,00%	0,00%
	43,43%	56,35%	50,01%	49,99%	-0,56%	-0,26%	0,00%	0,00%
	46,07%	53,92%	51,92%	47,95%	-0,35%	-0,17%	-0,11%	0,28%
	47,73%	52,02%	53,82%	46,37%	-0,15%	-0,07%	-0,23%	0,45%
	49,23%	50,65%	54,98%	45,36%	-0,09%	-0,02%	-0,21%	0,59%
	49,99%	50,01%	55,70%	44,86%	0,00%	0,00%	-0,19%	0,66%
	49,99%	50,01%	55,87%	44,86%	0,00%	0,00%	-0,13%	0,67%
	49,99%	50,01%	56,07%	44,82%	0,00%	0,00%	-0,07%	0,70%
	47,43%	52,11%	53,67%	46,90%	-0,23%	0,09%	-0,06%	0,38%
	45,43%	53,97%	51,90%	48,28%	-0,41%	-0,04%	-0,02%	0,33%
	44,21%	55,14%	50,61%	49,44%	-0,48%	0,00%	-0,01%	0,10%
	43,56%	55,90%	50,01%	49,99%	-0,55%	-0,03%	0,00%	0,00%
S12	43,44%	56,31%	50,01%	49,99%	-0,60%	0,03%	0,00%	0,00%
	43,39%	56,63%	50,01%	49,99%	-0,60%	0,02%	0,00%	0,00%
	46,04%	54,11%	51,93%	47,96%	-0,38%	0,01%	-0,10%	0,29%
	47,72%	52,11%	53,83%	46,40%	-0,16%	0,01%	-0,22%	0,48%
	49,22%	50,68%	54,99%	45,39%	-0,09%	0,01%	-0,20%	0,62%
	49,99%	50,01%	55,67%	44,88%	0,00%	0,00%	-0,21%	0,69%
	49,99%	50,01%	55,77%	44,88%	0,00%	0,00%	-0,23%	0,69%
	49,99%	50,01%	55,88%	44,84%	0,00%	0,00%	-0,26%	0,72%
	47,41%	52,11%	53,52%	46,92%	-0,24%	0,08%	-0,20%	0,41%
	45,38%	53,99%	51,82%	48,27%	-0,46%	-0,02%	-0,09%	0,32%
	44,17%	55,20%	50,58%	49,44%	-0,52%	0,05%	-0,03%	0,10%
	43,51%	56,00%	50,01%	49,99%	-0,60%	0,08%	0,00%	0,00%

S13	44,30%	55,97%	50,01%	49,99%	0,25%	-0,31%	0,00%	0,00%
	44,24%	56,15%	50,01%	49,99%	0,25%	-0,46%	0,00%	0,00%
	46,57%	53,78%	51,96%	47,68%	0,15%	-0,32%	-0,07%	0,01%
	47,97%	51,93%	53,92%	45,93%	0,09%	-0,16%	-0,13%	0,01%
	49,35%	50,62%	55,02%	44,79%	0,03%	-0,05%	-0,16%	0,03%
	49,99%	50,01%	55,75%	44,23%	0,00%	0,00%	-0,13%	0,04%
	49,99%	50,01%	55,97%	44,23%	0,00%	0,00%	-0,02%	0,04%
	49,99%	50,01%	56,25%	44,16%	0,00%	0,00%	0,12%	0,04%
	47,75%	52,00%	53,86%	46,53%	0,10%	-0,02%	0,14%	0,02%
	46,03%	53,98%	51,99%	47,95%	0,19%	-0,04%	0,07%	0,00%
	44,92%	55,07%	50,64%	49,34%	0,22%	-0,08%	0,02%	0,00%
	44,37%	55,76%	50,01%	49,99%	0,25%	-0,16%	0,00%	0,00%
S14	44,20%	56,11%	50,01%	49,99%	0,16%	-0,18%	0,00%	0,00%
	44,14%	56,43%	50,01%	49,99%	0,16%	-0,19%	0,00%	0,00%
	46,51%	53,99%	51,98%	47,73%	0,09%	-0,11%	-0,04%	0,06%
	47,93%	52,04%	53,96%	46,02%	0,05%	-0,06%	-0,09%	0,10%
	49,34%	50,65%	55,07%	44,89%	0,02%	-0,02%	-0,12%	0,12%
	49,99%	50,01%	55,75%	44,34%	0,00%	0,00%	-0,14%	0,15%
	49,99%	50,01%	55,85%	44,34%	0,00%	0,00%	-0,15%	0,15%
	49,99%	50,01%	55,98%	44,28%	0,00%	0,00%	-0,15%	0,16%
	47,71%	51,98%	53,64%	46,60%	0,06%	-0,05%	-0,08%	0,08%
	45,95%	53,92%	51,87%	48,00%	0,11%	-0,09%	-0,04%	0,05%
	44,82%	55,02%	50,60%	49,36%	0,13%	-0,12%	-0,01%	0,02%
	44,27%	55,77%	50,01%	49,99%	0,16%	-0,15%	0,00%	0,00%
S15	44,30%	55,97%	50,01%	49,99%	0,26%	-0,31%	0,00%	0,00%
	44,24%	56,15%	50,01%	49,99%	0,26%	-0,46%	0,00%	0,00%
	46,57%	53,78%	51,96%	47,68%	0,15%	-0,32%	-0,07%	0,01%
	47,97%	51,93%	53,92%	45,93%	0,09%	-0,16%	-0,13%	0,01%
	49,35%	50,62%	55,02%	44,79%	0,03%	-0,05%	-0,17%	0,03%
	49,99%	50,01%	55,75%	44,23%	0,00%	0,00%	-0,14%	0,04%
	49,99%	50,01%	55,97%	44,23%	0,00%	0,00%	-0,03%	0,05%
	49,99%	50,01%	56,25%	44,16%	0,00%	0,00%	0,12%	0,04%
	47,75%	52,01%	53,86%	46,53%	0,10%	-0,02%	0,14%	0,02%
	46,03%	53,98%	51,99%	47,95%	0,19%	-0,04%	0,07%	0,00%
	44,92%	55,07%	50,64%	49,34%	0,22%	-0,08%	0,02%	0,00%
	44,36%	55,77%	50,01%	49,99%	0,25%	-0,16%	0,00%	0,00%

S16	44,44%	55,82%	50,01%	49,99%	0,40%	-0,46%	0,00%	0,00%
	44,38%	55,99%	50,01%	49,99%	0,40%	-0,62%	0,00%	0,00%
	46,66%	53,68%	51,91%	47,74%	0,24%	-0,42%	-0,12%	0,07%
	48,01%	51,88%	53,82%	46,04%	0,14%	-0,22%	-0,23%	0,12%
	49,36%	50,60%	54,90%	44,93%	0,05%	-0,07%	-0,29%	0,16%
	49,99%	50,01%	55,61%	44,38%	0,00%	0,00%	-0,27%	0,19%
	49,99%	50,01%	55,83%	44,38%	0,00%	0,00%	-0,17%	0,19%
	49,99%	50,01%	56,11%	44,31%	0,00%	0,00%	-0,03%	0,19%
	47,80%	51,95%	53,77%	46,62%	0,15%	-0,08%	0,05%	0,11%
	46,13%	53,88%	51,94%	48,00%	0,29%	-0,14%	0,02%	0,05%
	45,04%	54,94%	50,62%	49,36%	0,35%	-0,21%	0,01%	0,02%
	44,50%	55,62%	50,01%	49,99%	0,39%	-0,31%	0,00%	0,00%
S17	44,36%	55,94%	50,01%	49,99%	0,32%	-0,34%	0,00%	0,00%
	44,30%	56,25%	50,01%	49,99%	0,32%	-0,36%	0,00%	0,00%
	46,60%	53,88%	51,94%	47,78%	0,18%	-0,21%	-0,09%	0,11%
	47,98%	51,98%	53,87%	46,12%	0,10%	-0,11%	-0,18%	0,20%
	49,35%	50,64%	54,94%	45,01%	0,04%	-0,03%	-0,24%	0,25%
	49,99%	50,01%	55,61%	44,48%	0,00%	0,00%	-0,28%	0,29%
	49,99%	50,01%	55,70%	44,49%	0,00%	0,00%	-0,30%	0,30%
	49,99%	50,01%	55,83%	44,43%	0,00%	0,00%	-0,30%	0,32%
	47,77%	51,93%	53,56%	46,68%	0,11%	-0,10%	-0,17%	0,17%
	46,05%	53,83%	51,83%	48,04%	0,21%	-0,18%	-0,09%	0,09%
	44,95%	54,90%	50,59%	49,38%	0,26%	-0,25%	-0,03%	0,03%
	44,42%	55,63%	50,01%	49,99%	0,30%	-0,30%	0,00%	0,00%
S18	44,45%	55,82%	50,01%	49,99%	0,41%	-0,46%	0,00%	0,00%
	44,40%	55,99%	50,01%	49,99%	0,41%	-0,62%	0,00%	0,00%
	46,65%	53,68%	51,91%	47,74%	0,24%	-0,41%	-0,11%	0,07%
	48,01%	51,88%	53,83%	46,03%	0,14%	-0,21%	-0,22%	0,12%
	49,37%	50,61%	54,90%	44,92%	0,05%	-0,07%	-0,29%	0,15%
	49,99%	50,01%	55,61%	44,38%	0,00%	0,00%	-0,28%	0,19%
	49,99%	50,01%	55,82%	44,39%	0,00%	0,00%	-0,18%	0,20%
	49,99%	50,01%	56,09%	44,32%	0,00%	0,00%	-0,04%	0,20%
	47,80%	51,96%	53,77%	46,62%	0,15%	-0,07%	0,05%	0,10%
	46,13%	53,88%	51,94%	48,00%	0,29%	-0,13%	0,02%	0,05%
	45,04%	54,95%	50,62%	49,36%	0,34%	-0,20%	0,01%	0,02%
	44,50%	55,62%	50,01%	49,99%	0,39%	-0,30%	0,00%	0,00%

Appendix

12

Determining of Seasonal Performance Factor

The SPF is determined through Equation [8A]:

$$SPF = \frac{E_{wells}}{E_{pump}} \tag{8A}$$

Where SPF is the Seasonal Performance Factor [-]; E_{wells} is the energy supplied by the wells [J] (i.e. the total energy demand); E_{pump} is total energy used by pump the total volume [J]

The energy needed to pump the total volume of water is determined through Equation [9A]:

$$E_{Wells} = P_{pump} u_{eq} \tag{9A}$$

Where P_{pump} is the power of the pump [J/s]; u_{eq} is equivalent full load hours [total pumped volume devided by maximum hourly discharge rate, [3600 s]].

Finally P_{pump} is determined through Equation [10A]:

$$P_{pump} = \frac{Q_{\max} H_{pump} \rho_w g}{\eta} \tag{10A}$$

Where $Q_{\max}$ is the maximum hourly discharge rate for the pumping system (Table 4.5) [175 m^3/h]; H_{pump} is the elevation head (considering a head of 5 meters below ground level, and frictional losses in the pipe system) [20 m]; ρ_w is the density of water [999,9 kg/m^3]; g is the gravitational acceleration [9,81 m/s^2]; η is the assumed efficiency of the underwater pump [0,4] (N.V.O.E., 2006).

Appendix

13

Thermal energy and financial results of optimizing strategies 1, 2 and 3.

SPF and Pumping Costs	50-50	Strategy 1	Strategy 2	Strategy 3	
Total Volume pumped in Hot wells	8.866.613	10.577.679	8.374.489	8.660.650	m3
Total Volume pumped in Cold wells	8.866.613	10.872.897	8.372.541	8.660.650	m3
Energy supply Hot wells	39.146.667	39.146.667	39.146.667	39.146.667	kWh
Energy supply Cold welss	39.146.667	39.146.667	39.146.667	39.146.667	kWh
Energy used for puming Hot wells	1.208.922	1.442.218	1.141.823	1.180.839	kWh
Energy used for pumping Cold wellss	1.208.922	1.482.469	1.141.557	1.180.839	kWh
SPF Hot wells	32,4	27,1	34,3	33,2	[-]
SPF Cold Welss	32,4	26,4	34,3	33,2	[-]
Pumping Costs	-546.916	-661.564	-516.501	-534.212	Euro

High value Thermal energy	50-50	Strategy 1	Strategy 2	Strategy 3	
High Hot thermal energy loss (12,5> C)	867.926	-	89.751	-	kWh
High Cold thermal energy loss (< 9 C)	2.031.406	212.309	1.944.290	1.436.738	kWh
Financial loss	61.920	-	6.403	-	Euro
Financial loss	459.504	48.024	439.798	324.990	Euro
High value thermal energy loss (C)	734	54	515	364	°C
		Savings	Savings	Savings	
		473.399	75.222	196.433	Euro
Net profit:		-188.165	-441.279	-337.778	Euro

Total Thermal Energy	50-50	Strategy 1	Strategy 2	Strategy 3	
Total Hot thermal energy loss (10-13 C)	1.867.956	122.324	1.653.073	1.387.257	kWh
Total Cold thermal enegy loss (7-10 C)	2.054.900	239.516	1.967.784	1.607.685	kWh
Financial loss	133.264	8.727	117.934	98.970	Euro
Financial loss	464.818	54.178	445.113	363.658	Euro
		Savings	Savings	Savings	
		535.177	35.036	135.454	Euro
Net profit:		-126.387	-481.465	-398.758	Euro

	Strategy 1	Strategy 2	Strategy 3	
Total thermal energy loss				
Cold Energy Demand 20 years	39.146.667	39.146.667	39.146.667	**kwh**
Cold Energy Demand 20 years	8.854.976	8.854.976	8.854.976	**euro**
Cold Energy Losses 20 years (50-50)	464.818	464.818	464.818	**euro**
Cold Energy Losses 20 years (opt)	54.178	445.113	363.658	**euro**
Hot Energy Demand 20 years	39.146.667	39.146.667	39.146.667	**kwh**
Hot Energy Demand 20 years	2.792.867	2.792.867	2.792.867	**euro**
Hot Energy Losses 20 years (50-50)	133.267	133.267	133.267	**euro**
Hot Energy Losses 20 years (opt)	8.727	117.936	98.972	**euro**
Cold Energy Savings	1.815.384	87.115	447.215	**kwh**
Cold Energy Savings	410.640	19.705	101.160	**euro/20 years**
Cold Energy Savings	20.532	985	5.058	**euro/year**
Cold Energy Savings (compared to 50-50)	88,3	4,2	21,8	**%**
Hot Energy Savings	1.745.632	214.883	480.699	**kwh**
Hot Energy Savings	124.540	15.331	34.295	**euro/20 years**
Hot Energy Savings	6.227	767	1.715	**euro/year**
Hot Energy Savings (compared to 50-50)	93,5	11,5	25,7	**%**
TOTAL savings	26.759	1.752	6.773	**euro/year**
TOTAL savings	535.180	35.036	135.455	**euro/20 years**
TOTAL savings	89,5	5,9	22,6	**%**
Total water pumped (50-50)	8.866.613	8.866.613	8.866.613	**m3**
Total water pumped (opt)	10.577.679	8.374.489	8.660.650	**m3**
Savings	-1.711.066	492.125	205.964	**m3/20 years**
Total water pumped (opt) per year	528.884	418.724	433.032	**m3/year**
High value temperature Loss (50-50)	595	595	595	**°C**
High value temperature Loss (Opt)	11	231	91	**°C**
Difference	585	365	504	**°C**